Aging alters the Langat Virus infection and pathogenesis in region-specific manner

Dissertation

for the acquirement of the academic degree

doctor rerum naturalium (Dr. rer. nat.)

approved by the Faculty of Natural Sciences
Otto-von-Guericke-Universität Magdeburg

Submitted by: **M.Sc. Angela Rose (geb. Wedekind)**

Born in: Zeven, 29.01.1992

Reviewer Prof. Dr. Andrea Kröger

Prof. Dr. Martin Pfeffer

handed in: 17.07.22 defended: 24.11.22

Abstract

The type I interferon (IFN) system, including a key player MAVS, is essential for the antiviral immune response. The interaction between the innate and the adaptive immune system is particularly critical here. Age-related phenomena such as immunosenescence and inflammaging lead to decreased number and function of immune cells and an imbalance between pro- and anti-inflammatory signaling pathways. All of these factors can contribute to older people developing more severe infections. Especially concerning neurotropic viral infections such as Tick-borne encephalitis virus (TBEV), the mortality in the elderly is significantly increased. Therefore, an efficient local immune response within the central nervous system (CNS) is crucial. In this study, we used the Langat Virus (LGTV), a *Flavivirus* of the TBEV serocomplex. We report that MAVS is essential in the antiviral response because *Mavs*$^{-/-}$ mice develop severe LGTV infection. MAVS protects the mice from high viral replication in the periphery and brain and increased mortality upon intraperitoneal infection. We report that aging increases the relevance of the antiviral activity of MAVS during LGTV infection because old *Mavs*$^{-/-}$ mice succumb to LGTV infection earlier than younger *Mavs*$^{-/-}$ mice. Age-related impairments of immune cells have often been discussed in the literature. In particular, it has been shown that innate immune cells in the CNS are affected during aging. There is a reduction in the number and activation of macrophages and dendritic cells in aged *Mavs*$^{-/-}$ mice. Furthermore, aging reduces type-I- and type-II-interferon-expression as well as IRF-1- and IRF-7-expression. There are many indications in the literature that the local antiviral response seems to be differentially regulated in specific brain regions and that this depends on aging processes. Our data show that cerebellar cells of young *Mavs*$^{-/-}$ mice were more susceptible to LGTV infection than those in old *Mavs*$^{-/-}$ mice. This correlates with the increased local expression of Ifi27la in old *Mavs*$^{-/-}$ mice. However, this locally increased antiviral activity in old *Mavs*$^{-/-}$ mice failed to protect against the increased viral spread or lethal LGTV infection. Accordingly, antiviral activity during LGTV infection appears to be age- and region-specifically regulated within the CNS.

Contents

1. Introduction

1.1. Antiviral immune response

The immune system of vertebrates is divided into innate and adaptive immunity. The innate immune system is the first line of defense against pathogens entering the body. This immune response is non-specific and rapid since it acts directly but always similarly to all pathogens [1]. Innate immunity consists of the skin and mucous membranes, immune cells, and antimicrobial peptides (defensins) [2]. Innate immune cells are neutrophils, macrophages, dendritic cells (DCs), or natural killer cells (NK cells). These cells recognize pathogens and foreign substances through germline-encoded receptors and are essential in inhibiting the early replication and spread of infectious agents. In contrast, adaptive immune cells have receptors generated by somatic mechanisms during the development of each organism. Therefore, a diverse repertoire of receptors with random specificities is generated. The adaptive immune cells are T- and B- lymphocytes [3]. There is a fundamental relationship between innate and adaptive immunity, as the efficiency of the adaptive immune response depends on the signals derived from the innate immune response. A link between innate and adaptive immunity is, for example, the release of type I Interferons (type I IFN), which enhances the immune response and stimulates antigen-presenting cells (APCs) [4, 5]. The antiviral response is induced to recognize pathogen-associated molecular patterns (PAMPs) via pathogen recognition receptors (PRRs) (**Figure 1**).This leads to the secretion of various cytokines to activate and recruit immune cells [6, 7]. Interferons (IFNs) are widely released cytokines with antiviral, antiproliferative, and immunomodulatory effects. The IFN family includes two main classes of related cytokines: the type I IFN and the type II IFN [8]. IFNγ belongs to type II IFN and is produced by NK cells, $CD4^+$, and $CD8^+$ T cells once antigen-specific immunity has developed. IFNα and IFNβ belong to the type I IFN and are produced by fibroblasts, epithelial cells, and APCs. In this study, type I IFNs refer to IFNα/β, the induced cytokines in viral infections. Type I IFNs act autocrine and paracrine, induce intracellular antimicrobial activity, and influence the development of innate and adaptive immune responses [9-11].

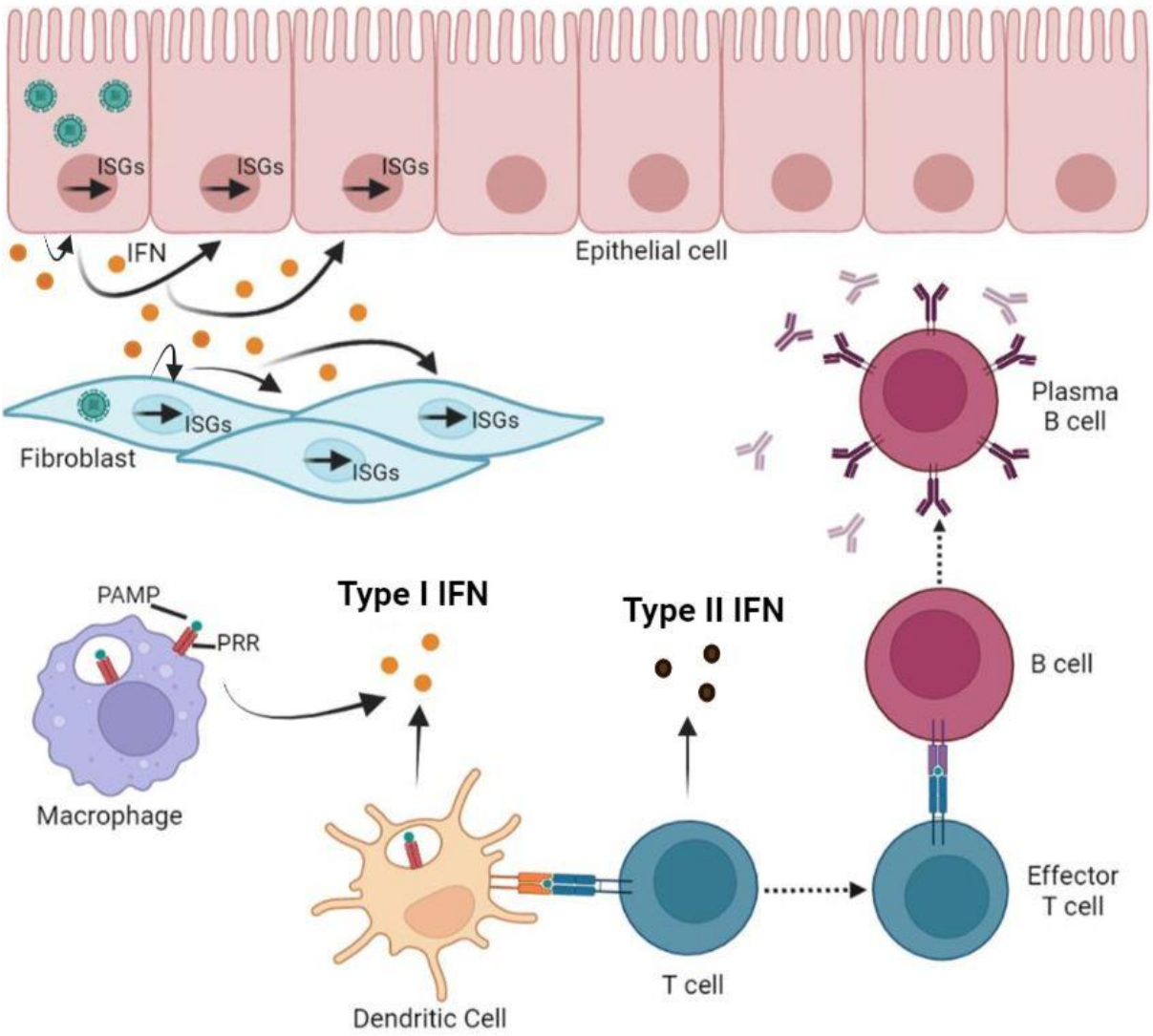

Figure 1: Antiviral immune response. Infected epithelial cells or fibroblasts release IFNs that induce the expression of ISGs in infected and neighboring cells. ISGs initiate an intracellular antimicrobial program to inhibit the spread of infectious agents. Innate immune cells such as macrophages and DCs can detect PAMPS via their PRRs on the plasma membrane, endosomes, and cytosol. Upon detection of pathogens, immune cells release type I IFNs (IFNα/β). IFNs enhance the antigen presentation and the production of immune response mediators such as cytokines and chemokines. IFNs also influence the cells of adaptive immunity. T cells secrete type II IFN (IFNγ), become effector T cells, and can stimulate B cells to turn into plasma cells. Consequently, plasma B cells can secrete virus-specific antibodies. The figure is adapted from Ivashkiv and Donlin (2014) [9] with BioRender.

1.1.1. Type I interferon signaling

The recognition of viral genomes induces the activation of the antiviral response. There are two types of PRRs, the toll-like receptors (TLRs) and the retinoic acid-inducible gene I-(RIG-I) like receptors (RLRs). TLRs detect viral nucleic acids in endosomes only in specialized cell types.

RIG-I is ubiquitously expressed and can recognize virus nucleic acid within cells in the cytosol [12, 13]. Upon binding of viral RNA ligands, RIG-I and melanoma differentiation-associated protein 5 (MDA5) recruit mitochondrial antiviral signaling protein (MAVS) (**Figure 2**). This initiates the activation of interferon regulatory factors (IRFs) and induces the expression of type I IFNs. Secreted IFNα and IFNβ bind to the interferon α receptor (IFNAR), resulting in the activation of the Janus kinase-1 (Jak1) and Tyrosine kinase-2 (Tyk2). This is followed by the activation of transcription-1 and transcription-2 (STAT1, STAT2). These signaling cascades induce the expression of interferon stimulating genes (ISGs), which have antiviral properties. Antiviral ISGs can target almost every step in the life cycle of a virus [14-16]. IRF-1 downstream of PRR-signaling regulates the induction of type I IFN-expression and, thus, the immune response to several viral infections [17, 18].

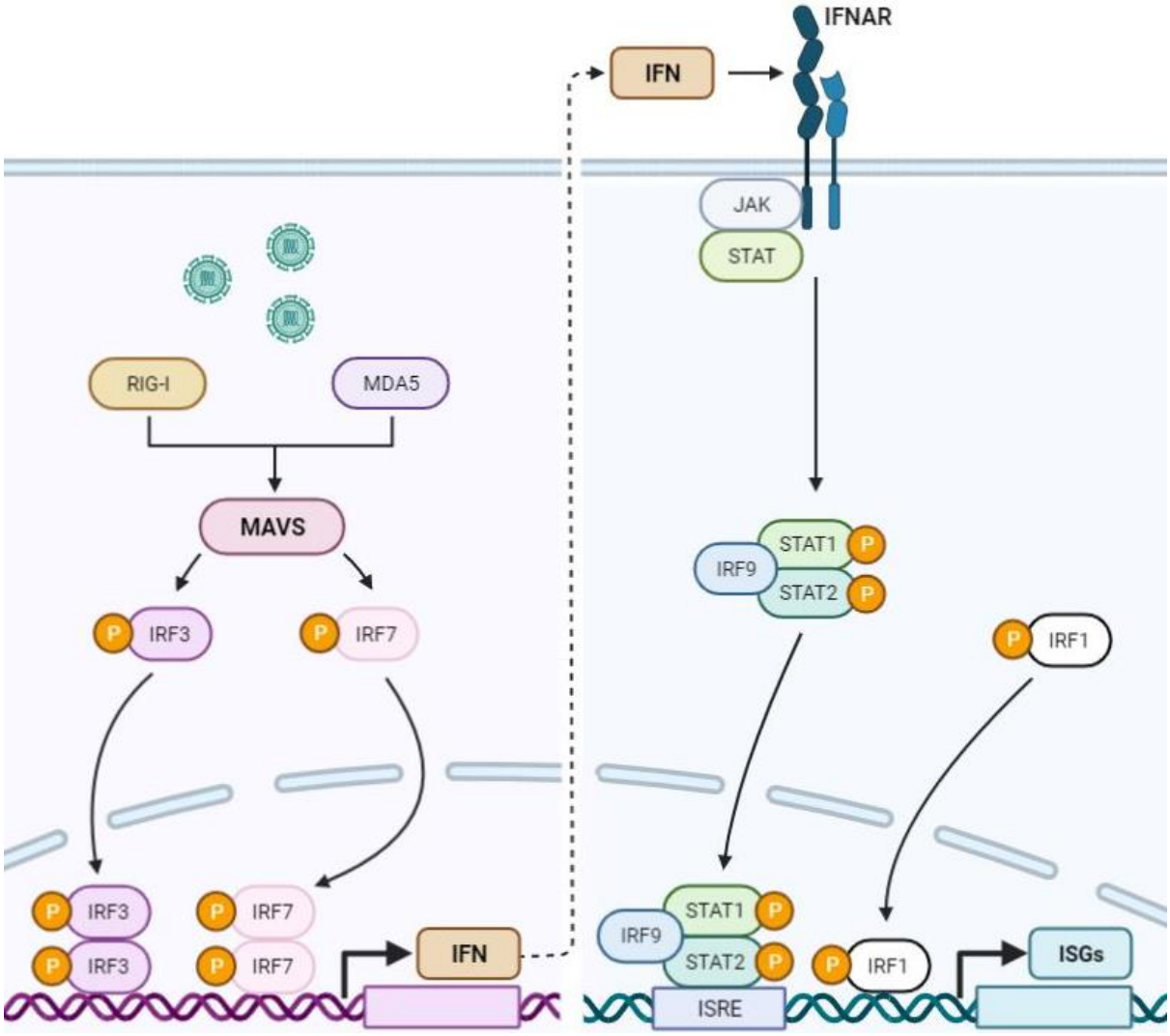

Figure 2: Type-I-IFN signaling. Viral RNA is recognized by receptors such as RIG-I/MDA5. Recognition of viral RNA by RIG-I leads to activation of MAVS and consequently activates IRF- 3/IRF-7 and transcriptional induction of type-I-IFNs. The secreted IFNs bind to IFNAR and induce JAK/STAT signaling. STATs form a transcription complex with IRF-9, which translocates to the nucleus and induces Interferon- induced genes (ISGs) to mediate antiviral and pro-inflammatory effects. IRF-1 is downstream of

PRR- signaling and regulates the induction of type I IFN-expression and, thus, the immune response to several virus infections. The figure is adapted from BioRender.

1.1.2. Type I IFN response in the brain

The central nervous system (CNS) contains highly differentiated cells that are essential for coordinating the functions of complex organisms. Neurons, glia, and endothelial cells are the main cell types that interact to maintain integrity and function. In the past, the blood-brain barrier (BBB) was thought to be the only barrier protecting the CNS from invading pathogens and immune cells [19, 20]. Nowadays, three different barrier structures have been described beside the BBB. The blood-cerebrospinal-fluid (blood-CSF), the meningeal, and the ventricular barrier. These physical barriers are impermeable to proteins or pathogens [21, 22]. Nonetheless, neurotropic viruses can use mechanisms to enter the CNS, such as infection of epithelial cells by the nasal route, axonal transport, crossing the BBB after viremia, or utilizing motile infected cells as Trojan horses [23, 24]. Therefore, the CNS is under constant cellular immune surveillance to protect the brain from invading pathogens and maintain homeostasis and optimal function. Once CNS infection occurs, resident cells such as neurons, astrocytes, oligodendrocytes, and microglia can produce IFNα/β [25]. IFNβ-expression results in rapidly induced ISG release during neurotropic virus infections [26] and highlights the relevance of type I IFNs in the antiviral defense [27]. Detje et al. (2009) show that IFNAR-signaling directly in the CNS was crucial for survival during viral infection [28]. In addition, circulating immune cells cross barriers and protect the cells of the CNS during viral infection [29-31]. $CD4^+$ and $CD8^+$ T cells are critical immune cells that interact with infected neurons, microglia, or astrocytes. This interaction is bidirectional. T cells secrete IFNγ to stimulate resident CNS cells and secrete soluble mediators to regulate T cell responses [32].

1.1.3. Specific immune response signatures in the CNS

Specialized immune mechanisms within the CNS are essential to control neurotropic viral infections. Van den Pol et al. (2014) show that ISG-expression was upregulated in uninfected brain regions by long-distant signaling during neurotropic viral infection [33]. Kim et al. (2000) show that an artificial immune response in the CNS was region- and cell-type-specific [34]. In addition, Kipp et al. (2008) show that astrocytes secrete a region-specific basal profile of cytokines during inflammation [35]. These results suggest that the immune response in the CNS is cell type-dependent and, thus, is differentially regulated in specific brain regions. Neurotropic viral infections are often detected in the olfactory bulb [36]. Several studies demonstrate effective, neuroprotective type I IFN signaling within the olfactory bulb, resulting in rapid viral clearance and inhibition of viral spread. Here, the expression of cytokines lowers the viral titer, which strongly correlates with the rapid infiltration of immune cells. This infiltration of immune cells is crucial in limiting viral replication and spread to other brain regions [37].

In-vitro studies with cortical neurons and cerebellar granule cell neurons show a region- and cell- type-specific antiviral response. Here, antiviral activity within the cerebrum in the cortical neurons was required to limit viral spread [38].

Several pathogens can use the blood-CSF barrier to enter the CNS. This barrier is built up from the choroid plexus, which is the source of CSF and is found in every cerebral ventricle [39]. In response to neuroinflammation, the choroid plexus epithelium can produce chemokines and cytokines, leading to the recruitment of immune cells. For this reason, the choroid plexus is described as a gateway to transport immune cells between CSF and the brain. These data indicate that those specific immune signatures in different brain regions such as the olfactory bulb, cerebrum, cerebellum, and choroid plexus influence the course and outcome of infections in the CNS [40] (**Figure 3**).

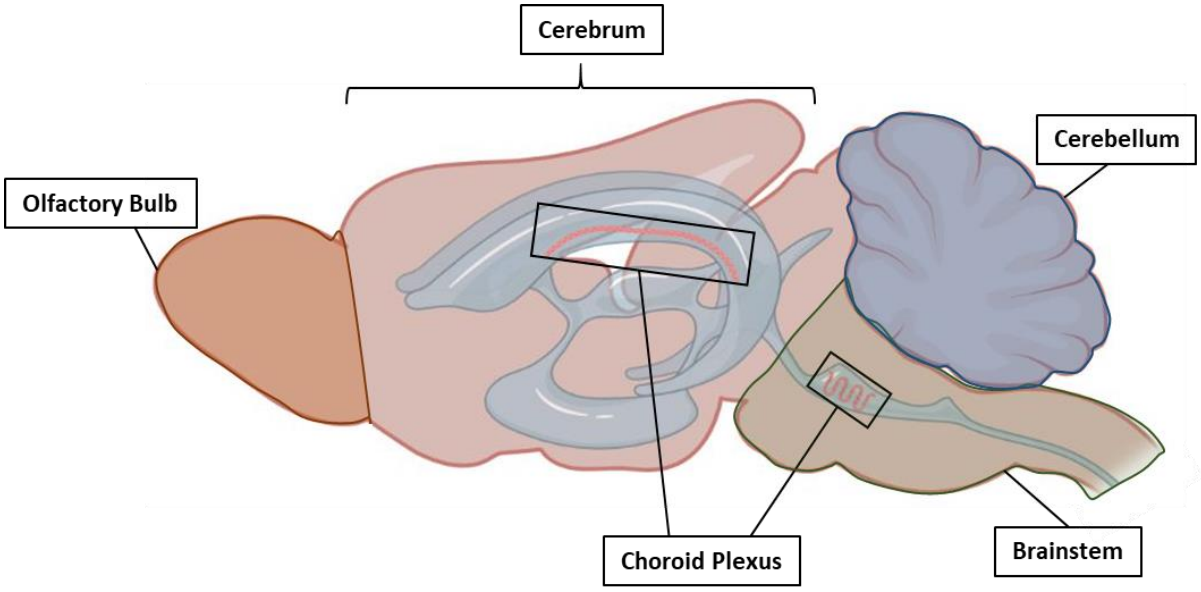

Figure 3: Brain regions of a mouse brain. The antiviral immune response within the CNS is regulated in a cell-type and region-specific manner. Specific immune signatures have been described in the olfactory bulb, cerebellum, cerebrum, and choroid plexus. The figure is modified with BioRender.

Baruch et al. (2014) show that the specific antiviral response within the choroid plexus was age-induced. Indeed, a type I IFN-dependent expression profile was induced by brain-derived signals in the CSF of old mice. This suggests that aging also influences the cell-type and region-specific antiviral response in the CNS [41].

1.2. Aging society and the risk of infections

By 2050, 2.1 billion people will be over 60 and 434 million over 80 years old. Increased life expectancy increases the risk of infections such as cardiovascular diseases, neurodegenerative diseases, type-2-diabetes, and cancer [42]. Aging is defined as the functional decline of living organisms over time. There are conserved hallmarks of aging derived from a few aging processes [43]. These aging processes affect the entire human body, including the brain.

1.2.1. Hallmarks of brain aging

Environmental factors play an important role in structural changes in the brain during aging. Erickson et al. (2011) show that aerobic training increases hippocampus volume [44]. Cherbuin et al. (2015) show that massive energy intake and obesity increase hippocampal atrophy [45]. On the other hand, during normal aging, the human brain loses its elasticity and shrinks by reducing the gray and white matter and expanding cerebral ventricles [46]. In 2018, Mattson and Arumugam defined the ten hallmarks of brain aging, which consist of oxidative damage, mitochondrial dysfunction, impaired molecular waste disposal, impaired DNA repair, stem cell exhaustion, impaired adaptive stress response signaling, dysregulated neuronal calcium homeostasis, aberrant neuronal network activity, and glial cell activation and inflammation. All factors are associated with disturbed energy metabolism. Telomere damage and cell senescence are considered factors in peripheral proliferative tissues but have not been established as hallmarks of brain aging [47]. In particular, the brain of old organisms changes, which is reflected in severe neuronal damage. Neurodegenerative diseases such as Alzheimer's, Parkinson's, or multiple sclerosis are typical in the elderly [47]. Neuronal damage is associated with the chronic alarming of the innate immune response [48]. There is a low level of persistent infiltrated immune cells and a higher level of various pro-inflammatory cytokines and chemokines in the tissue and the systemic milieu. This is called inflammaging. Furthermore, cells in an irreversible state of arrested cell proliferation and altered function accumulate in the elderly, also known as immunosenescence [42].

1.2.2. Immunosenescence and inflammaging

Populations of immune cells and immune function of the innate and the adaptive immune compartments are reduced in aged organisms [49] (**Figure 4**). Studies have shown age-related changes in frequency and function in monocytes, macrophages, NK cells, and DCs [50]. Macrophages and DCs of old donors showed an impaired type I IFN secretion, migration, and antigen presentation [51]. These immune cells produce more pro-inflammatory mediators that lead to a chronic inflammatory status in the elderly. This condition is also known as inflammaging. Consequently, older subjects have an impaired immune response and are more susceptible to viral pathogens than younger subjects [51]. This inflammatory reaction also has an immunopathological effect on the CNS [52]. In addition, T cell and B cell expansion and function are impaired, resulting in dysregulated signaling and cytokine secretion [53]. Age-related changes reduce circulating naïve T cells, resulting in the accumulation of terminally differentiated T cells [54, 55]. Consequently, T cell receptor (TCR) diversity is limited, and the ability to respond to vaccines and emerging pathogens is reduced. In neurotropic viral infections, T cells play an essential role by releasing IFNγ and interacting with cells of the CNS. $CD8^+$ T cells directly eliminate infected cells, and $CD4^+$ T cells support this process [56].

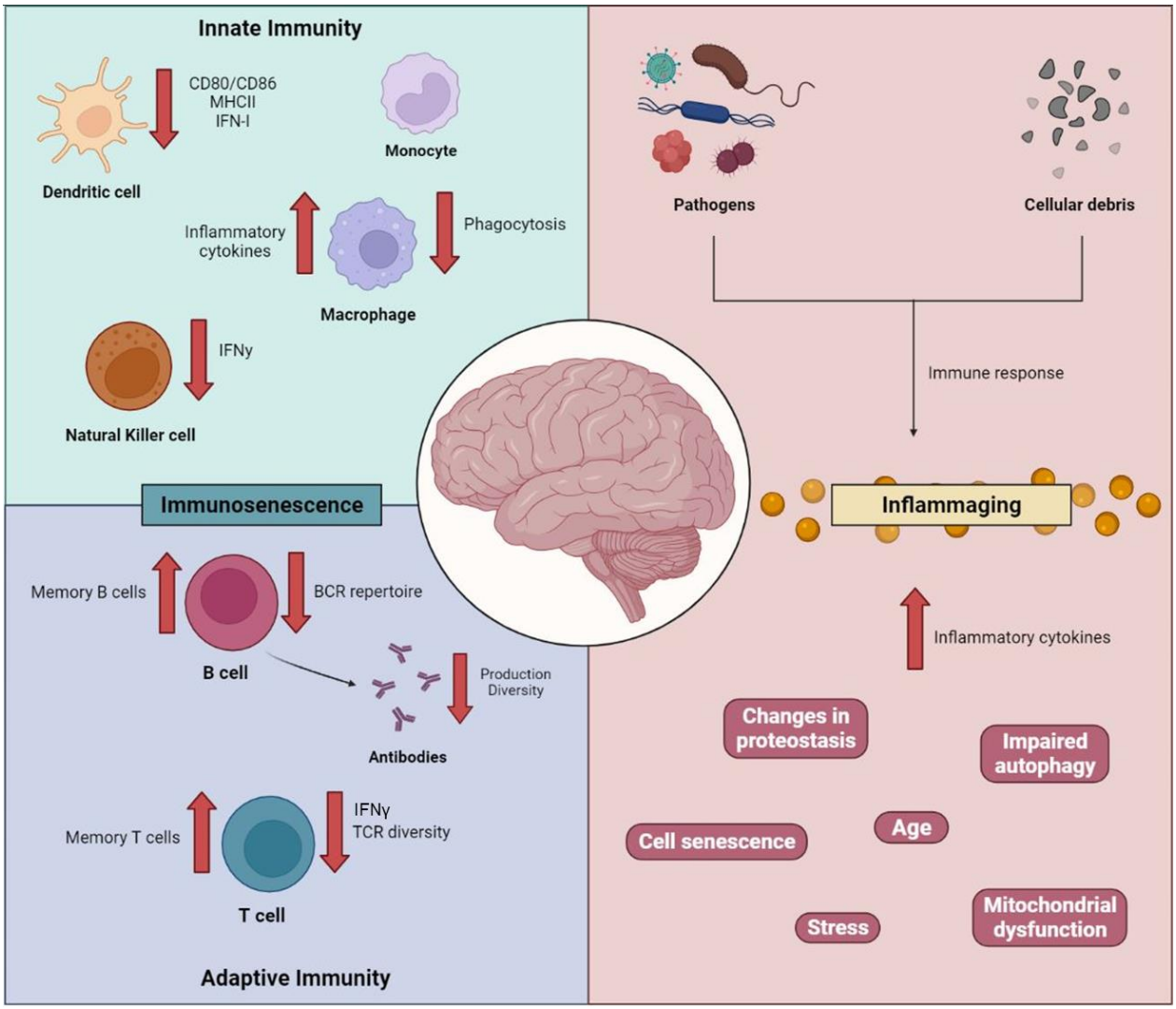

Figure 4: Immunosenescence and inflammaging. Significant immunological changes observed during immunosenescence are shown on the left: Aging leads to multiple impairments in the function and response of innate and adaptive immune cells. On the right: numerous factors dysregulate intracellular homeostasis during aging and increase the secretion of inflammatory cytokines and chemokines, termed inflammaging.

1.2.3. Severity of neurotropic virus infections in the elderly

Neurotropic viruses can infect neurons directly, causing apoptosis or degeneration of neurons and leading to CNS pathology [57, 58]. The limited ability of the CNS to regenerate challenges the immune system to eliminate pathogens without damaging healthy neurons. Under normal conditions, class I major histocompatibility complex (MHC-I molecule) expression on neurons is limited, protecting them from $CD8^+$ T cells [52]. Animal models of neurological diseases have shown that T cells are essential players during CNS inflammation due to their direct contact with neurons. The interaction between T cells and neurons is bidirectional. Neurons promote T cell apoptosis by producing anti-inflammatory cytokines. At the same time, $CD8^+$ T cells eliminate viruses from infected neurons in a MHC-I-dependent manner through cytotoxic granules. During inflammation, secretion of IFNγ produced by $CD8^+$ T cells enhances the expression of MHC-I molecules on neurons and promotes neurotoxicity [59-61]. These factors can lead to a higher burden of neurotropic viral infections in an aged organism [50], leading to higher morbidity and mortality [48].

1.3. Tick-Borne Encephalitis Virus

The Tick-Borne Encephalitis Virus (TBEV) belongs to the family *Flaviviridae* and the genus *Flavivirus*. It is a critical human pathogen causing millions of infections worldwide. Arthropods transmit more than 70 different viruses within the flavivirus. *Mosquito-borne viruses* such as Dengue Virus (DENV), Japanese Encephalitis Virus (JEV), West Nile Virus (WNV), Yellow Fever Virus (YFV), and Zika Virus (ZIKV). Or *tick-borne viruses* such as TBEV, Langat Virus (LGVT), Omsk Hemorrhagic Fever Virus (OHFV), Powassan Virus (POWV), and Louping-Ill Virus (LIV) [46, 62-67]. Cases are known of humans being infected with TBEV through consumption of unpasteurized contaminated dairy products [68]. Infected people usually do not develop any clinical symptoms, but some develop a severe course of infection. This is related to the neuroinvasiveness and neurovirulence of TBEV. It can enter the central nervous system (CNS) after peripheral inoculation and replicate in the cells of the CNS [57]. The entire mechanism of how the virus enters the brain is still unknown [64, 69].

1.3.1. Virus Structure

All members of *Flavivirus* have a very similar structure of their virion, genomic organization, and life circle. Mature virions are round, enveloped, and around 50 nm in diameter. The viral genome is a positively charged, single-strand RNA of 11-kilo base pairs. The genomic RNA contains a single open reading frame (ORF) that encodes for a polyprotein. That polyprotein is cleaved into three structural proteins (capsid (C) protein, envelope (E) protein, and the membrane (M) protein) and seven non-structural proteins (NS1, NS2A, NS2B, NS3, NS4A, NS4B, and NS5) (**Figure 5**) [70-72]. An immature virion contains a precursor membrane, the prM protein. Cleavage of the prM protein into M protein occurs during virion exit from the cells. The E protein plays an essential role by interacting with receptors, mediating cell entry, and protecting the virion from nucleases [62, 65, 73].

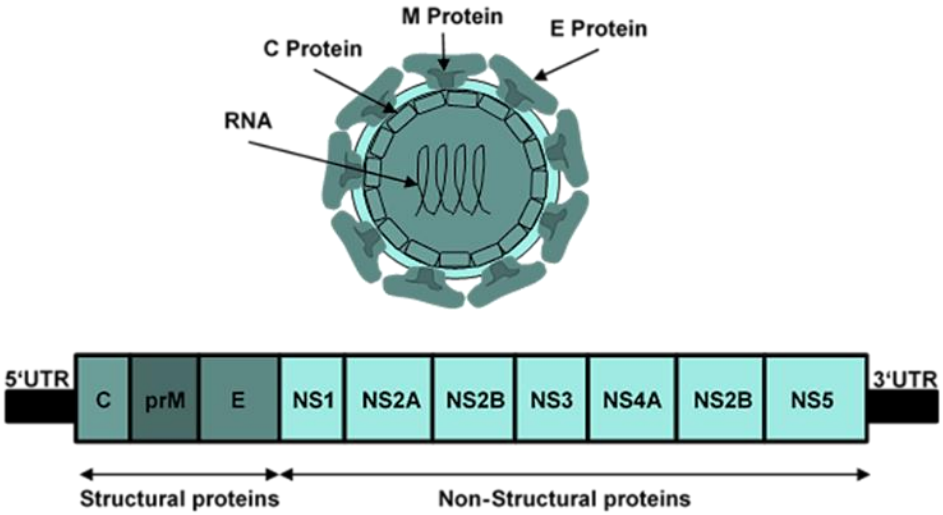

Figure 5: Schematic virus structure of flaviviruses. The virus contains three structural proteins the capsid (C) protein, the envelope (E) protein, and the membrane (M) protein. Likewise, seven non-structural proteins: NS1, NS2A, NS2B, NS3, NS4A, NS4B, and NS5. An immature virion contains a precursor membrane, the prM protein. Cleavage of the prM protein into M protein occurs during virion exit from cells.

1.3.2. Clinical outcome

Neurotropic viruses such as TBEV lead to dangerous human infections in large parts of Europe and Asia. The incidence of TBEV increases every year. This is related to climatic, ecological, environmental, and socioeconomic changes. TBEV results in more than 10000 new cases worldwide each year. The increasing geographic spread and higher morbidity of TBEV have recently highlighted it as a public health concern [62, 66, 74]. The clinical outcome of TBEV depends on the virus strain, the infection dose, and the patient's age. After a tick bite with subsequent transmission of TBEV, the incubation period is mostly 7- 14 days. In one-third of the infected patients, the TBE infection shows a biphasic course, which begins with unspecific symptoms such as headaches, muscle pain, and fever. This initial phase lasts about eight days. An asymptomatic phase (1-20 days) follows. About one-third of patients develop hemorrhagic fever, encephalitis, meningitis, or meningoencephalitis in the second phase. The neurovirulence of TBEV leads to apoptosis or degeneration of neurons, which is considered the leading cause of neurological disease [57, 75] (**Figure 6**).

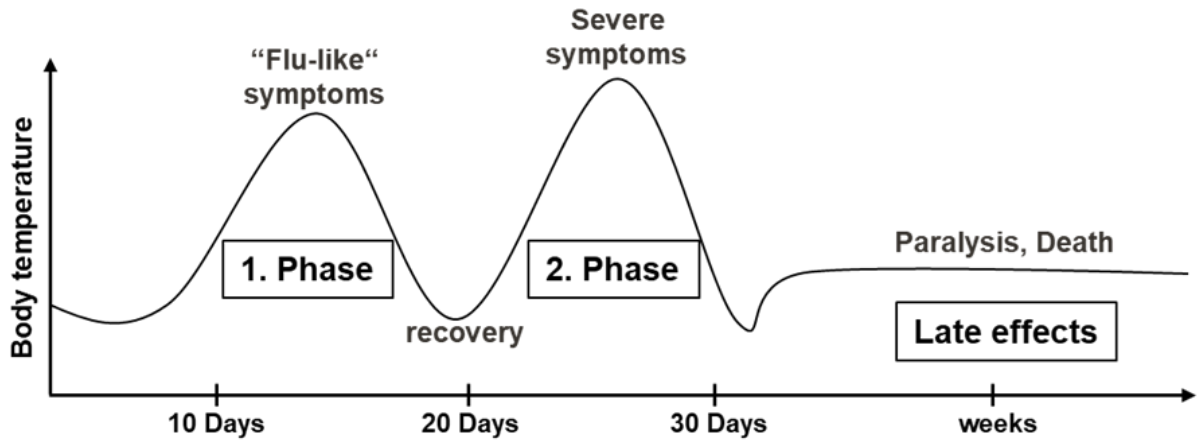

Figure 6: The biphasic course of TBEV infection. The initial phase with flu-like symptoms lasts about a week. An asymptomatic phase follows. About one-third of patients develop hemorrhagic fever, encephalitis, meningitis, or meningoencephalitis in the second phase. These patients can suffer from long-term effects.

On the one hand, mortality of TBEV depends on the viral subtype. The European virus has a mortality rate between 0.5–2 %, the Siberian between 2-3 %, and the Far Eastern around 40 %. The European type is mainly transmitted by *Ixodes ricinus*, and the Siberian and the Far Eastern type is primarily transmitted by *Ixodes persulcatus* [66, 76-78]. On the other hand, older patients are more likely to develop severe meningoencephalitis with chronic neurological impairment or death [62, 63, 79]. The risk of infection is significantly increased in patients over 50 years [80, 81]. The mortality rate in the elderly is 15 times higher than in younger people [82].

1.3.3. LGTV as an infection model for TBEV

LGTV was first isolated in Malaysia from a pool of *Ixodes granulatus* and *Haemaphysalis* spp. It is a naturally attenuated member of the TBEV serocomplex of flaviviruses [65]. LGTV shares 82– 88 % amino acid identity with TBEV and is classified as a flavivirus with low pathogenicity in humans, as it mainly causes symptoms in immunocompromised patients [63, 73]. In mice, TBEV infection causes typically severe symptoms with a lethal outcome. Since about 30 % of TBEV-infected humans and about 30 % of LGTV-infected mice develop symptoms, LGTV infections in mice are comparable to TBEV infections in humans. Therefore, LGTV can be used as an infection model for TBEV [83].

2. Aim of the thesis

TBEV is an important human pathogen causing millions of infections worldwide [65]. Because it is a neurotropic virus, it can invade and replicate in the CNS [57]. Although TBEV infections are mostly asymptomatic, patients can develop severe neurological disorders [75]. Interestingly, the mortality rate from TBEV infection is highly increased in patients over 50 years [82]. Aging processes affect the entire human body, including the brain. Cells of the immune system are involved with age, leading to decreased antiviral activity within the CNS [49, 50]. Therefore, neurotropic viral infections represent a high burden for the elderly, leading to increased morbidity and mortality [81]. The type I IFN system, including the critical player MAVS, is an essential component of antiviral immunity [27]. MAVS is necessary for the local IFN response in the CNS by reducing viral load and spread [84]. The antiviral activity in the CNS can be regulated differently in specific brain regions [34, 35]. Aging processes can also influence this regulation [41]. In this context, a particular focus was placed on type I IFN signaling during aging. The TBEV strain LGTV was used as an infection model to study the effects of aging on antiviral activity. Since LGTV is a neurotropic virus, we aimed to uncover the effects of aging on the antiviral function of MAVS in specific brain regions of mice. In addition, we sought to find the effects of aging on the frequency and activation of specific immune cells in the cerebrum and cerebellum during LGTV infection. Finally, our efforts aimed to determine whether MAVS-dependent antiviral activity is age- and region-specifically regulated.

3. Results

Aging plays an essential role in susceptibility to infection [49]. This is particularly important in CNS infection with Tick-Borne Encephalitis virus (TBEV), in which older people suffer more from the consequences than younger people [81]. These consequences include severe encephalitis, meningoencephalitis, and persistent impairment of mobility and memory [75]. As a result, hospitalization rates for TBE-associated diseases are increasing among older people [82]. The immune system is crucial in host defense against viral infections, and the implication is that aging negatively affects immunity [42, 85]. With increasing age, decreasing adaptive immunity likely plays a significant role in the higher morbidity and mortality of virus-infected elderly [49]. However, an effective immune response results from a carefully balanced interplay of innate and adaptive immunity [86]. The innate immune system is the first line of defense against invading pathogens. Recent studies have provided experimental and clinical evidence that the innate immune system contributes to the impaired response to viral infection with age [87]. However, this focuses on the expression level of innate immune receptors and loss of function in innate immune cells such as dendritic cells and natural killer cells [88]. Here we concentrate on how the innate immune system influences virus recognition during aging and what consequences this has on the course of infection in specific immune-privileged organs of the CNS.

We use the Langat virus (LGTV) as a model virus for TBEV infections in the CNS. To investigate the role of MAVS in the antiviral response of aged mice, mice of different ages were compared. Young adult mice with mature immune systems (2-3 months: young), older adults mice with initial impairments of the immune system (10 – 12 months: adult), and very old mice with impairments of the immune system (18-24 months: old) were used. The influence of aging on morbidity and mortality as well as the immune response in the brain was investigated.

3.1. The importance of MAVS in antiviral defense increases with age

In TBEV or LGTV infections, the type I IFN response is crucial for protecting mice [89, 90]. Recognition of PAMPs by RIG-I leads to activation of MAVS and induces secretion of IFNα and IFNβ. Subsequently, signaling cascades induce the expression of multiple ISGs with antiviral properties. The detection of PAMPS by TLRs also activates type I IFN signaling. Despite an intact TLR-system, a depletion of MAVS leads to a higher susceptibility to viral infections [91]. In addition, several studies show that MAVS controls viral replication during neurotropic viral infection. Consequently, it is a significant factor in inhibiting viral spread [92-94]. MAVS is also very important for the local IFN response in the brain, reducing viral load and viral spread during LGTV infection [84].

To investigate whether MAVS influences the antiviral response during aging, C57BL/6OlaHsd (WT) and *Mavs*$^{-/-}$ mice of different ages were infected systemically by intraperitoneal LGTV injection to analyze mouse survival (**Figure 7**).

All WT mice survived LGTV infection without clinical symptoms, independent of the age of the mice (**Figure 7A**). This indicates that aging did not strongly influence the survival of WT mice during LGTV infection.

As expected, the depletion of MAVS resulted in severe clinical symptoms. Most of the mice developed hunchback, lethargy, fur ruffling, and weight loss (**Figure 7B**). Severely infected young *Mavs*$^{-/-}$ mice died within 6-8 days post-infection (dpi), but 25 % survived the LGTV infection. Adult and old *Mavs*$^{-/-}$ mice reached humanized endpoints within 6-7 dpi. Old *Mavs*$^{-/-}$ mice showed a lower median survival time than adult mice. However, this difference was not significant. In contrast, young *Mavs*$^{-/-}$ mice showed an increased median survival time than adult or old mice. Therefore, young *Mavs*$^{-/-}$ mice had a significant survival advantage compared to adult or old mice. The data confirmed that MAVS protects mice from lethal LGTV infection, and aging increases the susceptibility of mice to LGTV infection.

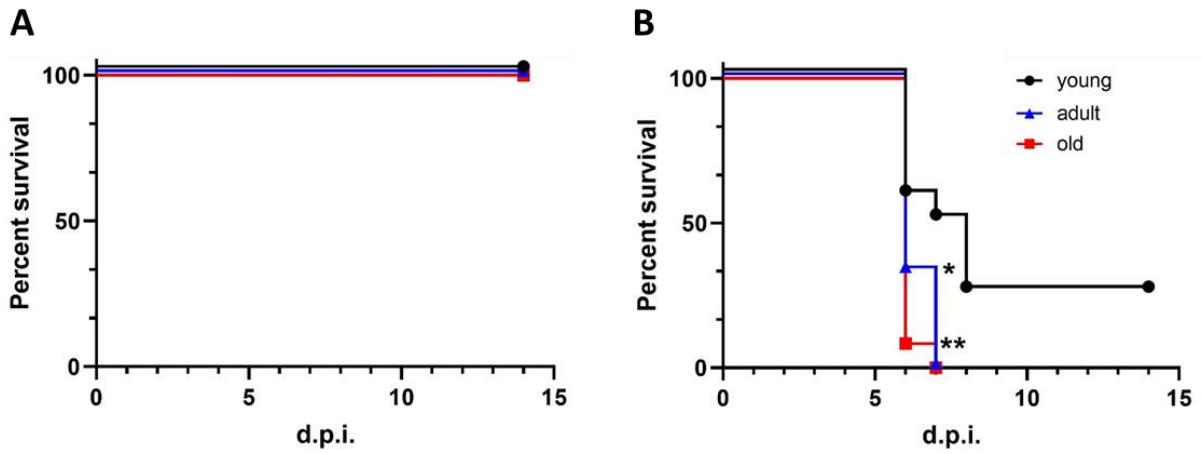

Figure 7: Impact of MAVS on antiviral response during aging Survival analysis of WT and *Mavs*$^{-/-}$ mice of three different ages (young: 2-3 months (n=12); adult: 10-12 months (n=12); old: 18-24 months (n=12)). Mice were infected intraperitoneally with 10^4 FFU LGTV. Kaplan-Meier curves of infected mice are shown. A: WT mice. B: *Mavs*$^{-/-}$ mice. The data are representative of at least two independent experiments. Survival differences between young and adult and young and old mice were tested for statistical significance using the Mantel-Cox test (p-value: * < 0,05; ** < 0,01).

3.2. Relevance of MAVS-dependent antiviral activity increases with age

MAVS is an essential factor in inducing the antiviral response through the expression of IFNs [94]. During LGTV infection, *Mavs*$^{-/-}$ mice show increased viral replication and rapid neuroinvasion, indicating an essential role of MAVS in both peripheral organs and the CNS [84]. To investigate whether age-related increased susceptibility to LGTV infection in *Mavs*$^{-/-}$ mice correlates with viral replication, viral load was determined at six dpi and terminal endpoint (endpoint). Viral replication was determined using quantitative real-time polymerase chain reaction (qRT-PCR) in the spleen, inguinal lymph nodes (LN, **Figure 8**), and the brain (**Figure 9**) of mice.

In the lymph nodes of WT mice, the overall viral load was low with a slight but not significant increase with age at six dpi (**Figure 8A**). The depletion of MAVS resulted in an increased viral load in the lymph nodes of mice at six dpi. This increase was significant in adult *Mavs*$^{-/-}$ mice compared to WT mice. In the lymph nodes of *Mavs*$^{-/-}$ mice, the viral load was slightly increased with the age of mice. This increase was significant in adult *Mavs*$^{-/-}$ mice compared to young *Mavs*$^{-/-}$ mice at six dpi.
Analysis at the endpoint showed that lymph nodes of WT mice of all ages had a low viral load with no significant differences (**Figure 8B**). In the lymph nodes of *Mavs*$^{-/-}$ mice, the viral load was similarly low in young and adult mice as in WT mice, while the viral load was slightly but not significantly increased in old mice compared to WT mice.

In the spleen of WT mice, the overall viral load was low and no age-related differences were detected at six dpi (**Figure 8C**). In the spleen of *Mavs*$^{-/-}$ mice, the viral load was similarly low as in WT mice, with no age-dependent differences at six dpi.
At endpoint analysis, in the spleen of WT mice, the viral load was low with no significant differences during aging (**Figure 8D**). The depletion of MAVS resulted in a significantly increased viral load in adult and old mice. In the spleen of *Mavs*$^{-/-}$ mice, the viral load was increased with the age of the mice. This increase was highly significant between young and adult *Mavs*$^{-/-}$ mice and between adult and old *Mavs*$^{-/-}$ mice at endpoint analysis.

The data suggest that the relevance of the inhibitory antiviral effect of MAVS during aging is increased in the spleen at endpoint analysis. However, the viral load is not mainly affected in the periphery of mice, independent of age and MAVS. Therefore, viral loads in the peripheral organs are unlikely to cause death in *Mavs*$^{-/-}$ mice.

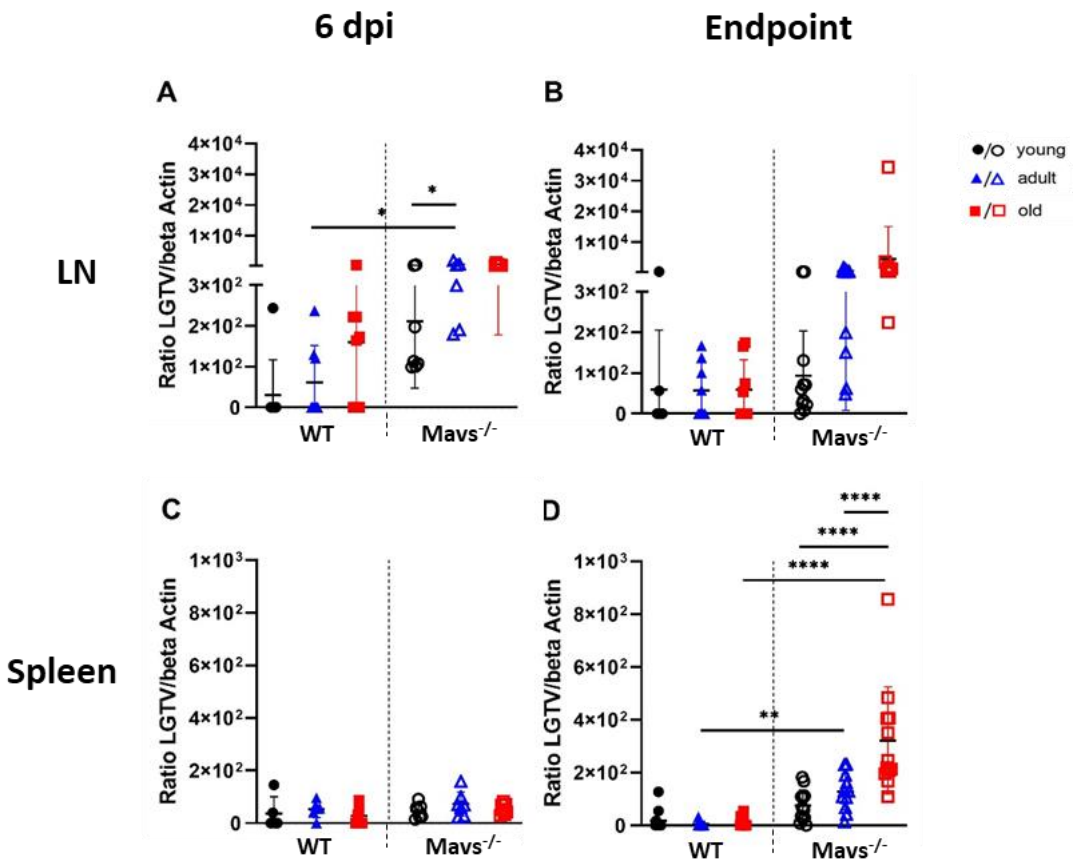

Figure 8: Antiviral effect of MAVS in the spleen increases with age. WT and *Mavs*$^{-/-}$ mice of three different ages (young: 2-3 months (n=10 (WT), n=12 (MAVS)); adult: 10-12 months (n=10 (WT), n=12 (MAVS)); old: 18– 24 months (n=10 (WT), n=12 (MAVS)), were infected intraperitoneal with 10^4 FFU LGTV. Spleen and inguinal lymph nodes were collected at six dpi and endpoint of the survival experiments. The relative quantitative viral RNA was determined in comparison to β-actin. Results were combined from three independent experiments. Viral load in lymph nodes at six dpi (A) and endpoint of infection (B); spleens at six dpi (C) and endpoint of infection (D). RNA-level differences were tested for statistical significance using the two way ANOVA multiple comparison test (p-value: * < 0,05; ** < 0,01; **** < 0,0001)

Since LGTV is a neurotropic virus, we further analyzed the viral load in the brain of infected mice (**Figure 9**). At six dpi, WT mice had an overall low viral load in the brain with no significant differences during aging (**Figure 9A**). The depletion of MAVS resulted in an overall increased viral load in mice, with a significant increase in young mice. In the brain of *Mavs*$^{-/-}$ mice, the viral load was significantly increased in young mice compared to adult mice. However, the viral load was slightly increased in old *Mavs*$^{-/-}$ mice compared to adult *Mavs*$^{-/-}$ mice. Therefore, aging did not affect the viral load in the brain of *Mavs*$^{-/-}$ mice.

At endpoint analysis, WT mice had an overall low viral load in the brain with no significant differences during aging (**Figure 9B**). The depletion of MAVS resulted in an overall increased viral load in mice. This increase was significant in adult *Mavs*$^{-/-}$ mice compared to WT mice. In the brain of *Mavs*$^{-/-}$ mice, although the viral load was slightly increased with the age of mice, this increase was not significant.

The data support knowledge of the inhibitory antiviral effect of MAVS in the CNS. However, aging does not influence the viral load in the CNS of mice and is unlikely to be the cause of the early death in aged *Mavs*$^{-/-}$ mice.

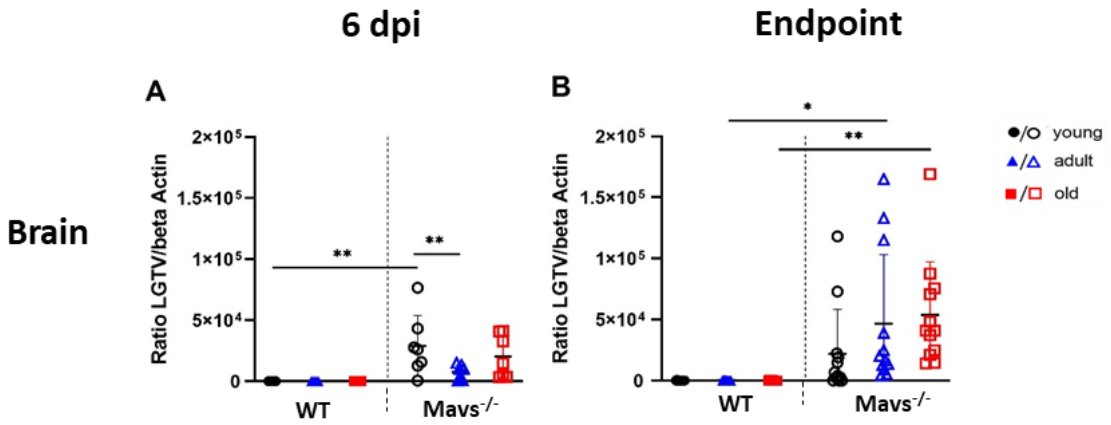

Figure 9: Antiviral effect of MAVS during CNS LGTV infection is age-independent. WT and *Mavs*$^{-/-}$ mice of three different ages (young: 2-3 months (n=10 (WT), n=12 (MAVS)); adult: 10-12 months (n=10 (WT), n=12 (MAVS)); old: 18-24 months (n=10 (WT), n=12 (MAVS)), were infected intraperitoneal with 10^4 FFU LGTV. Brains were collected at six dpi and the endpoint of survival experiments. The relative quantitative viral RNA was determined in comparison to β-actin. Results were combined from three independent experiments. A: Analysis of collected brains at six dpi. B: Analysis of the collected brains at the endpoint of infection. RNA-level differences were tested for statistical significance using the two-way ANOVA multiple comparison test (p-value: * < 0,05; ** < 0,01).

3.3. Impact of aging on immune cell composition and function of CNS immunity

Neurotropic virus infections are associated with CNS inflammation, leading to the infiltration of immune cells [42]. In aged organisms, innate and adaptive immune cells are affected. Age-related changes in immunity lead to a decreased number and impaired function of immune cells [49, 93]. To investigate whether immune cells infiltrate into the CNS during LGTV infection and this infiltration is altered with age, WT and Mavs$^{-/-}$ mice of different ages were systemically infected with LGTV and immune cells of the cerebrum and the cerebellum were analyzed by flow cytometry.

The gating strategy of the analysis is shown in **Figure 10**. First, brain cells were determined through their size (forward scatter: FSC-A) and shape (sideward scatter: SSC-A). Single cells were separated through the area and height of the sideward scatter (SSC-A: SSC-H). Live-Dead-staining enabled the determination of living cells. Infiltrating cells were CD45^{+} cells and were divided into lymphocytes (CD11b^{-} CD45^{+}), monocytes (CD11b^{+} CD45^{+}) and separated from microglial cells (CD11b^{+} CD45^{-}). The staining of CD3 separated T cells from non-T cells. CD3^{+} cells such as Th cells and CTLs were distinguished with CD4 and CD8 staining. CD3^{-} cells were separated into B cells (CD19^{+}), macrophages (F4/80^{+}) and dendritic cells (DCs, CD11c^{+}). The staining of CD86 determined at least the activation of CD3^{-} and microglial cells.

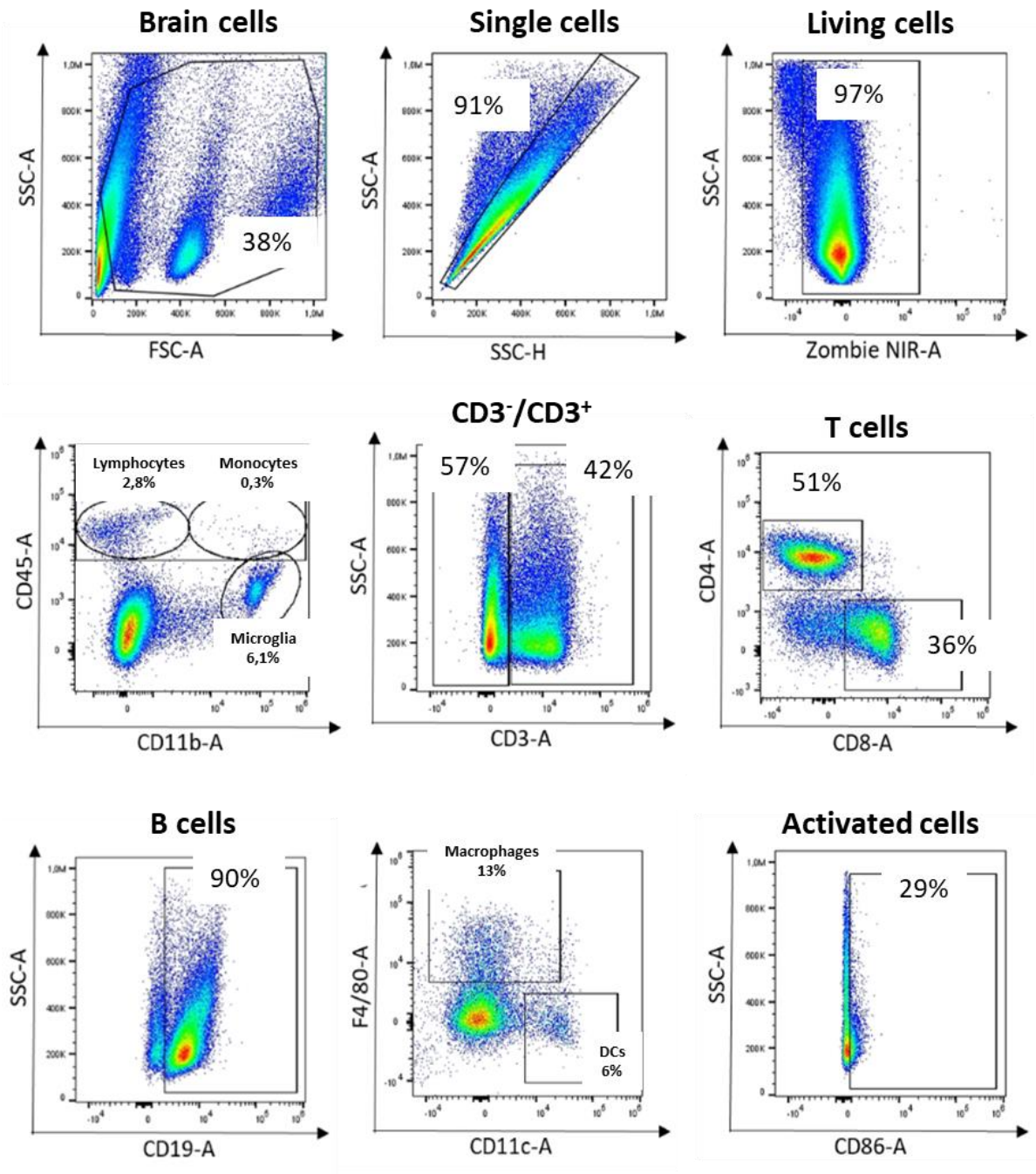

Figure 10: Gating strategy of immune cell panel. Brain cells were determined through forward (size) and sideward (shape) scatter. Single cells were isolated through the area and the height of the sideward scatter. Living cells were separated through the live-dead-staining. Afterwards, the infiltrating cells ($CD11b^+$ $CD45^+$) were isolated from microglial cells ($CD11b^+$ $CD45^-$). The staining of CD3 separated T cells from non-T cells. With the staining of CD4 and CD8, Th cells and CTLs could be distinguished. $CD3^-$ cells were separated into B cells, macrophages, and dendritic cells. B cells were defined as $CD19^+$ cells, macrophages as $F4/80^+$ cells, and DCs as $CD11c^+$ cells. The staining of CD86 determined the activation of $CD3^-$ and microglial cells.

The LGTV infection resulted in an increased frequency of $CD45^+$ cells in the CNS of mice. This is shown in **Figure 11** as an example. $CD45^+$ cells of the cerebrum from uninfected young $Mavs^{-/-}$ mice (D0) were compared to $CD45^+$ cells of the cerebrum from infected young $Mavs^{-/-}$ mice (D6). In the cerebrum of infected young $Mavs^{-/-}$ mice, frequency of $CD45^+$ cells was about 7 %, while in the cerebrum of uninfected young $Mavs^{-/-}$ mice almost no $CD45^+$ cells were evident. Interestingly, these infiltrating $CD45^+$ cells of infected young $Mavs^{-/-}$ mice contained more than 6 % monocytes. The data suggest that LGTV infection increases the infiltration of immune cells, such as lymphocytes and monocytes, into the CNS of mice. Whether aging affects the frequency and composition of specific infiltrating cells during LGTV CNS infection in an MAVS-dependent manner is analyzed in the following sections.

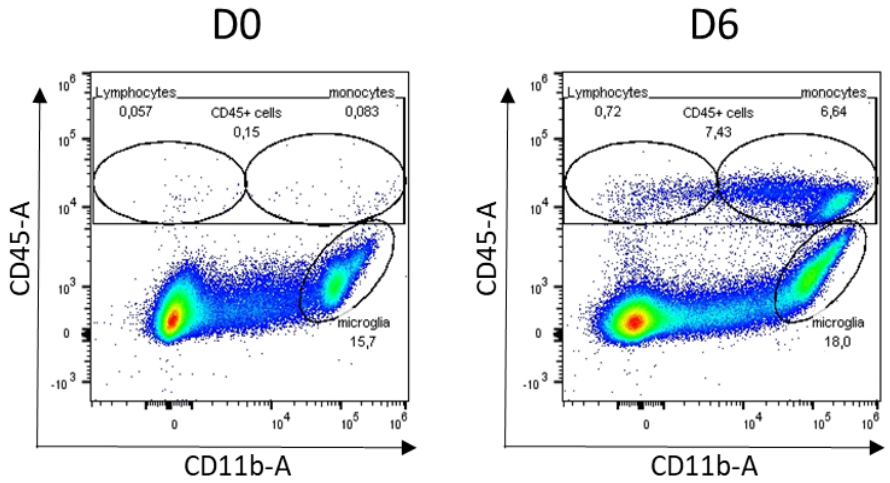

Figure 11: LGTV infection lead to the increased infiltration of immune cells. Infiltrating cells ($CD11b^+$ $CD45^+$) and microglial cells ($CD11b^+$ $CD45^-$) of the cerebrum were shown. Isolated brain cells of uninfected young *Mavs*$^{-/-}$ mice (D0) and LGTV-infected young *Mavs*$^{-/-}$ mice (D6) were compared.

3.3.1. Effect of aging on B cell infiltration and activation

Aging affects the B cell compartment, since the elderly have significantly reduced B cell repertoire and numbers of B cell lineages, resulting in a less efficient response and more severe viral infections [94, 95]. To analyze whether age-related changes in infiltrating B cells could be the reason for the increased susceptibility of aged $Mavs^{-/-}$ mice, the effect of aging on infiltrating B cells frequency and activation in LGTV-infected mice will be investigated using flow cytometry. B cells were characterized as $CD3^-$ $CD19^+$ cells, and their activation status was analyzed by CD86- expression level.

In the cerebrum of WT mice, the frequency of B cells was similar in all age groups; no effect of aging was detectable (**Figure 12A**). In the cerebrum of *Mavs*$^{-/-}$ mice, the frequency of B cells was comparable to WT mice; no effect of aging was evident.
Since not only the cell number but also the activation status of cells could influence the immune response, the activation of infiltrating B cells was determined. In the cerebrum of WT mice, the frequency of activated B cells was very low and the same in all age groups; no effect of aging was detectable (**Figure 12C**). The depletion of MAVS resulted in a significantly increased frequency of B cells in young mice, while the frequency of B cells was similar in adult and old mice. In the cerebrum of Mavs$^{-/-}$ mice, the frequency of B cells was slightly decreased with the age of mice, this decrease was not significant.

In the cerebellum of WT mice, the frequency of B cells was the same in all age groups; no effect of aging was evident (**Figure 12B**). The depletion of MAVS resulted in a significantly increased frequency of B cells in young mice, while the frequency of B cells was similar in adult and old mice. In the cerebellum of Mavs$^{-/-}$ mice, the frequency of B cells was slightly decreased with the age of mice, this decrease was not significant.
The frequency of activated B cells in the cerebellum of WT mice was low in all age groups; no effect of aging was evident (**Figure 12D**). The depletion of MAVS resulted in a significantly increased frequency of activated B cells in young mice, while the frequency of activated B cells was similar in old mice. In the cerebellum of Mavs$^{-/-}$ mice, the frequency of activated B cells was decreased with the age of mice. This decrease was significant between young and old *Mavs*$^{-/-}$ mice.

The data indicate that B cell infiltration into the CNS during LGTV infection is age-independent. However, MAVS may reduce B cell infiltration into the cerebellum as well as activated B cell infiltration into the CNS in an age-dependent manner.

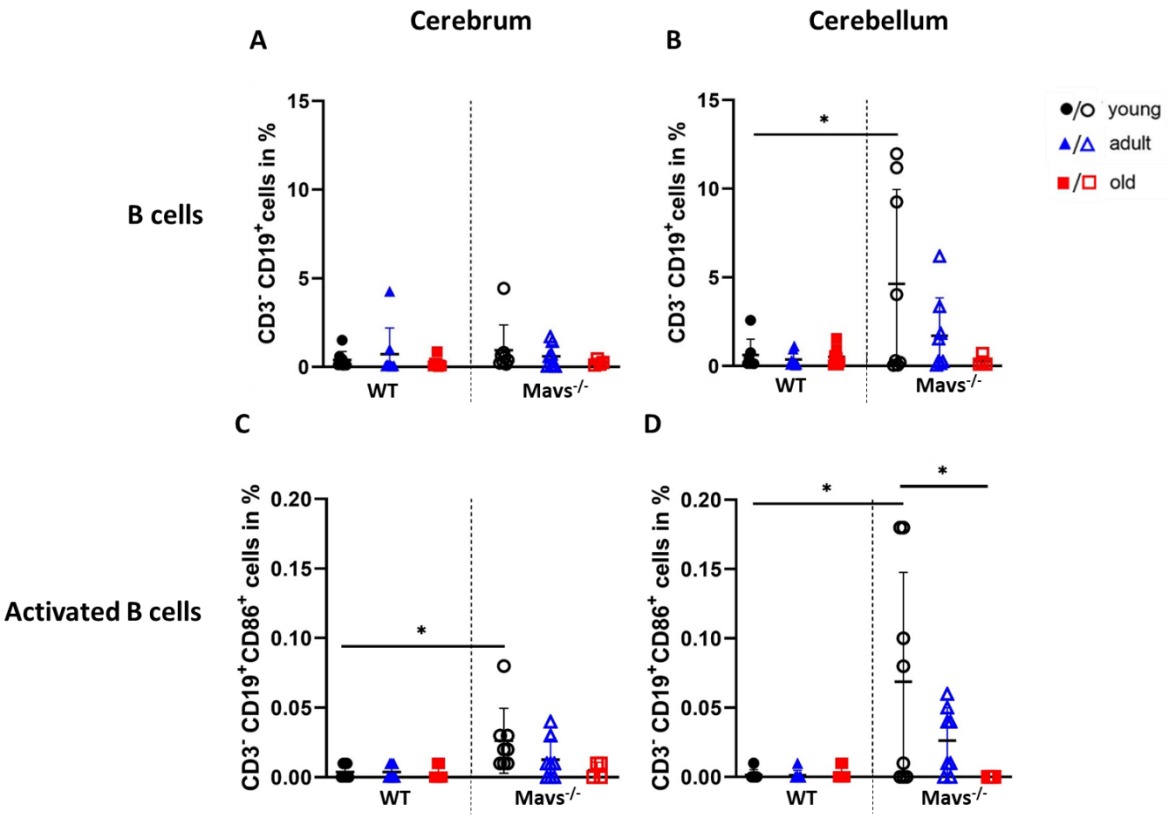

Figure 12: Aging affects B cell infiltration and activation in the CNS in a region- and MAVS-dependent manner. WT and *Mavs*$^{-/-}$ mice of three different ages (young: 2-3 months (n=8); adult: 2- 3 months (n=8); old: 18-24 months (n=8)), were infected intraperitoneal with 10^4 FFU LGTV. Immune cells were isolated at six dpi. The frequency of CD3$^-$ CD19$^+$ B cells in the A: Cerebrum and B: Cerebellum and the frequency of CD3$^-$ CD19$^+$ CD86$^+$ activated B cells in the C: Cerebrum and D: Cerebellum were analyzed by flow cytometry. Differences in the frequency of immune cells were tested for statistical significance using the two-way ANOVA multiple comparison test (p-value: * < 0,05).

3.3.2. Effect of aging on T cell infiltration

Aging affects the T cell compartment, since the elderly have significantly reduced T cell repertoire and numbers of T cell lineages, resulting in a less efficient response and more severe viral infections [53, 54]. To analyze whether age-related changes in infiltrating T cells could be the reason for the increased susceptibility of aged Mavs$^{-/-}$ mice, the effect of aging on the frequency of infiltrating Th cells and CTLs in LGTV-infected mice will be investigated using flow cytometry. Th cells were characterized as CD3$^+$ CD4$^+$ T cells, and CTLs as CD3$^+$ CD8$^+$ T cells.

In the cerebrum of WT mice, the frequency of CTLs was similar in all age groups; no effect of aging was detectable (**Figure 13A**). In the cerebrum of *Mavs*$^{-/-}$ mice, the frequency of CTLs was comparable to WT mice; no effect of aging was detectable.

In the cerebellum of WT mice, the frequency of CTLs was increased with the age of mice, this increase was significant between young and old mice (**Figure 13B**). Young or adult *Mavs*$^{-/-}$ mice had a similar frequency of CTLs in the cerebellum as young WT mice, whereas old Mavs$^{-/-}$ mice had a significantly decreased frequency of CTLs compared to WT mice. In the cerebellum of *Mavs*$^{-/-}$ mice, the frequency of CTLs was similar in all age groups; no effect of aging was detectable.

The data suggest that the infiltration of CTLs into the CNS of LGTV infected mice is age- independent. However, the infiltration of CTLs into the cerebellum of old LGTV-infected mice may be MAVS-dependent.

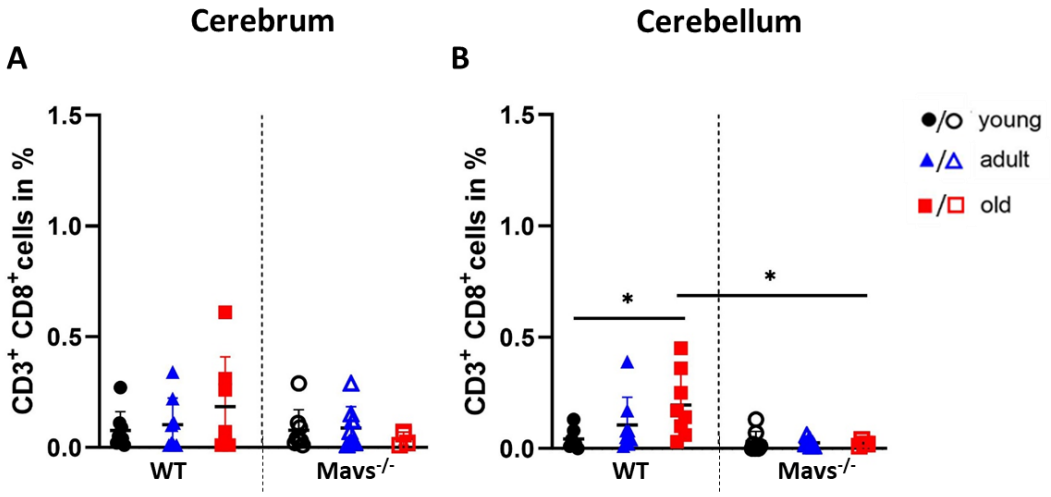

Figure 13: CTL infiltration into the CNS is age-independent. WT and *Mavs*$^{-/-}$ mice of three different ages (young: 2-3 months (n=8); adult: 2-3 months (n=8); old: 18-24 months (n=8)), were infected intraperitoneal with 10^4 FFU LGTV. Immune cells were isolated at six dpi. The frequency of CTLs ($CD3^+$ $CD8^+$ T cells) was analyzed using flow cytometry in the A: Cerebrum and B: Cerebellum. Differences in the frequency of immune cells were tested for statistical significance using the two-way ANOVA multiple comparison test (p-value: * < 0,05).

In the cerebrum of WT mice, the frequency of Th cells was similar in all age groups; no effect of aging was detectable (**Figure 14A**). The depletion of MAVS resulted in an overall slightly increased frequency of Th cells in mice. However, this increase was not significant. In the cerebrum of Mavs$^{-/-}$ mice, the frequency of Th cells was slightly decreased with the age of mice, this decrease was not significant.

In the cerebellum of WT mice, the frequency of Th cells was similar in all age groups; no effect of aging was evident (**Figure 14B**). In the absence of MAVS, the frequency of Th cells was slightly increased in young and adult mice, whereas the frequency of Th cells was slightly decreased in old mice. However, these differences were not significant. In the cerebellum of *Mavs*$^{-/-}$ mice, the frequency of Th cells decreased slightly with the age of mice, this decrease was not significant.

The data indicate that the infiltration of Th cells into the CNS of LGTV infected mice is age- independent.

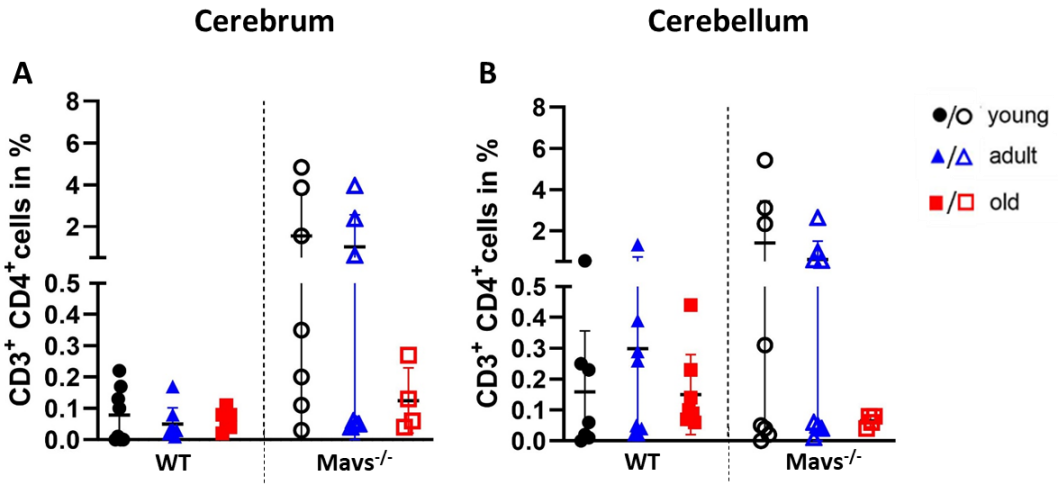

Figure 14: T cell infiltration into the CNS is age-independent. WT and *Mavs*$^{-/-}$ mice of three different ages (young: 2-3 months (n=8); adult: 2-3 months (n=8); old: 18-24 months (n=8)), were infected intraperitoneal with 10^4 FFU LGTV. Immune cells were isolated at six dpi. The frequency of Th cells ($CD3^+$ $CD4^+$ T cells) was analyzed using flow cytometry in the A: Cerebrum and B: Cerebellum.

3.3.3. Effect of aging on the infiltration and activation of dendritic cells

The primary function of dendritic cells (DCs) is the recognition of pathogens and antigen presentation. Thus, DCs can induce the adaptive immune response by the secretion of type I IFNs [95]. Aging could lead to a reduced number and impaired type I IFN production, antigen processing, phagocytosis, and migration of DCs [76, 88, 96]. To analyze whether age-related changes in infiltrating dendritic cells could be the reason for the increased susceptibility of aged Mavs$^{-/-}$ mice, the effect of aging on infiltrating DC frequency and activation in LGTV-infected mice will be investigated using flow cytometry. DCs were characterized as $CD3^-$ $CD11c^+$, and their activation status was analyzed by CD86- expression level.

In the cerebrum of WT mice, the frequency of DCs was similar in all age groups; no effect of aging was evident (**Figure 15A**). In the absence of MAVS, the frequency of DCs was significantly increased in young mice, whereas the frequency of DCs was comparable in adult and old mice. In the cerebrum of Mavs $^{-/-}$ mice, the frequency of DCs was decreased with the age of mice. This decrease was significant between young and adult *Mavs*$^{-/-}$ mice as well as between young and old *Mavs*$^{-/-}$ mice.
Since not only the cell number but also the activation status of cells could influence the immune response, the activation of infiltrating DCs was determined. In the cerebrum of WT mice, the frequency of activated DCs was very low in all age groups; no effect of aging was detected (**Figure 15C**). In the absence of MAVS, the frequency of activated DCs was significantly increased in young mice, while the frequency of activated DCs was similar in adult or old mice. In the cerebrum of *Mavs*$^{-/-}$ mice, the frequency of activated DCs was decreased with the age of the mice; this decrease was significant between young and adult as well as between young and old mice.

In the cerebellum of WT mice, the frequency of DCs was low in all age groups; no effect of aging was evident (**Figure 15B**). In the absence of MAVS, the frequency of DCs was slightly increased in young and adult mice; this increase was not significant. In the cerebellum of *Mavs*$^{-/-}$ mice, the frequency of DCs was decreased with the age of the mice; this decrease was significant between young and old mice.
The frequency of activated DCs in the cerebellum of WT mice was very low in all age groups; no effect of aging was detected (**Figure 15D**). In the absence of MAVS, the frequency of activated DCs was significantly increased in young mice, while the frequency of activated DCs was similar in adult and old mice. In the cerebellum of *Mavs*$^{-/-}$ mice, the frequency of activated DCs was decreased with the age of mice. This decrease was significant between young and adult *Mavs*$^{-/-}$ mice as well as between young and old *Mavs*$^{-/-}$ mice.

The data indicate that the infiltration and activation of DCs is age- dependent during LGTV infection in the CNS of mice. Further, MAVS reduces the infiltration and activation of DCs in an age-dependent manner.

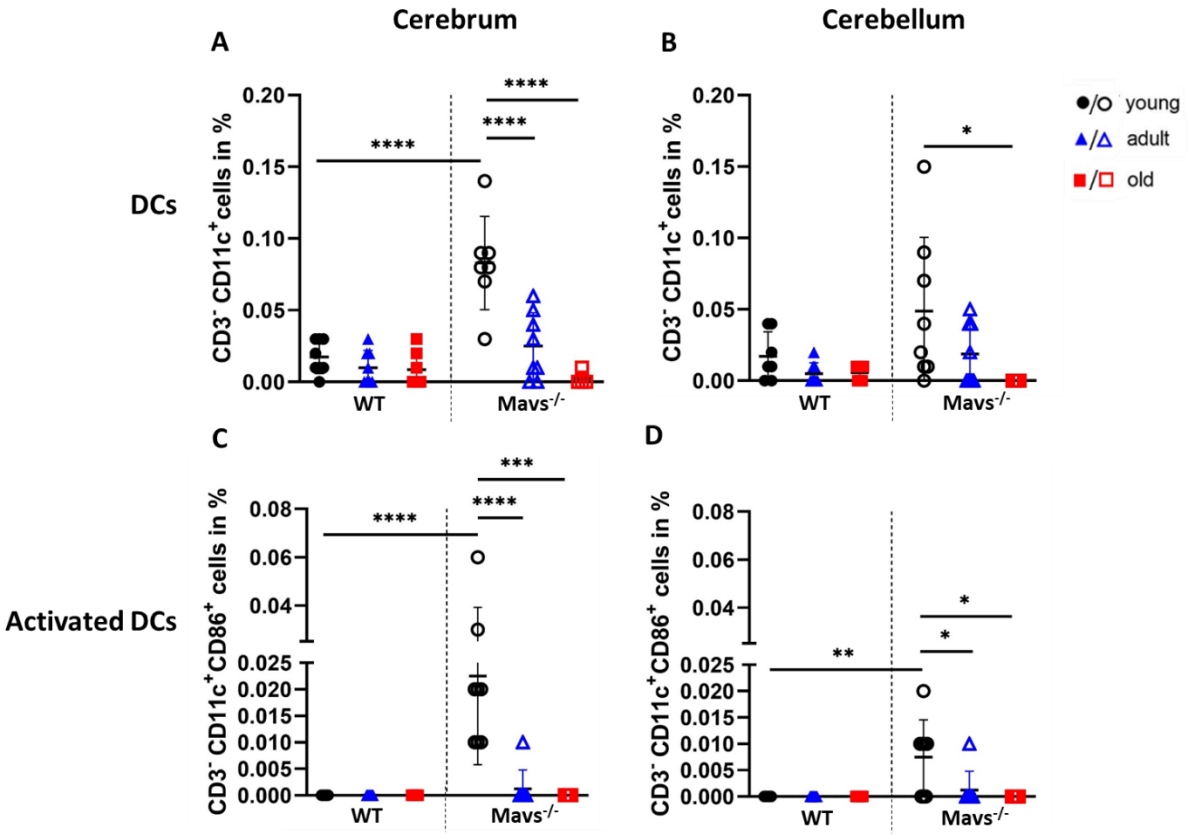

Figure 15: Aging influences DC infiltration and activation in the CNS in a MAVS-dependent manner. WT and *Mavs*$^{-/-}$ mice of three different ages (young: 2-3 months (n=8); adult: 2-3 months (n=8); old: 18- 24 months (n=8)), were infected intraperitoneal with 10^4 FFU LGTV. Immune cells were isolated at six dpi. The frequency of CD3$^-$ CD11c$^+$ DCs in the A: Cerebrum and B: Cerebellum and the frequency of CD3$^-$ CD11c$^+$ CD86$^+$ activated DCs in the C: Cerebrum and D: Cerebellum were analyzed by flow cytometry. Differences in the frequency of immune cells were tested for statistical significance using the two-way ANOVA multiple comparison test (p-value: * < 0,05; ** < 0,01; *** < 0,001; **** < 0,0001).

3.3.4. Effect of aging on the infiltration and activation of macrophages

Macrophages have a central role in maintaining tissue homeostasis and organizing the immune response. Aging lead to an impaired function of macrophages, such as reduced cytotoxicity, intracellular killing, motility, type I IFN production, and antigen presentation. These age-related changes in resident macrophages seem to contribute to the increased morbidity and mortality in infections [76, 88, 97]. To analyze whether age-related changes in infiltrating macrophages could be the reason for the increased susceptibility of aged Mavs$^{-/-}$ mice, the effects of aging on infiltrating macrophages' frequency and activation in LGTV-infected mice will be investigated using flow cytometry. Macrophages were characterized as CD3$^-$ F4/80$^+$, and their activation status was analyzed by CD86-expression level.

In the cerebrum of WT mice, the frequency of macrophages was low in all age groups; no effect of aging was detectable (**Figure 16A**). In the absence of MAVS, the frequency of macrophages was increased in young and adult mice, with a significant difference in young mice. Old *Mavs*$^{-/-}$ mice had a similar frequency of macrophages as WT mice. In the cerebrum of *Mavs*$^{-/-}$ mice, the frequency of macrophages was significantly decreased with the age of the mice; this decrease was significant between young and old mice.

Since not only the cell number but also the activation status of cells could influence the immune response, the activation of infiltrating macrophages cells was determined. In the cerebrum of WT mice, the frequency of activated macrophages was very low in all age groups; no effect of aging was detectable (**Figure 16C**). The depletion of MAVS resulted in a significantly increased frequency of activated macrophages in young mice. In the cerebrum of *Mavs*$^{-/-}$ mice, the frequency of activated macrophages was significantly decreased with the age of mice; this decrease was significant between young and old mice.

In the cerebellum of WT mice, the frequency of macrophages was similar in all age groups; no effect of aging was visible (**Figure 16B**). In the cerebellum of *Mavs*$^{-/-}$, the frequency of macrophages was similar to WT mice; no effect of aging was detectable.

The frequency of activated macrophages in the cerebellum WT mice was similar in all age groups; no effect of aging was detected (**Figure 16D**). In the cerebellum of *Mavs*$^{-/-}$, the frequency of activated macrophages was similar to WT mice; no effect of aging was detectable.

The data suggest that the infiltration of macrophages into the cerebrum of LGTV infected mice is age- and MAVS-dependent. Further, MAVS reduces the infiltration of activated macrophages into the cerebrum of LGTV infected mice in an age-dependent manner. In contrast, the infiltration and activation of macrophages in the cerebellum of LGTV-infected mice is independent of age.

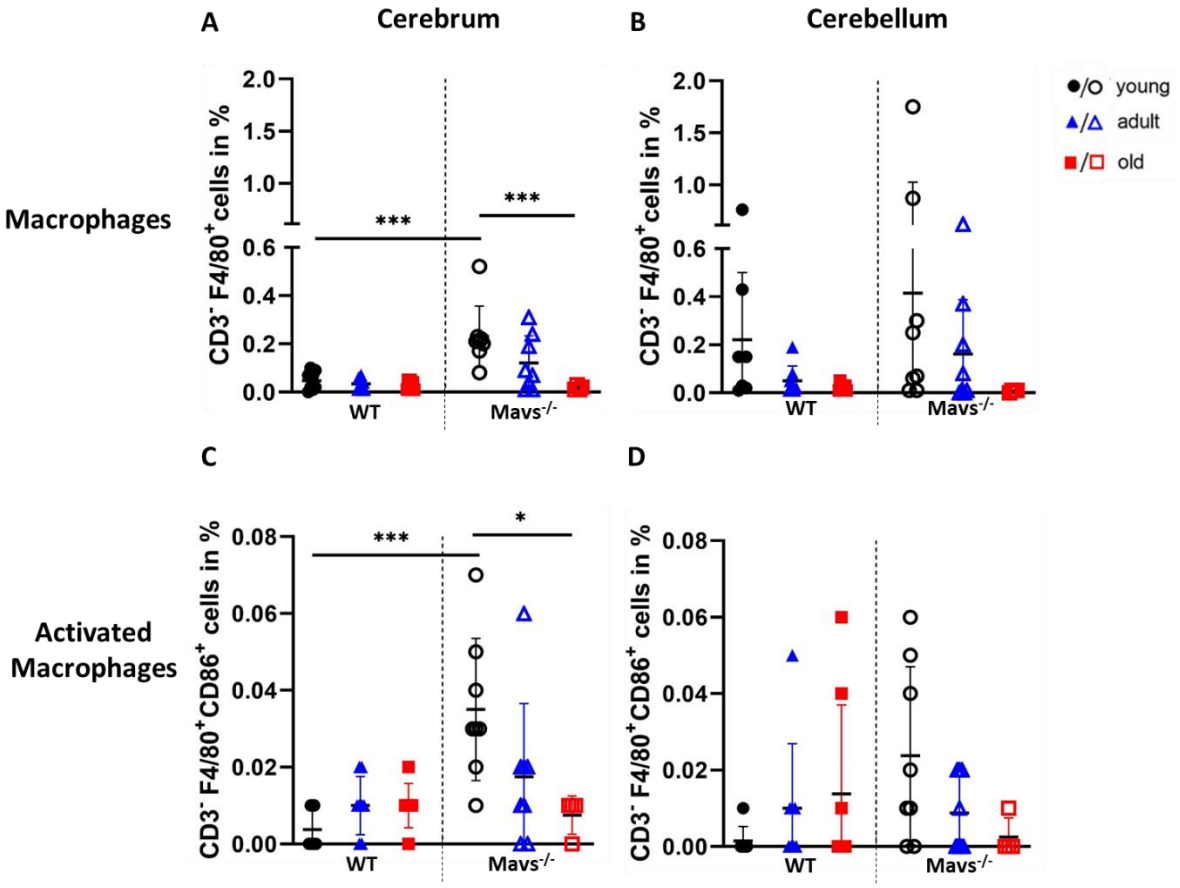

Figure 16: Aging affects infiltration and activation of macrophages in the CNS in a region- and MAVS-specific manner. WT and *Mavs*$^{-/-}$ mice of three different ages (young: 2-3 months (n=8); adult: 2- 3 months (n=8); old: 18-24 months (n=8)), were infected intraperitoneal with 10^4 FFU LGTV. Immune cells were isolated at six dpi. The frequency of CD3$^-$ F4/80$^+$ macrophages in the A: Cerebrum and B: Cerebellum and the frequency of CD3$^-$ F4/80$^+$ CD86$^+$ activated macrophages in the C: Cerebrum and D: Cerebellum were analyzed by flow cytometry. Differences in the frequency of immune cells were tested for statistical significance using the two-way ANOVA multiple comparison test (p-value: * < 0,05; *** < 0,001).

3.3.5. Effect of aging on the frequency and activation of microglia

Microglial cells have a central role in maintaining tissue homeostasis and organizing immune responses in the brain [98-100]. Aging lead to chronic impaired activation, resulting in a reduced type I IFN production, and a decreased phagocytosis of microglia [48, 87]. This loss in function can determine the severity of viral infections. To analyze whether age-related changes in microglia could be the reason for the increased susceptibility of old Mavs$^{-/-}$ mice, the effects of aging on microglia frequency and activation in LGTV-infected mice will be investigated using flow cytometry. Microglia cells were characterized as CD45$^-$ CD11b$^+$ cells, and their activation status was analyzed by CD86-expression level.

In the cerebrum of WT mice, the frequency of microglia was similar in all age groups; no effect of aging was detectable (**Figure 17A**). In the cerebrum of *Mavs*$^{-/-}$ mice, the frequency of microglia was similar to WT mice; no effect of aging was evident.

Since not only the cell number but also the activation status of cells could influence the immune response, the activation of microglia was determined. In the cerebrum of WT mice, frequency of activated microglia was very low in young mice (**Figure 17C**). Adult or old WT mice had a highly significantly increased frequency of microglia compared to young WT mice. Further, adult WT mice had an increased frequency of microglia compared to old WT mice. In the absence of MAVS, the frequency of activated microglia was similar in young mice, whereas the frequency of activated microglia was decreased in adult and old mice with a significant difference in adult mice. In the cerebrum of *Mavs*$^{-/-}$ mice, the frequency of activated microglia was increased with the age of mice. This increase was significant between young and adult *Mavs*$^{-/-}$ mice as well as between young and old *Mavs*$^{-/-}$ mice.

In the cerebellum of WT mice, the frequency of microglia was decreased with the age the mice, this decrease was significant between young and adult as well as between young and old mice (**Figure 17B**). Young WT mice had a significantly increased frequency of microglia in the cerebellum compared to Mavs$^{-/-}$ mice, whereas adult and old WT mice had a similarly low frequency of microglia as Mavs$^{-/-}$ mice. In the cerebellum of Mavs$^{-/-}$ mice, the frequency of microglia was low in all age groups; no effect of aging was evident.

The frequency of activated microglia in the cerebellum of WT mice was very low in young mice, but significantly increased with the age of the mice (**Figure 17D)**. The depletion of MAVS resulted in a significantly decreased frequency of activated microglia in adult mice, whereas the frequency of activated microglia was similar in young and old mice. In the cerebellum of *Mavs*$^{-/-}$ mice, the frequency of activated microglia was slightly increased with the age of the mice. However, no significant differences were detected.

The data suggest that the frequency of microglia in the cerebellum of LGTV infected mice is age- and MAVS-dependent. Interestingly, the frequency of microglia in the cerebrum is age and MAVS-independent. Further, MAVS supports the activation of microglia in the CNS of LGTV-infected mice in an age-dependent manner.

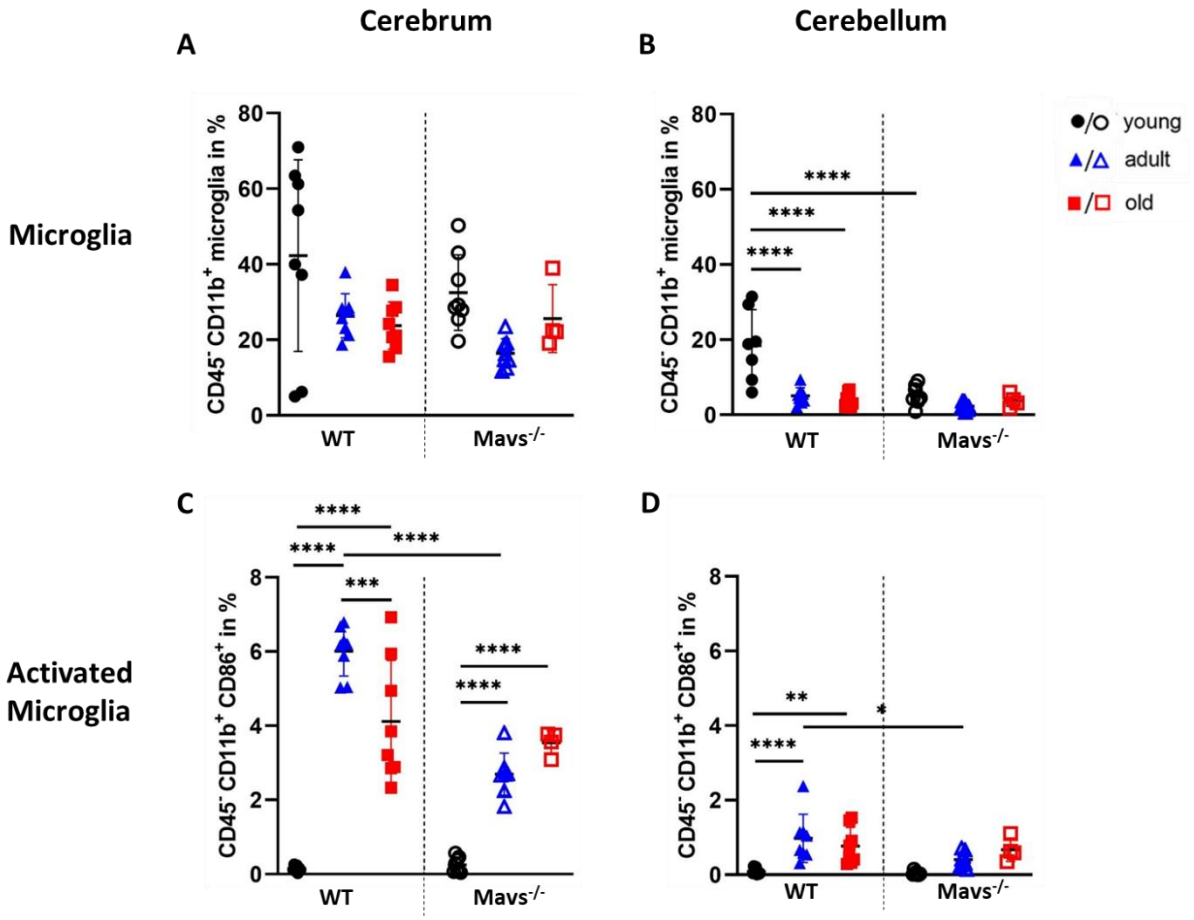

Figure 17: Aging affects frequency and activation of microglia are in a MAVS- and region-specific manner. WT and *Mavs*$^{-/-}$ mice of three different ages (young: 2-3 months (n=8); adult: 2-3 months (n=8); old: 18-24 months (n=8)), were infected intraperitoneal with 10^4 FFU LGTV. Immune cells were isolated at six dpi. The frequency of CD45$^-$ CD11b$^+$ microglia in the A: Cerebrum and B: Cerebellum and the frequency of CD45$^-$ CD11b$^+$ CD86$^+$ activated microglia in the C: Cerebrum and D: Cerebellum were analyzed by flow cytometry. Differences in the frequency of immune cells were tested for statistical significance using the two-way ANOVA multiple comparison test (p-value: * < 0,05; ** < 0,01; *** < 0,001; **** < 0,0001).

3.4. MAVS-dependent antiviral response is age- and region-specific

The local antiviral response in the CNS is critical for inhibiting the viral replication of neurotropic viruses. This response is differently regulated at several levels. Both, specific cell types and subpopulations of cell types can determine the antiviral response [101]. Additionally, the antiviral immune response in the CNS is regulated region-specific [41].

To investigate whether aging influences the function of MAVS in a region-specific manner during CNS infection, WT and *Mavs*$^{-/-}$ mice of different ages were infected systemically by intraperitoneal LGTV injection. Brains were isolated at six dpi and fixed. Specific brain regions, such as the olfactory bulb (**Figure 18**), cerebrum (**Figure 19**), choroid plexus (**Figure 20**), and cerebellum (**Figure 21**) were analyzed by immunohistochemistry. Sagittal sections of the brains of LGTV-infected WT and *Mavs*$^{-/-}$ mice of different ages were examined for LGTV non-structural protein 3 (NS3), infiltrating immune cells (CD45), neurons (NeuN), and cell nuclei (DAPI). The quantification of NS3^{+} and CD45^{+} cells from three independent experiments is visualized in graphs.

Immunohistological analyses of the olfactory bulb showed no detection of NS3^{+} cells (green) in WT mice of all age groups (**Figure 18A**). The depletion of MAVS resulted in detecting many NS3^{+} cells in the olfactory bulb of mice, but the quantification of NS3^{+} cells showed no age-related differences in Mavs$^{-/-}$ mice (**Figure 18B**).
CD45^{+} cells were detectable in the olfactory bulb of WT mice independent of the age of the mice, but the quantification showed no age-related differences (**Figure 18C**). The depletion of MAVS resulted in detecting many CD45^{+} cells in the olfactory bulb of mice. The quantification of CD45^{+} cells in *Mavs*$^{-/-}$ mice showed a decrease with the age of the mice, this decrease was significant between young and adult as well as between young and old mice.

The data indicate that MAVS is crucial in controlling viral replication in the olfactory bulb of mice independent of age. Furthermore, LGTV infection in the absence of MAVS leads to the increased infiltration of immune cells into the olfactory bulb in an age-dependent manner.

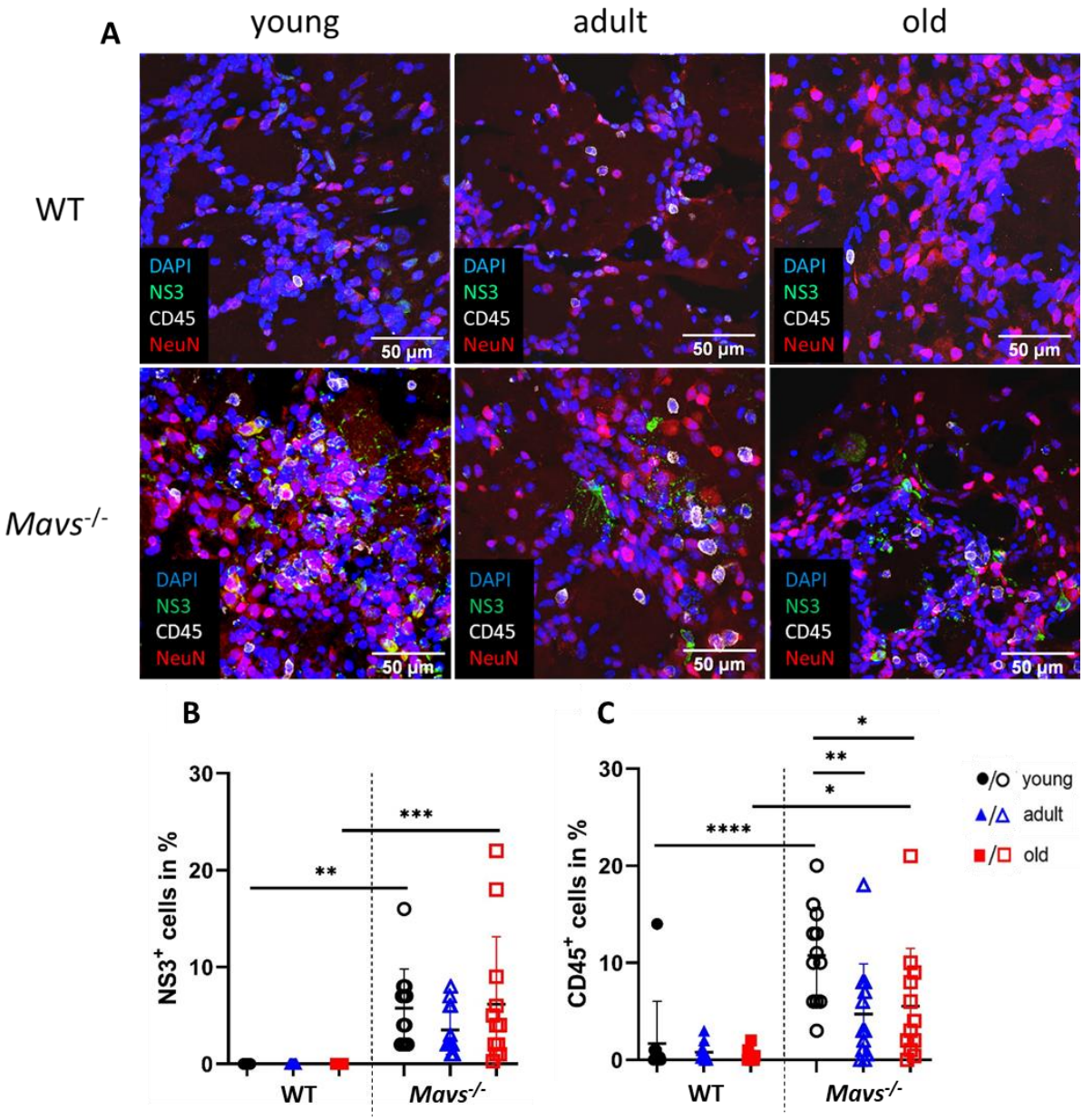

Figure 18: MAVS affects immune cell infiltration into the olfactory bulb in an age-specific manner. WT and *Mavs*$^{-/-}$ mice of three different ages (young: 2-3 months (n=10); adult: 10-12 months (n=10); old: 18- 24 months (n=10)), were infected intraperitoneal with 10^4 FFU LGTV. Brains were isolated at six dpi, fixed, and analyzed by immunohistochemistry. A: The staining of the NS3 protein of LGTV (green), infiltrating CD45$^+$ immune cells (white), nucleus-staining (DAPI, blue), and NeuN$^+$ neurons (red) in WT and *Mavs*$^{-/-}$ mice are shown. Stained cells were count by ImageJ. The quantifications of B: NS3$^+$cells and C: CD45$^+$ cells are shown. Differences in the frequency of NS3$^+$ and CD45$^+$ cells were tested for statistical significance using the two-way ANOVA multiple comparison test (p-value: * <0,05; ** < 0,01; *** < 0,001; **** < 0,0001).

Immunohistological analyses of the cerebrum showed no detection of $NS3^+$ cells in WT mice of all age groups (**Figure 19A**). The depletion of MAVS resulting in the detection of $NS3^+$ cells in in the cerebrum of mice. The quantification of $NS3^+$ cells in *Mavs*$^{-/-}$ mice showed a decrease with the age of the mice, this decrease was significant between young and old mice (**Figure 19B**). Almost no $CD45^+$ cells were detectable in the cerebrum of WT mice. Although, the quantification showed a few $CD45^+$ cells in the cerebrum of adult WT mice, no age-related differences were detected (**Figure 19C**). The depletion of MAVS led to an increase in $CD45^+$ cells in the cerebrum of young mice. The quantification of $CD45^+$ cells in *Mavs*$^{-/-}$ mice showed a significant decrease in adult mice compared to young mice, whereas no significant difference was detected between young and old mice.

The data suggest that MAVS is important in controlling viral replication in the cerebrum of mice in an age-dependent manner. Further, LGTV infection in the absence of MAVS leads to the infiltration of immune cells into the cerebrum in an age-dependent manner.

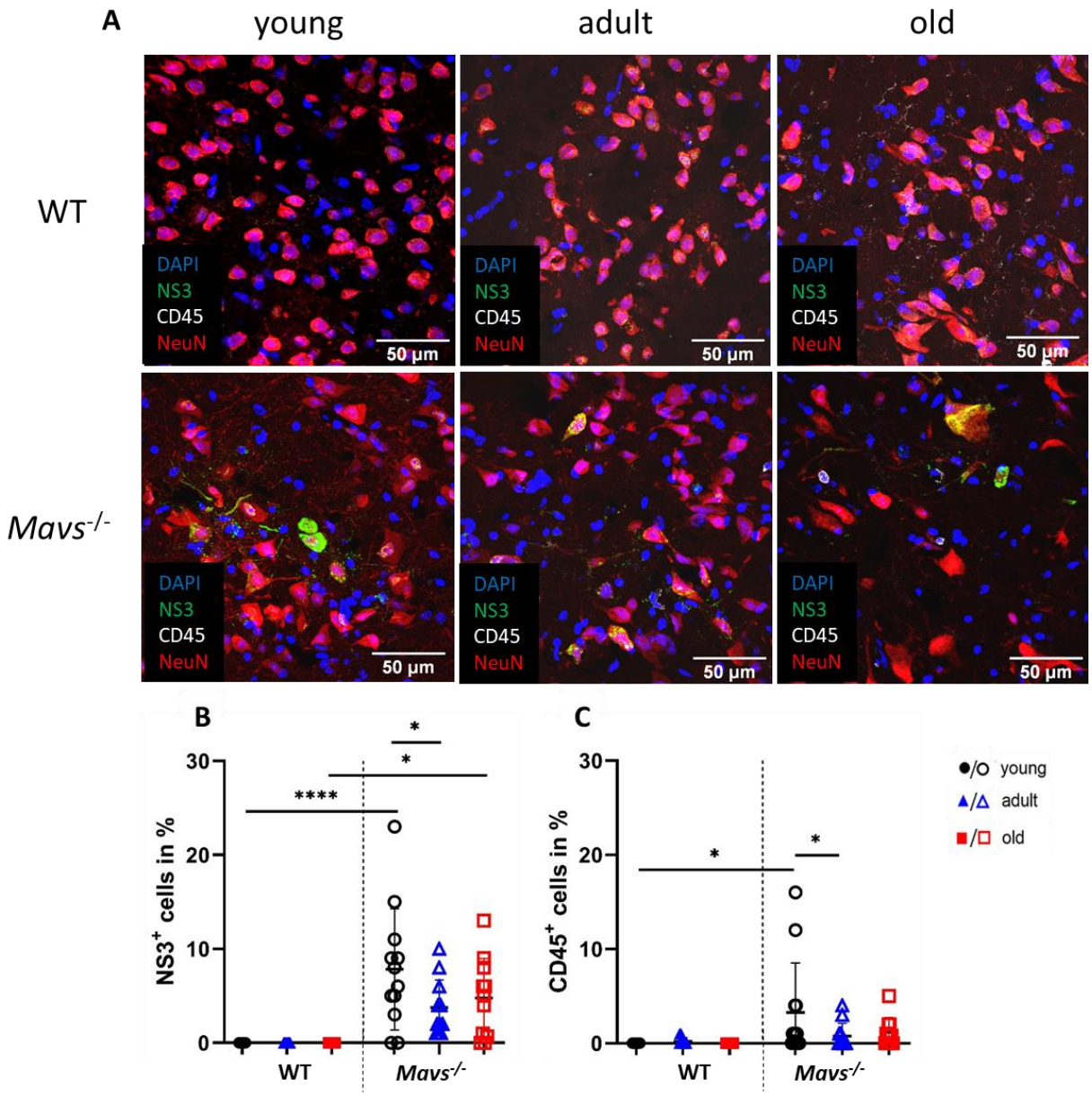

Figure 19: MAVS influences LGTV replication and immune cell infiltration in the cerebrum in an age-specific manner. WT and *Mavs*$^{-/-}$ mice of three different ages (young: 2-3 months (n=10); adult: 10- 12 months (n=10); old: 18-24 months (n=10)), were infected intraperitoneal with 10^4 FFU LGTV. Brains were isolated at six dpi, fixed, and analyzed by immunohistochemistry. A: The staining of the NS3 protein of LGTV (green), infiltrating CD45$^+$ immune cells (white), nucleus-staining (DAPI, blue), and NeuN$^+$ neurons (red) in WT and *Mavs*$^{-/-}$ mice are shown. Stained cells were counted by ImageJ. The quantifications of B: NS3$^+$cells and C: CD45$^+$ cells are shown. Differences in the frequency of NS3$^+$ and CD45$^+$ cells were tested for statistical significance using the two-way ANOVA multiple comparison test (p-value: * <0,05; **** < 0,0001).

The epithelium of the choroid plexus can produce chemokines and cytokines, leading to the recruitment of immune cells. For this reason, the choroid plexus is described as a gateway for the transport of immune cells between CSF and the brain. Immunohistological analyses of the choroid plexus showed no detection of $NS3^+$ cells in WT mice of all age groups (**Figure 20A**). In contrast, the quantification of $NS3^+$ cells in the choroid plexus of *Mavs*$^{-/-}$ mice showed significant age-related differences. While in young *Mavs*$^{-/-}$ mice no $NS3^+$ cells were detected, in adult and old *Mavs*$^{-/-}$ mice many $NS3^+$ cells were detected (**Figure 20B**).
$CD45^+$ cells were detected in the choroid plexus of WT mice of all age groups with no significant differences (**Figure 20C**). The frequency of $CD45^+$ cells in the choroid plexus of *Mavs*$^{-/-}$ mice decreased with the age of the mice, this decrease was significant between young and adult as well as between young and old mice.

The data reveal that MAVS has an important impact to control viral replication in the choroid plexus in an age-dependent manner. Furthermore, the depletion of MAVS increases immune cell infiltration into the choroid plexus in an age-dependent manner.

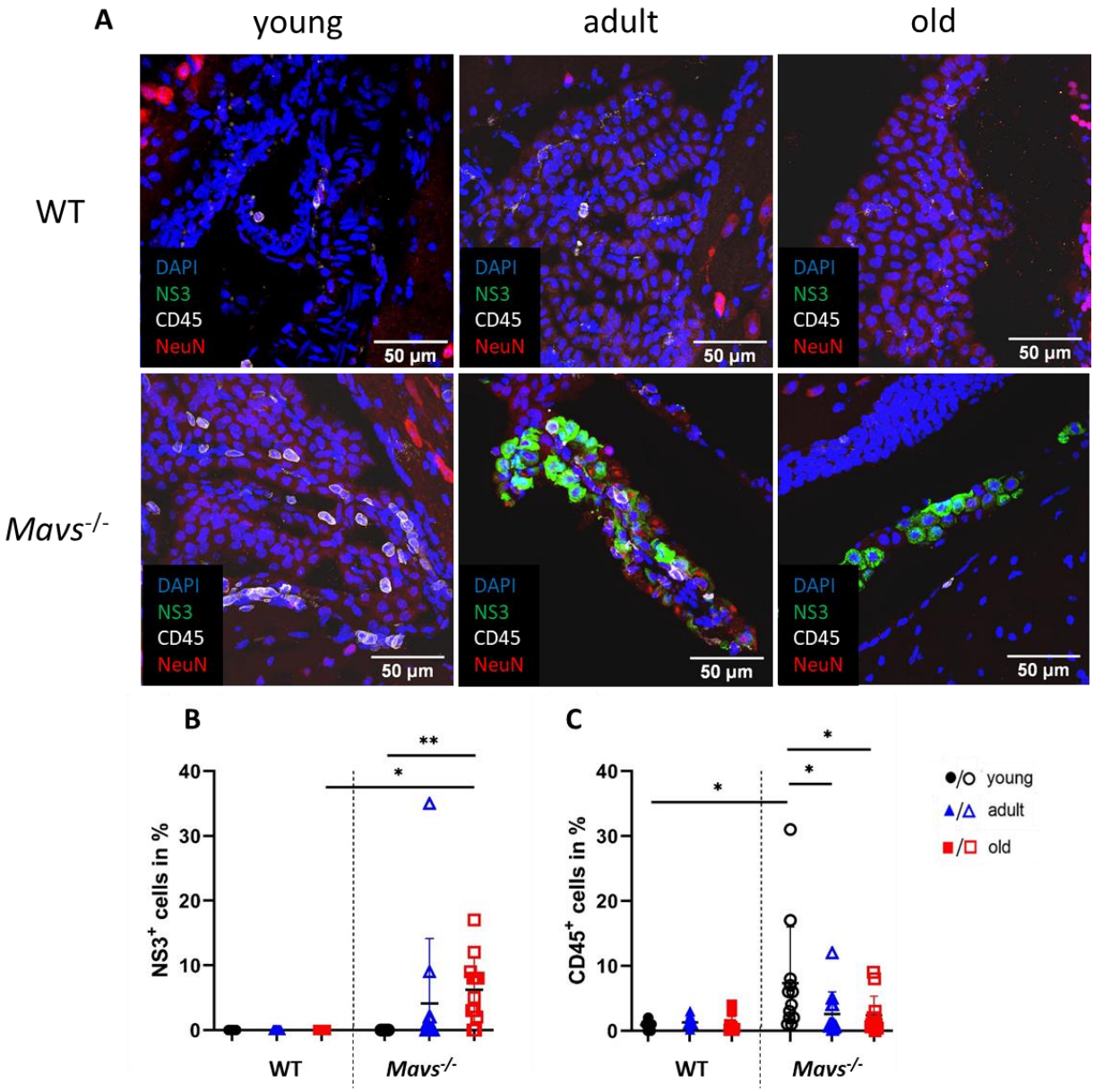

Figure 20: MAVS regulates LGTV replication and immune cell infiltration in the choroid plexus age-specific. WT and *Mavs*$^{-/-}$ mice of three different ages (young: 2-3 months (n=10); adult: 10-12 months (n=10); old: 18-24 months (n=10)), were infected intraperitoneal with 10^4 FFU LGTV. Brains were isolated at six dpi, fixed, and analyzed by immunohistochemistry. A: The staining of the NS3 protein of LGTV (green), infiltrating CD45$^+$ immune cells (white), nucleus-staining (DAPI, blue), and NeuN$^+$ neurons (red) in WT and *Mavs*$^{-/-}$ mice are shown. Stained cells were counted by ImageJ. The quantifications of B: NS3$^+$cells and C: CD45$^+$ cells are shown. Differences in the frequency of infected cells were tested for statistical significance using the two-way ANOVA multiple comparison test (p- value: * < 0,005; ** <0,01).

Immunohistological analyses of the cerebellum showed no detection of $NS3^+$ cells in WT mice of all age groups (**Figure 21A**). The same was demonstrated in the cerebellum of adult and old *Mavs*$^{-/-}$ mice. In contrast, many $NS3^+$ cells were detected in the cerebellum of young *Mavs*$^{-/-}$ mice, with a significant increase in young *Mavs*$^{-/-}$ mice compared to WT mice (**Figure 21B**).
No $CD45^+$ cells were detected in the cerebellum of WT mice of all age groups (**Figure 21C**). The same was demonstrated in the cerebellum of adult and old *Mavs*$^{-/-}$ mice. In contrast, many $CD45^+$ cells were detected in young *Mavs*$^{-/-}$ mice, with a significant increase in young *Mavs*$^{-/-}$ mice compared to young WT mice.

The data indicate that MAVS play a crucial role in controlling viral replication in the cerebellum of mice in an age-dependent manner. Further, the depletion of MAVS increases the infiltration of immune cells in an age-dependent manner.

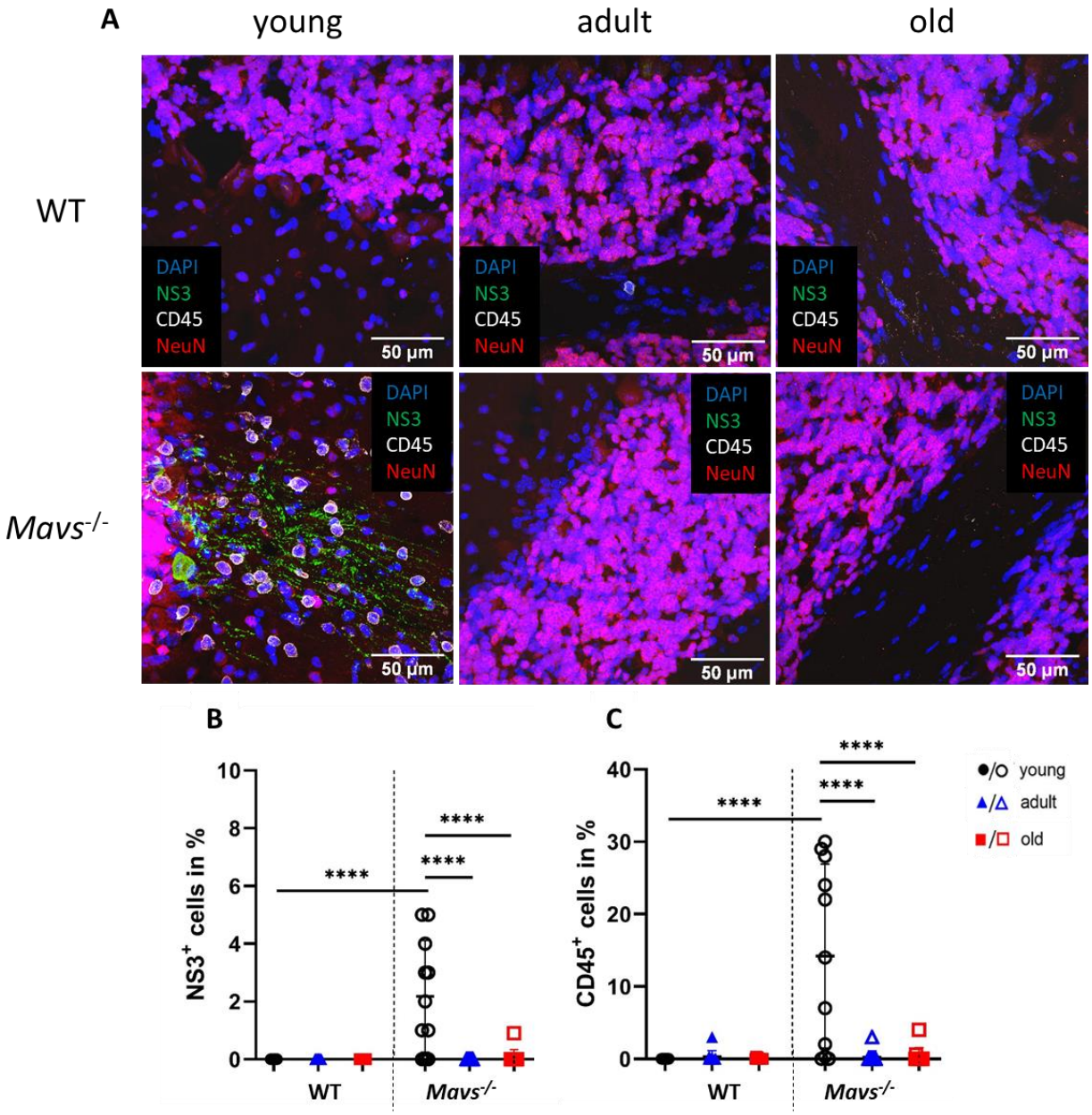

Figure 21: MAVS regulated LGTV replication and immune cell infiltration age-specific. WT and *Mavs*$^{-/-}$ mice of three different ages (young: 2-3 months (n=10); adult: 10-12 months (n=10); old: 18-24 months (n=10)), were infected intraperitoneal with 10^4 FFU LGTV. Brains were isolated at six dpi, fixed, and analyzed by immunohistochemistry. A: The staining of the NS3 protein of LGTV (green), infiltrating CD45$^+$ immune cells (white), nucleus-staining (DAPI, blue), and NeuN$^+$ neurons (red) in WT and *Mavs*$^{-/-}$ mice are shown. Stained cells were counted by ImageJ. The quantifications of B: NS3$^+$cells and C: CD45$^+$ cells are shown. Differences in the frequency of infected cells were tested for statistical significance using the two-way ANOVA multiple comparison test (p-value: **** <0,0001).

3.5. MAVS controls viral replication in the CNS

Immunohistological analysis has limited sensitivity to show the distribution of infected cells, Therefore, qRT-PCR analysis was performed to determine the viral load in the different brain regions (**Figure 22)**.

In the olfactory bulb of WT, the viral load mice was low with no influence of the age of the mice (**Figure 22A**). The depletion of MAVS led to an overall increased viral load, independent of the age of the mice. Interestingly, young *Mavs*$^{-/-}$ mice showed the highest viral load, which decreased significantly with the age of the mice.

In the cerebrum of WT, the viral load mice was low with no influence of the age of the mice (**Figure 22B**), similar to the viral load in the olfactory bulb of WT mice. In the absence of MAVS, the viral load was significantly increased in young mice. In the cerebrum of *Mavs*$^{-/-}$ mice, the viral load decreased with the age of the mice, this decrease was significant between young and adult as well as between young and old mice.

In the cerebellum of WT mice, the viral load was low independent of the age of the mice (**Figure 22C**), comparable to the viral load in the olfactory bulb and cerebrum of WT mice. The depletion of MAVS resulted in an increased viral load in mice. While the viral load was very high in young *Mavs*$^{-/-}$ mice compared to WT mice, the viral load in adult and old *Mavs*$^{-/-}$ mice was slightly increased compared to WT mice. In the cerebellum of *Mavs*$^{-/-}$ mice, an effect of age on the viral load was demonstrated. The highest viral load was detected in young *Mavs*$^{-/-}$ mice, which decreased significantly with the age of the mice.

Although, old *Mavs*$^{-/-}$ mice succumbed to LGTV infection while old WT mice survived, the viral load in the cerebellum of old *Mavs*$^{-/-}$ mice was very similar to WT mice. Adult *Mavs*$^{-/-}$ mice succumbed to LGTV infection while adult WT mice survived, however the viral load in the cerebellum of adult *Mavs*$^{-/-}$ mice was very similar to WT mice.

The data suggest that the antiviral effect of MAVS is age and region-specific. Furthermore, MAVS plays a critical role in inhibiting viral replication of LGTV. However, the data indicate that virus replication may not be the key factor in the death of mice. Young *Mavs*$^{-/-}$ mice survived the infection better than adult and old mice, despite having a low viral load in specific brain regions.

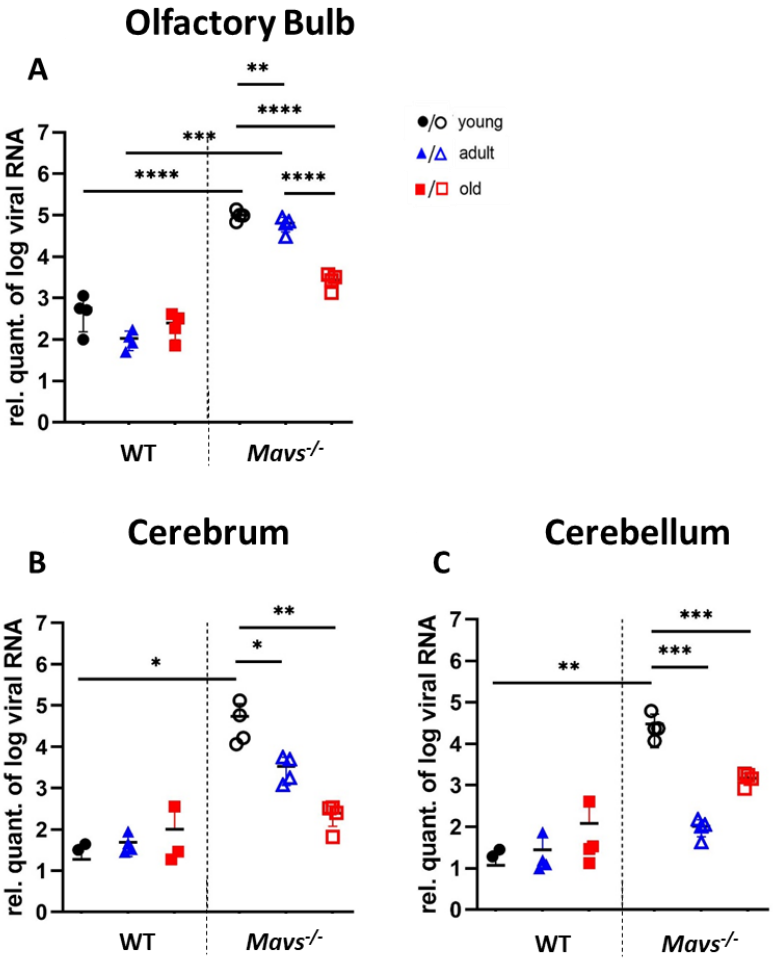

Figure 22: The antiviral effect of MAVS is age- and region-specific. WT and *Mavs*$^{-/-}$ mice of three different ages (young: 2-3 months (n=10); adult: 10-12 months (n=10); old: 18-24 months (n=10)), were infected intraperitoneal with 10^4 FFU LGTV. Viral RNA were determined using qRT-PCR and normalized to the expression of β-actin at six dpi. A: olfactory bulb, B: cerebrum, C: choroid plexus, and D: cerebellum. Differences in the expression of viral RNA were tested for statistical significance using the two-way ANOVA multiple comparison test (p-value: * < 0,05; ** < 0,01; *** < 0,001; **** < 0,0001).

3.6. Antiviral interferon activity is regulated age- and region-specifically

IFNs play an essential role in controlling neuroinflammation caused by neurotropic flaviviruses. IFNs, such as IFNβ and IFNγ, activate the Jak/STAT-signaling pathway resulting in the expression of ISGs. Several studies have shown that aging leads to the alteration of IFNAR-signaling and, thus, increased susceptibility to viral infections [102-104]. Here, the antiviral response may depend on the localization of the virus but also the cell type-specific expression of IFNs and ISGs in different brain regions [105].

3.6.1. IFNβ-/IFNγ-expression is age- and region-specifically regulated

IFNβ has antiviral, antiproliferative, and immunomodulatory effects [106]. It can reduce the number of inflammatory cells in the brain and thus ensure the preservation of neurons [107].

IFNγ has antiviral and immunomodulatory properties and is mainly expressed by NK cells, Th cells and CTLs. In order to investigate whether aging alone has an influence on the expression of IFNs, endogenous IFN-expression levels in young, adult and old naïve WT and *Mavs*$^{-/-}$ mice were determined by qRT-PCR. Further, to investigate whether aging affects the antiviral activity in specific brain regions during infection, LGTV-induced IFN-expression levels were determined. Therefore, WT and *Mavs*$^{-/-}$ mice of different ages were infected systemically by intraperitoneal LGTV injection. Brains of infected mice were isolated at six dpi.

Analysis of the endogenous IFNβ-expression in the olfactory bulb of WT mice showed similarly low expression levels that were independent of the age of the mice (**Figure 23, D0**). In the olfactory bulb, the depletion of MAVS did not lead to significant differences in the endogenous IFNβ-expression levels, independent of the age of the mice.
In the cerebrum of WT mice, the endogenous IFNβ-expression levels were similarly low, independent of the age of the mice. The depletion of MAVS led to significantly increased endogenous IFNβ-expression levels in mice, independent of the age of the mice.
In the cerebellum of WT mice, the endogenous IFNβ-expression levels were similarly low, independent of the age of the mice. The depletion of MAVS led to significantly increased endogenous IFNβ-expression levels in young mice, while the depletion of MAVS did not influence the endogenous IFNβ-expression levels in old mice. In the cerebellum of *Mavs*$^{-/-}$ mice, the endogenous IFNβ-expression levels were slightly decreased in old mice compared to young or adult mice. However, this decrease was not significant.
The data indicate that aging had no significant impact on the endogenous expression of IFNβ in the analyzed brain regions. Nevertheless, the endogenous IFNβ-expression in the cerebrum and cerebellum of mice appear to be MAVS-dependent. This effect does not seem to play a major role for the increased susceptibility of aged *Mavs*$^{-/-}$ mice, since no significant age-related differences are evident.

The LGTV-induced expression levels of IFNβ were analyzed after six dpi in the olfactory bulb, cerebrum, and cerebellum of mice (**Figure 23, D6**). In the olfactory bulb of WT mice, LGTV infection did not lead to an induction of IFNβ-expression in mice, independent of the age of the mice. The depletion of MAVS resulted in significantly increased IFNβ-expression levels in young and adult mice. In the olfactory bulb of *Mavs*$^{-/-}$ mice, the IFNβ-expression levels decreased significantly with the age of the mice. LGTV infection did not lead to induction of IFNβ- expression in old *Mavs*$^{-/-}$ mice.
In the cerebrum of WT, LGTV infection did not lead to an induction of IFNβ-expression in mice, independent of the age of the mice. While in the absence of MAVS, the IFNβ-expression levels were increased in mice, with a highly significant difference in young mice. In the cerebrum of

Mavs$^{-/-}$ mice, the IFNβ-expression levels were decreased with the age of the mice, this decrease was significant between young and adult as well as between young and old mice.

In the cerebellum of WT, LGTV infection did not lead to an induction of IFNβ-expression in mice, independent of the age of the mice. In the absence of MAVS, the IFNβ-expression levels were increased in mice, with a significant difference in young mice. In the cerebellum of *Mavs*$^{-/-}$ mice, the IFNβ-expression levels were slightly significantly decreased in adult mice compared to young mice, while the IFNβ-expression levels were similar in young and old mice.

The data indicate that aging had an impact on the LGTV-induced expression of IFNβ in the analyzed brain regions in a MAVS-dependent manner. Furthermore, the IFNβ-expression is differentially regulated in specific brain regions. This effect can be responsible for the increased susceptibility of aged *Mavs*$^{-/-}$ mice, since there is an age-dependent effect on the expression of IFNβ.

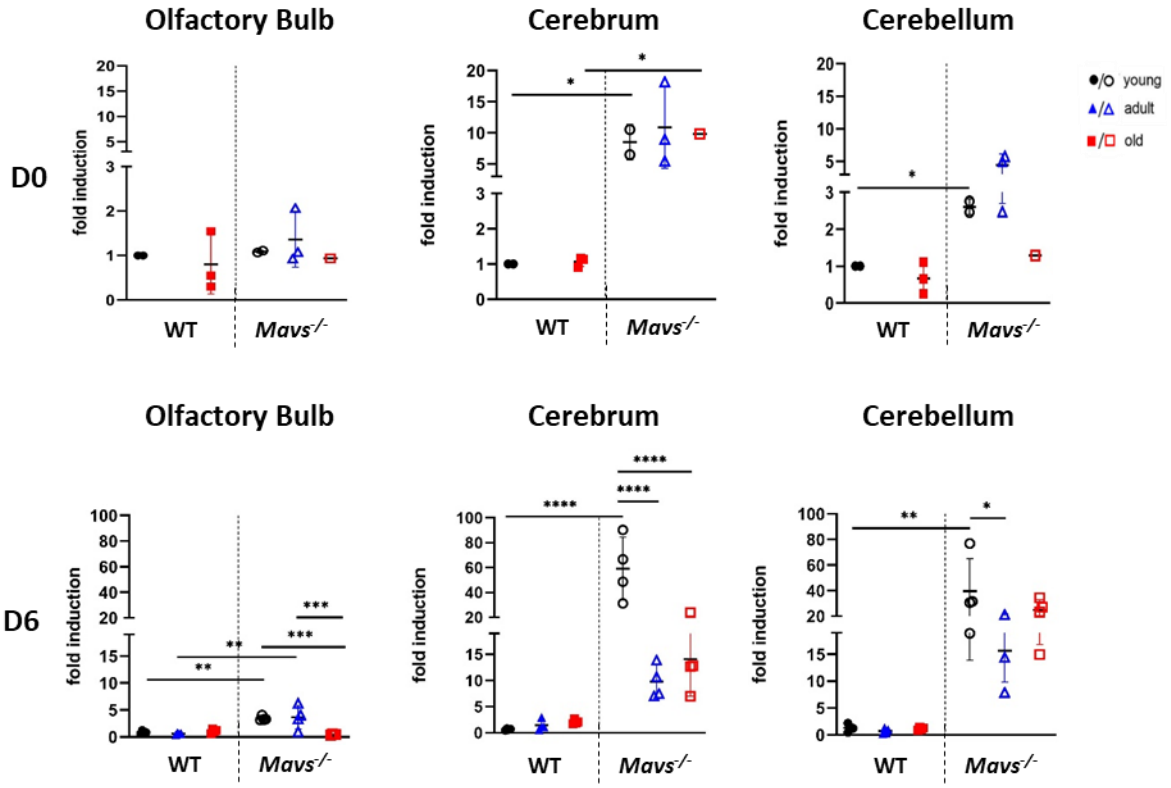

Figure 23: MAVS regulates LGTV-induced IFNβ-expression a region- and age-specific manner. Naïve WT and *Mavs*$^{-/-}$ mice of three different ages (young: 2-3 months (D0: n=2; D6: n=4); adult: 10-12 months (D0: n=0; D6: n=3); old: 18-24 months (D0: n=1 (MAVS), n=3 (WT); D6: n=3 (WT), n=4 (MAVS)). Brains of naïve mice were isolated without infection (D0) and brains of infected mice were isolated at six dpi (D6). The LGTV-induced expression of IFNβ was determined using qRT-PCR and normalized to the endogenous IFNβ-expression of naïve young WT mice. The IFNβ-expression was analyzed in the olfactory bulb, cerebrum, and cerebellum. Differences in the expression of IFNβ were tested for statistical

significance using the two-way ANOVA multiple comparison test (p-value: * < 0,05; ** < 0,01; *** < 0,001; **** < 0,0001).

Analysis of the endogenous IFNγ-expression in WT mice showed similarly low expression levels in the olfactory bulb, cerebrum, and cerebellum that were independent of the age of the mice (**Figure 24, D0**).
The depletion of MAVS did not lead to significant differences in the endogenous IFNγ-expression levels in the olfactory bulb, cerebrum and cerebellum of mice, which was independent of the age of the mice.
The data indicate that aging had no impact on the endogenous expression of IFNγ in the CNS of mice. This effect does not seem to be responsible for the increased susceptibility of aged *Mavs*$^{-/-}$ mice, since no age-related differences are evident.

The LGTV-induced expression levels of IFNγ were analyzed after six dpi in the olfactory bulb, cerebrum, and cerebellum of mice (**Figure 24, D6**). In the olfactory bulb of WT mice, LGTV infection did not lead to induction of IFNγ-expression in mice, independent of the age of the mice. The depletion of MAVS led to slightly increased IFNγ-expression levels in young mice. However, this increase was not significant. In the olfactory bulb of *Mavs*$^{-/-}$ mice, the IFNγ- expression levels decreased significantly with the age of mice. LGTV infection did not lead to induction of IFNγ-expression in adult or old *Mavs*$^{-/-}$ mice.
In the cerebrum of WT, LGTV infection did not lead to induction of IFNγ-expression in mice, independent of the age of the mice. The depletion of MAVS resulted in significantly increased IFNγ- expression levels in young mice. In the cerebrum of *Mavs*$^{-/-}$ mice, the IFNγ-expression levels decreased significantly with the age of mice. LGTV infection did not lead to induction of IFNγ- expression in adult and old *Mavs*$^{-/-}$ mice.
In the cerebellum of WT, LGTV infection did not lead to an induction of IFNγ-expression in mice, independent of the age of the mice. The depletion of MAVS led to increased IFNγ-expression levels in mice, independent of the age of the mice. In the cerebellum of *Mavs*$^{-/-}$ mice, the IFNγ- expression levels decreased slightly with the age the mice. This decrease was significant between young and old mice.
The data indicate that aging had an impact on the LGTV-induced expression of IFNγ in the analyzed brain regions in a MAVS-dependent manner. Furthermore, the IFNγ-expression is differentially regulated in specific brain regions. This effect can be responsible for the increased susceptibility of aged *Mavs*$^{-/-}$ mice, since there is an age-dependent effect on the expression of IFNγ.

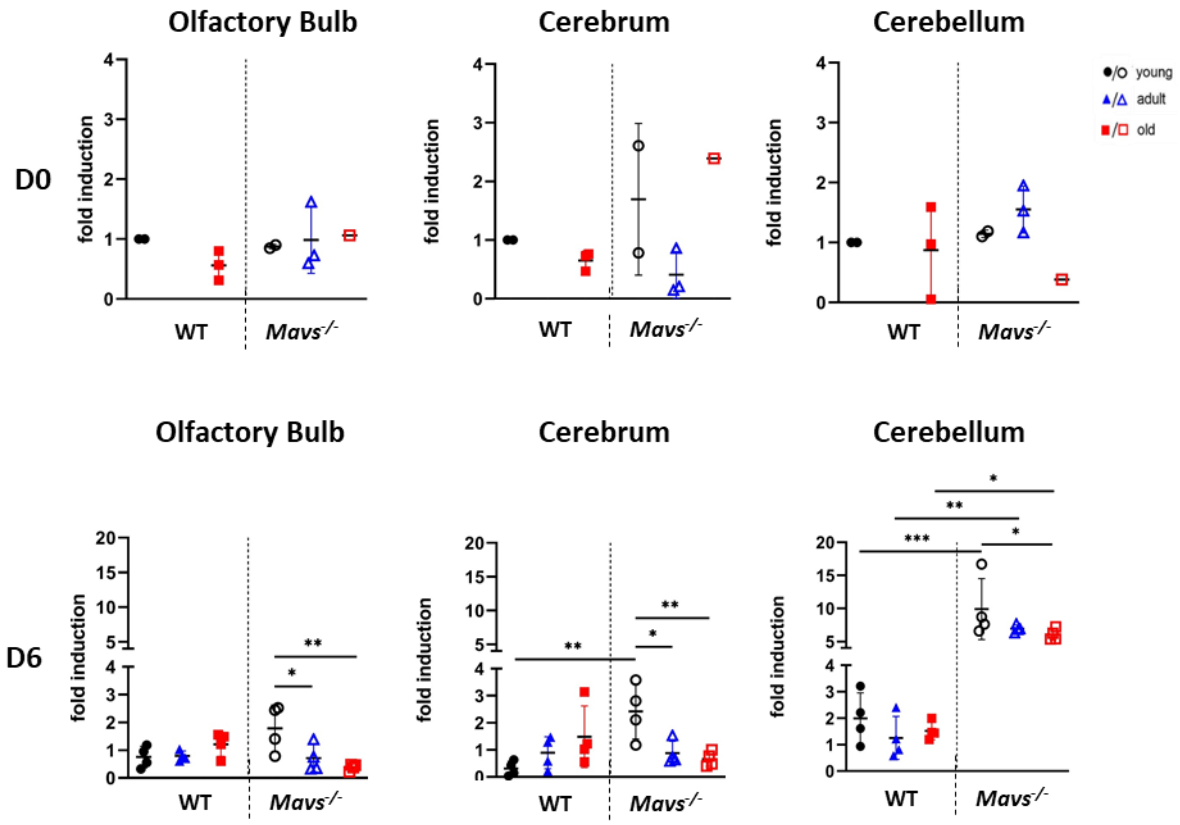

Figure 24: MAVS regulates LGTV-induced IFNγ-expression region- and age-specifically. Naïve WT and *Mavs*$^{-/-}$ mice of three different ages (young: 2-3 months (D0: n=2; D6: n=4); adult: 10-12 months (D0: n=0; D6: n=3); old: 18-24 months (D0: n=1 (MAVS), n=3 (WT); D6: n=3 (WT), n=4 (MAVS)). Brains of naïve mice were isolated without infection (D0) and brains of infected mice were isolated at six dpi (D6). The LGTV-induced expression of IFNγ was determined using qRT-PCR and normalized to the endogenous IFNγ-expression of naïve young WT mice. The IFNγ-expression was analyzed in the olfactory bulb, cerebrum, and cerebellum. Differences in the expression of IFNs were tested for statistical significance using the two-way ANOVA multiple comparison test (p-value: * < 0,05; ** < 0,01; *** < 0,001).

3.6.2. IRF-1/IRF-7 expression is age- and region-specifically regulated

The transcription factors of the interferon regulatory factor (IRF) family are important regulators of both IFN-dependent and IFN-independent antiviral response. They also play a crucial role in antiviral response in the CNS [17, 108]. In addition to host defense, they have a variety of functions, including cell cycle regulation, apoptosis, and the development and homeostasis of immune cells. Studies have shown that IRF-1 inhibits viruses' cell-type- and viral-specific [109]. Aging leads to impaired regulation of IRF-1/IRF-7, which contributes to increased susceptibility to viral infections in the elderly [102, 104, 110].

In order to investigate whether aging alone has an influence on the expression of IRFs, endogenous IRF-expression levels in young, adult, and old naïve WT and *Mavs*$^{-/-}$ mice were determined by qRT-PCR. Further, to investigate whether aging affects the antiviral activity in specific brain regions during infection, LGTV-induced IRF-expression levels were determined. Therefore, WT and *Mavs*$^{-/-}$ mice of different ages were infected systemically by intraperitoneal LGTV injection. Brains of infected mice were isolated at six dpi.

Analysis of the endogenous IRF-1-expression in WT mice showed similarly low expression levels in the olfactory bulb that were independent of the age of the mice (**Figure 25, D0**). In the olfactory bulb, the depletion of MAVS did not lead to increased endogenous IRF-1-expression levels in mice, independent of the age of the mice.
In the cerebrum of WT mice, the endogenous IRF-1-expression levels were low in young mice but significantly increased in old mice. The depletion of MAVS led to significantly increased IRF- 1- expression levels in young mice, whereas the depletion of MAVS led to significantly decreased IRF-1-expression levels in old mice. However, in the cerebrum of *Mavs*$^{-/-}$ mice, no age- related differences were evident.
In the cerebellum of WT mice, the endogenous IRF-1-expression levels were similar in all age groups; no age-related differences were evident. The depletion of MAVS did not lead to significant differences in the endogenous IRF-1-expression levels in mice, independent of the age of the mice.
The data indicate that aging had an impact on the endogenous expression of IRF-1 in the cerebrum of mice, which is MAVS-dependent. However, this effect does not seem to be responsible for the increased susceptibility of aged *Mavs*$^{-/-}$ mice, since no age-related differences are visible in *Mavs*$^{-/-}$ mice.

The LGTV-induced expression levels of IRF-1 were analyzed after six dpi in the olfactory bulb, cerebrum, and cerebellum of mice (**Figure 25**, **D6**). In the olfactory bulb of WT mice, LGTV infection did not significantly increased IRF-1-expression, independent of the age of the mice.
In the olfactory bulb of *Mavs*$^{-/-}$ mice, LGTV infection did not lead to induction of IRF- 1- expression in young and old mice, while the IRF-1-expression levels were slightly significantly increased in adult mice compared to old mice.
In the cerebrum of WT mice, LGTV infection did not lead to induction of IRF-1-expression, independent of the age of the mice. While the depletion of MAVS led to induction of IRF- 1- expression in mice, with a significant difference in young mice. In the cerebrum of *Mavs*$^{-/-}$ mice, the IRF-1-expression levels decreased with the age of the mice, this decrease was significant between young and adult as well as between young and old mice.

In the cerebellum of WT mice, LGTV infection did not lead to induction of IRF-1-expression, independent of the age of the mice. While the depletion of MAVS led to induction of IRF- 1- expression in mice, with a significant difference in young mice. In the cerebellum of *Mavs*$^{-/-}$ mice, the IRF-1-expression levels decreased with the age of the mice, with significant differences between young and adult as well as between young and old mice.

The data indicate that aging had an impact on the LGTV-induced expression of IRF-1 in the analyzed brain regions in a MAVS-dependent manner. Furthermore, the induced IRF- 1- expression is differentially regulated in specific brain regions. This effect can be responsible for the increased susceptibility of aged *Mavs*$^{-/-}$ mice, since there is an age-dependent effect on the expression of IRF-1.

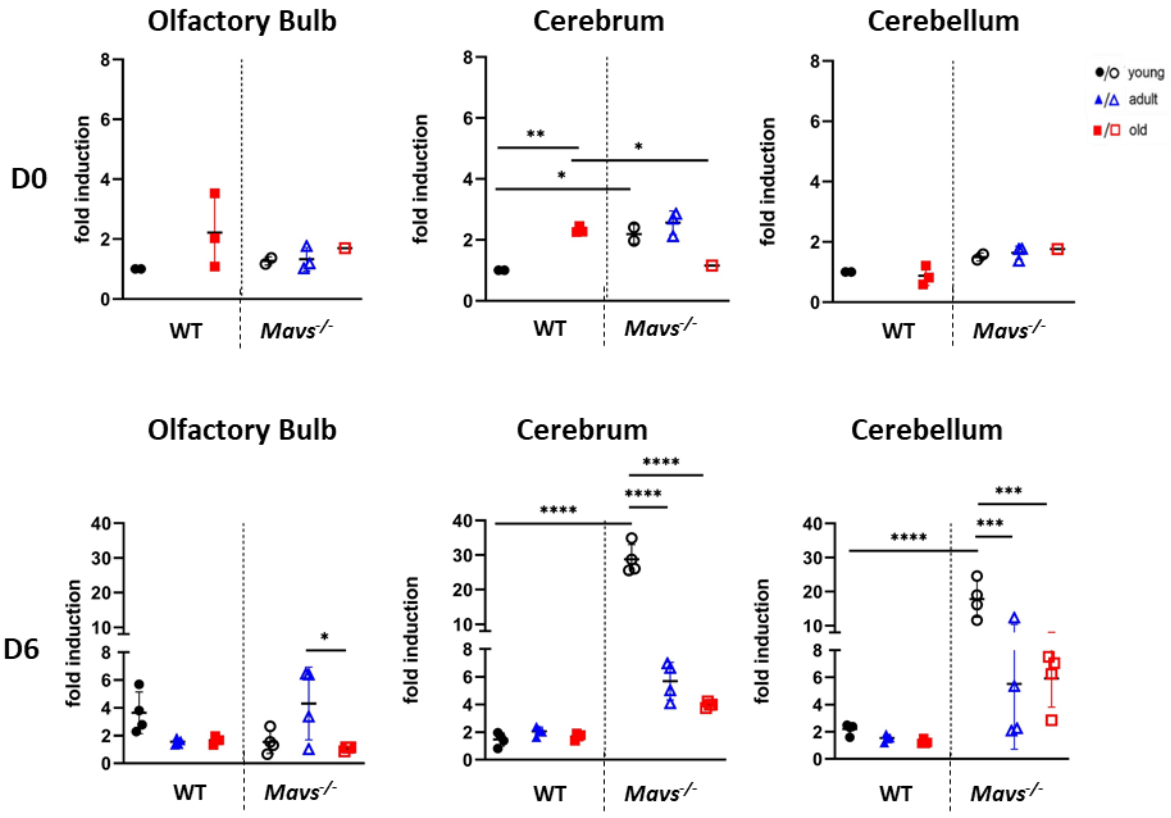

Figure 25: MAVS regulates IRF-1 expression region- and age-specifically. Naïve WT and *Mavs*$^{-/-}$ mice of three different ages (young: 2-3 months (D0: n=2; D6: n=4); adult: 10-12 months (D0: n=0; D6: n=3); old: 18-24 months (D0: n=1 (MAVS), n=3 (WT); D6: n=3 (WT), n=4 (MAVS)). Brains of naïve mice were isolated without infection (D0) and brains of infected mice were isolated at six dpi (D6). The LGTV-induced expression of IRF-1 was determined using qRT-PCR and normalized to the endogenous IRF-1-expression of naïve young WT mice. The IFNβ-expression was analyzed in the olfactory bulb, cerebrum, and cerebellum. Differences in the expression of IRFs were tested for statistical significance using the two-way ANOVA multiple comparison test (p-value: ** < 0,01).

Analysis of the endogenous IRF-7-expression levels in WT mice showed no significant differences in the olfactory bulb, cerebrum, and cerebellum that were independent of the age of the mice (**Figure 26, D0**).
The endogenous IRF-7-expression levels in *Mavs*$^{-/-}$ mice were similarly low in the olfactory bulb, cerebrum, and cerebellum that were independent of the age of the mice.
The data indicate that aging did not lead to significant differences in the endogenous expression of IRF-7 in the analyzed brain regions of mice, which is independent of MAVS. This effect does not seem to be responsible for the increased susceptibility of aged *Mavs*$^{-/-}$ mice, since no age- related differences are visible in *Mavs*$^{-/-}$ mice.

The LGTV-induced expression levels of IRF-7 were analyzed after six dpi in the olfactory bulb, cerebrum, and cerebellum of mice (**Figure 26**, **D6**). In the olfactory bulb of WT, LGTV infection led to induction of IRF-7-expression in young mice, while LGTV infection did not lead to induction of IRF-7-expression in adult or old mice. The depletion of MAVS led to highly significantly increased IRF-7-expression levels in young mice and slightly significantly increased IRF- 7- expression levels in adult mice. In the olfactory bulb of *Mavs*$^{-/-}$ mice, the IRF-7-expression levels decreased significantly with the age of mice.
In the cerebrum of WT mice, the IRF-7-expression levels were similarly low, independent of the age of the mice. While the depletion of MAVS led to induction of IRF-7-expression in mice, with a significant difference in young mice. In the cerebrum of *Mavs*$^{-/-}$ mice, the IRF-7-expression levels decreased with the age of the mice, this decrease was significant between young and old mice.
In the cerebellum of WT mice, LGTV infection led to induction of IRF-7-expression in young mice, while LGTV infection did not lead to induction of IRF-7-expression in adult or old mice. The depletion of MAVS led to slightly increased IRF-7-expression levels in young mice. However, this increase was not significant. In the cerebellum of *Mavs*$^{-/-}$ mice, the IRF-7-expression levels decreased with the age of mice, this decrease was significant between young and old mice.
The data indicate that aging had an impact on the LGTV-induced expression of IRF-7 in the analyzed brain regions in a MAVS-dependent manner. Furthermore, the induced IRF- 7- expression is differentially regulated in specific brain regions. This effect can be responsible for the increased susceptibility of aged *Mavs*$^{-/-}$ mice, since there is an age- dependent effect on the expression of IRF-7.

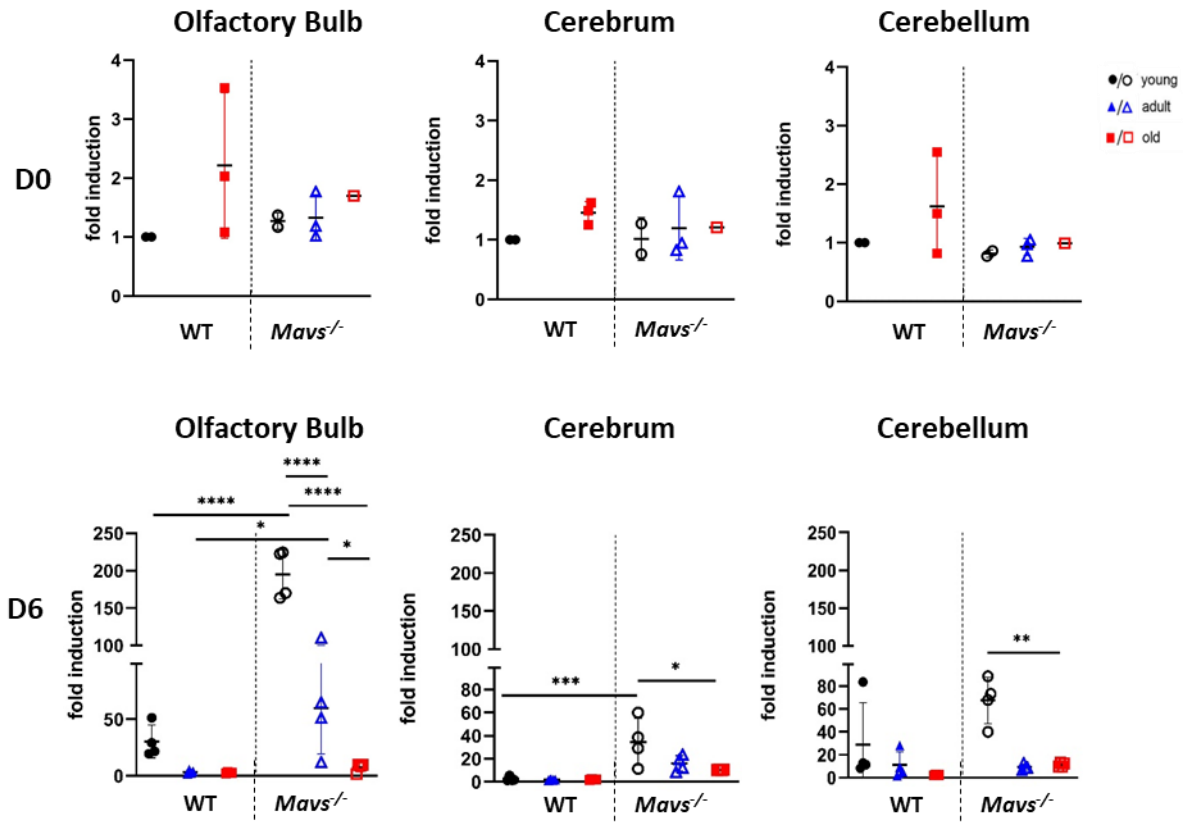

Figure 26: MAVS regulates the LGTV-induced IRF7-expression region- and age-specific. Naïve WT and *Mavs*$^{-/-}$ mice of three different ages (young: 2-3 months (D0: n=2; D6: n=4); adult: 10-12 months (D0: n=0; D6: n=3); old: 18-24 months (D0: n=1 (MAVS), n=3 (WT); D6: n=3 (WT), n=4 (MAVS)) were infected intraperitoneal with 10^4 FFU LGTV. Brains of naïve mice were isolated without infection (D0) and brains of infected mice were isolated at six dpi (D6). The LGTV-induced expression of IRF-7 was determined using qRT-PCR and normalized to the endogenous IFNβ-expression of naïve young WT mice. The IRF-7-expression was analyzed in the olfactory bulb, cerebrum, and cerebellum. Differences in the expression of IRFs were tested for statistical significance using the two-way ANOVA multiple comparison test (p-value: * < 0,05; ** < 0,01; *** < 0,001; **** < 0,0001).

3.6.3. ISG-expression is age- and region-specifically regulated

In addition to determining the expression levels of IRFs, the analysis of ISG-expression levels was crucial. ISGs can modulate the viral entry, replication, and assembly. However, the specific function of most ISGs *in vivo* is still unknown [111].

OAS-1 plays a critical role in cell apoptosis, growth, differentiation, and gene regulation. It is essential for stimulating the innate antiviral immune response by activating RNase L to cleave viral RNA [112]. In order to investigate whether aging alone has an influence on the expression of OAS-1, endogenous expression levels in young, adult, and old naïve WT and *Mavs*$^{-/-}$ mice were determined by qRT-PCR. Further, to investigate whether aging affects the antiviral activity in specific brain regions during aging, LGTV-induced OAS-1-expression was determined. Therefore,

WT and *Mavs*$^{-/-}$ mice of different ages were infected systemically by intraperitoneal LGTV injection. Brains of infected mice were isolated at six dpi.

Analysis of the endogenous OAS-1-expression levels in WT mice showed no age-related differences in the olfactory bulb, cerebrum, and cerebellum (**Figure 27, D0**).

The depletion of MAVS did not lead to significant differences in the endogenous OAS- 1- expression in the olfactory bulb, cerebrum, and cerebellum, independent of the age of mice.

The data indicate that aging had no impact on the endogenous expression of OAS-1 in the analyzed brain regions of mice, which is independent of MAVS. This effect does not seem to be responsible for the increased susceptibility of aged *Mavs*$^{-/-}$ mice, since no age-related differences are visible in *Mavs*$^{-/-}$ mice.

The LGTV-induced expression levels of OAS-1 were analyzed after six dpi in the olfactory bulb, cerebrum, and cerebellum of mice (**Figure 27**, **D6**). In the olfactory bulb of WT mice, LGTV infection led to induction of OAS-1-expression in young mice, while LGTV infection did not lead to induction of OAS-1-expression in adult or old mice. The depletion of MAVS led to highly significantly increased OAS-1-expression levels in young mice and slightly significantly increased OAS-1-expression levels in adult mice. In the olfactory bulb of *Mavs*$^{-/-}$ mice, the OAS- 1- expression levels decreased with the age of the mice. Old *Mavs*$^{-/-}$ mice had low OAS- 1- expression levels similar to WT mice.

In the cerebrum of WT mice, LGTV infection did not lead to induction of OAS-1-expression in young and adult mice, while LGTV infection led to induction of OAS-1-expression in old mice. The depletion of MAVS led to highly significantly increased OAS-1-expression levels in young mice. In the cerebrum of *Mavs*$^{-/-}$ mice, the OAS-1-expression levels decreased significantly with the age of mice. Adult and old *Mavs*$^{-/-}$ mice had similar OAS-1-expression levels as old WT mice.

In the cerebellum of WT mice, LGTV infection led to induction of OAS-1-expression in young mice, while LGTV infection did not lead to induction of OAS-1-expression in adult or old mice. The depletion of MAVS led to significantly increased OAS-1-expression levels in young mice. In the cerebellum of *Mavs*$^{-/-}$ mice, the OAS-1-expression levels decreased slightly with the age of mice, however this decrease was not significant. Adult and old *Mavs*$^{-/-}$ mice had similar OAS- 1- expression levels as old WT mice.

The data indicate that aging had an impact on the LGTV-induced expression of OAS-1 in the olfactory bulb and cerebrum in a MAVS-dependent manner. This effect can be responsible for the increased susceptibility of aged *Mavs*$^{-/-}$ mice, since there is an age-dependent effect on the expression of OAS-1.

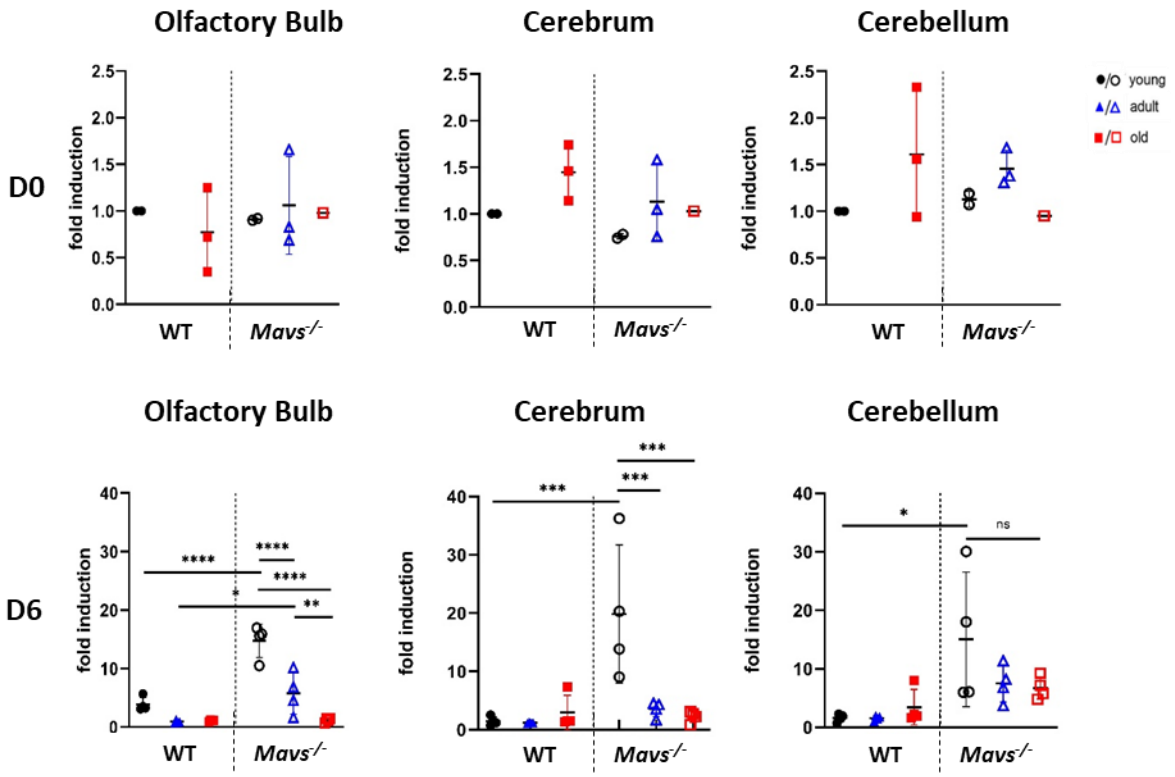

Figure 27: MAVS regulates the LGTV-induced OAS-1-expression region- and age-specific. Naïve WT and *Mavs*$^{-/-}$ mice of three different ages (young: 2-3 months (D0: n=2; D6: n=4); adult: 10-12 months (D0: n=0; D6: n=3); old: 18-24 months (D0: n=1 (MAVS), n=3 (WT); D6: n=3 (WT), n=4 (MAVS)). Brains of naïve mice were isolated without infection (D0) and brains of infected mice were isolated at six dpi (D6). The LGTV-induced expression of OAS-1 was determined using qRT- PCR and normalized to the endogenous IFNβ-expression of naïve young WT mice. The OAS- 1- expression was analyzed in the olfactory bulb, cerebrum, and cerebellum. Differences in the expression of ISGs were tested for statistical significance using the two-way ANOVA multiple comparison test (p-value: * < 0,05; ** < 0,01; *** < 0,001; **** < 0,0001, ns: not significant).

Rsad-2, also known as viperin, can inhibit soluble protein secretion, inhibit virus replication, and modulate cellular signaling [113-115]. It is dispensable to restrict virus replication and the induction of innate immunity [116]. Studies have shown that Rsad-2-activity is region- and cell- type-specific, which plays a fundamental role in enhanced virus replication and increased lethality during neurotropic viral infection in aging [38, 111]. In order to investigate whether aging alone has an influence on the expression of Rsad-2, endogenous expression levels in young, adult and old naïve WT and *Mavs*$^{-/-}$ mice were determined by qRT-PCR. Further, to investigate whether aging affects the antiviral activity in specific brain regions during aging, LGTV-induced Rsad- 2- expression was determined. Therefore, WT and *Mavs*$^{-/-}$ mice of different ages were infected systemically by intraperitoneal LGTV injection. Brains of infected mice were isolated at six dpi.

Analysis of the endogenous Rsad-2-expression levels in WT mice showed similarly low expression levels with no age-related differences in the olfactory bulb, cerebrum, and cerebellum (**Figure 28, D0**).

The depletion of MAVS did not lead to significant differences in the endogenous Rsad- 2- expression in the analyzed brain regions, independent of the age of mice.

The data indicate that aging had no impact on the endogenous expression of Rsad-2 in the analyzed brain regions of mice, which is independent of MAVS. This effect does not seem to be responsible for the increased susceptibility of aged *Mavs*$^{-/-}$ mice, since no age-related differences are visible in *Mavs*$^{-/-}$ mice.

The LGTV-induced expression levels of Rsad-2 were analyzed after six dpi in the olfactory bulb, cerebrum, and cerebellum of mice (**Figure 28, D6**). In the olfactory bulb of WT mice, LGTV infection led to slightly increased Rsad-2-expression levels in young mice, while LGTV infection did not lead to induction of Rsad-2-expression in adult or old mice. However, no age-related differences were detectable in the olfactory bulb of WT mice. The depletion of MAVS led to significantly increased Rsad-2-expression levels in young and adult mice. In the olfactory bulb of *Mavs*$^{-/-}$ mice, the Rsad-2-expression levels decreased significantly with the age of the mice. LGTV infection did not lead to induction of Rsad-2-expression in old *Mavs*$^{-/-}$ mice.

In the cerebrum of WT mice, LGTV infection did not lead to induction of Rsad-2-expression, independent of the age of the mice. In the cerebrum of *Mavs*$^{-/-}$ mice, LGTV infection led to induction of Rsad-2-expression in young mice, while LGTV infection did not lead to induction of Rsad-2-expression in adult and old mice.

In the cerebellum of WT mice, LGTV infection did not lead to induction of Rsad-2-expression, independent of the age of the mice. In the cerebellum of *Mavs*$^{-/-}$ mice, LGTV infection led to induction of Rsad-2-expression in young mice, while LGTV infection did not lead to induction of Rsad-2-expression in adult and old mice.

The data indicate that aging had an impact on the LGTV-induced expression of Rsad-2 in the analyzed brain regions in a MAVS-dependent manner. This effect can be responsible for the increased susceptibility of aged *Mavs*$^{-/-}$ mice, since there is an age-dependent effect on the expression of Rsad-2.

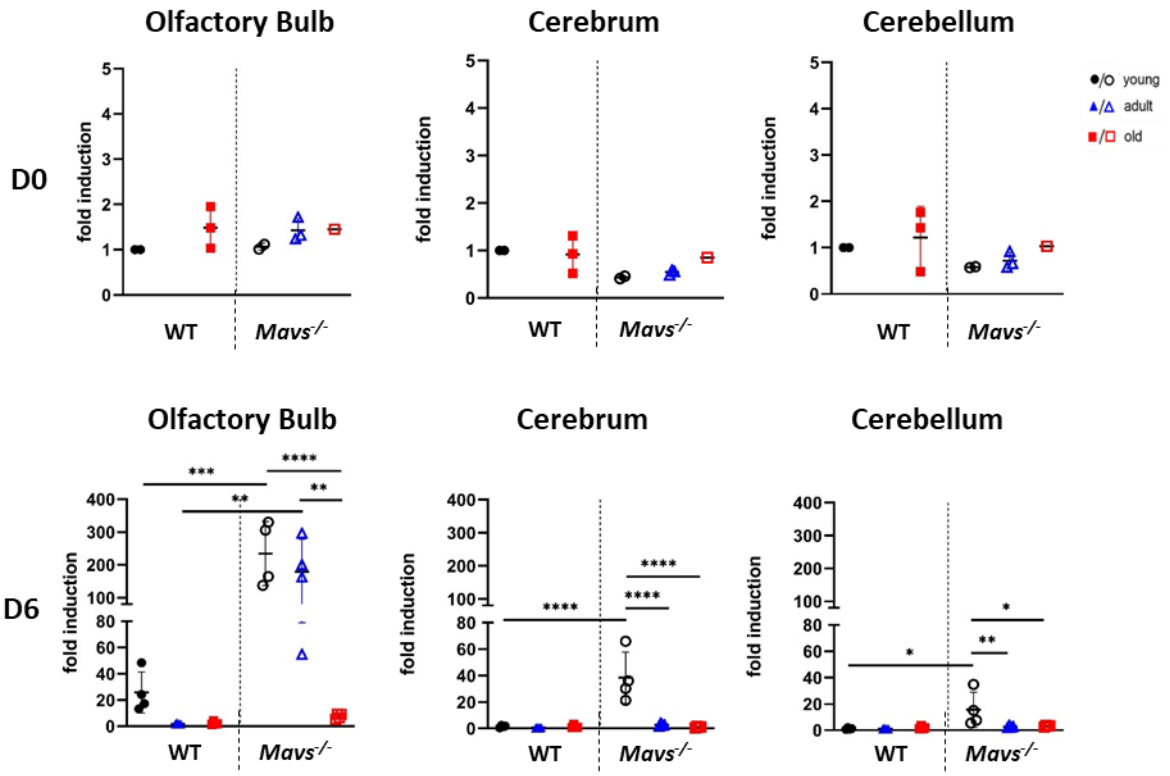

Figure 28: MAVS regulates LGTV-induced Rsad-2-expression age-and region-specific. Naïve WT and *Mavs*$^{-/-}$ mice of three different ages (young: 2-3 months (D0: n=2; D6: n=4); adult: 10-12 months (D0: n=0; D6: n=3); old: 18-24 months (D0: n=1 (MAVS), n=3 (WT); D6: n=3 (WT), n=4 (MAVS)). Brains of naïve mice were isolated without infection (D0) and brains of infected mice were isolated at six dpi (D6). The LGTV-induced expression of Rsad-2 was determined using qRT-PCR and normalized to the endogenous Rsad-2-expression of naïve young WT mice. The IFNβ-expression was analyzed in the olfactory bulb, cerebrum, and cerebellum. Differences in the expression of ISGs were tested for statistical significance using the two-way ANOVA multiple comparison test (p-value: * < 0,05; ** < 0,01; *** < 0,001; **** < 0,0001).

The ISG Ifi27la, also named Ifi27, modulates inflammatory events and immunity in the brain [117]. It plays an essential role by inhibiting the virus gene expression and virus replication [118]. Studies have shown that Ifi27 protects mice against mortality by regulating the antiviral response in neurotropic virus infections is cell-type and region-specific [101, 119].

In order to investigate whether aging alone has an influence on the expression of Ifi27, the endogenous expression levels in young, adult and old naïve mice were first examined by qRT- PCR. Afterwards, to investigate whether aging affects the antiviral activity in specific brain regions, the LGTV-induced Ifi27-expression was determined in the olfactory bulb, cerebrum, and cerebellum by qRT-PCR. Therefore, WT and *Mavs*$^{-/-}$ mice of different ages were infected systemically by intraperitoneal LGTV injection. Brains of infected mice were isolated at six dpi.

Analysis of the endogenous Ifi27-expression levels in the olfactory bulb of WT mice were low and showed no age-related differences (**Figure 29, D0**). In the olfactory bulb, the depletion of MAVS did not lead to significant differences in the endogenous Ifi27-expression levels, independent of the age of mice.
In the cerebrum of WT mice, the endogenous Ifi27-expression levels were significantly increased with the age of the mice. The depletion of MAVS did not influence endogenous Ifi27- expression levels in young mice, whereas the depletion of MAVS led to slightly significantly decreased endogenous Ifi27-expression in old mice.
In the cerebellum of WT mice, the Ifi27-expression levels were low and had no age-related differences. The depletion of MAVS did not lead to significant differences in the endogenous Ifi27- expression levels, independent of the age of mice.
The data indicate that aging had an impact on the endogenous expression of Ifi27 in the cerebrum of mice, which is regulated MAVS-dependently. However, this effect does not seem to be responsible for the increased susceptibility of aged *Mavs*$^{-/-}$ mice, since no age-related differences are visible in *Mavs*$^{-/-}$ mice.

The LGTV-induced expression levels of Ifi27 were analyzed after six dpi in the olfactory bulb, cerebrum, and cerebellum of mice (**Figure 29**, **D6**). In the olfactory bulb of WT mice, LGTV infection led to induction of Ifi27-expression in young mice, however these differences were not significant. The depletion of MAVS led to increased Ifi27-expression levels in mice, with a significant difference in young mice. In the olfactory bulb of *Mavs*$^{-/-}$ mice, the Ifi27-expression levels decreased significantly with the age of the mice.
In the cerebrum of WT mice, LGTV infection led to slightly increased Ifi27-expression levels in mice, independent of the age of mice. The depletion of MAVS led to significantly increased Ifi27- expression levels in mice, with significant differences in young and adult mice. Old *Mavs*$^{-/-}$ mice had significantly decreased Ifi27-expression levels compared to young mice.
In the cerebellum of WT mice, LGTV infection did not lead to induction of Ifi27-expression in mice, independent of the age of mice. The depletion of MAVS led to induction of Ifi27- expression in mice, independent of the age of the mice. In the cerebellum of *Mavs*$^{-/-}$ mice, the Ifi27-expression levels increased significantly with the age of the mice. Young *Mavs*$^{-/-}$ mice had slightly increased Ifi27-expression levels compared to WT mice, while adult and old *Mavs*$^{-/-}$ mice had highly increased Ifi27-expression levels compared to WT mice.
The data indicate that aging had an impact on the LGTV-induced expression of Ifi27 in a MAVS- and region-dependent manner. Since cerebellar cells of aged *Mavs*$^{-/-}$ mice are not highly susceptible to LGTV, this increased Ifi27-expression might have a protective effect in the cerebellum of aged *Mavs*$^{-/-}$ mice. However, this effect does not protect aged *Mavs*$^{-/-}$ mice against lethal LGTV infection.

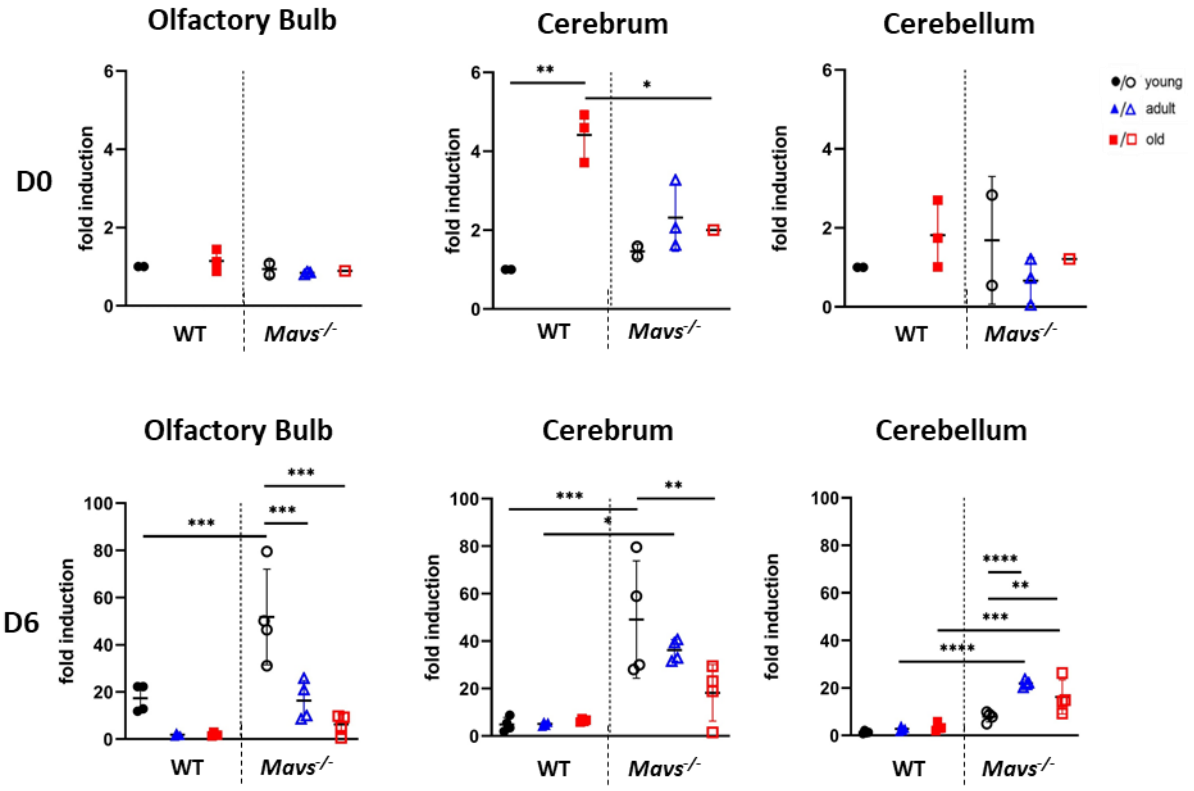

Figure 29: MAVS influences endogenous Ifi27-expression in the cerebrum. Naïve WT and *Mavs*$^{-/-}$ mice of three different ages (young: 2-3 months (D0: n=2; D6: n=4); adult: 10-12 months (D0: n=0; D6: n=3); old: 18-24 months (D0: n=1 (MAVS), n=3 (WT); D6: n=3 (WT), n=4 (MAVS)). Brains of naïve mice were isolated without infection (D0) and brains of infected mice were isolated at six dpi (D6). The LGTV-induced expression of Ifi27 was determined using qRT-PCR and normalized to the endogenous IFNβ-expression of naïve young WT mice. The Ifi27-expression was analyzed in the olfactory bulb, cerebrum, and cerebellum. Differences in the endogenous expression of Ifi27la was tested for statistical significance using the two-way ANOVA multiple comparison test (p- value: * < 0,05; ** < 0,01).

4. Discussion

Several studies have reported that the morbidity, severity, and mortality from viral infections increase with age. This correlation between aging and increasing disease severity has been observed also in TBEV infections. The ability of the immune response decreases with age. This is due to age-related changes in innate and adaptive immune responses. The innate immune response in the brain is important for antiviral defenses in neurotropic viral infections. MAVS thereby mediates direct antiviral activity in LGTV infections in the brain. We therefore examined the effects of age on antiviral immunity in the CNS of MAVS$^{-/-}$ mice.

Our results indicate that aging leads to an increased susceptible in Mavs$^{-/-}$ mice during LGTV infections. Although there is evidence that brain virus titer is directly related to mortality, we could not demonstrate an age-dependent increase in brain viral load in aged Mavs$^{-/-}$ mice. Detailed analyses have shown that virus distribution in different brain regions is regulated in an age-dependent manner. Specific antiviral genes are differentially regulated in brain regions and may be responsible for age-dependent differential regulation of the antiviral response.

4.1. Role of MAVS in antiviral activity during aging

The intracellular innate immune response and type I IFN signaling provide a first-line of defense against viral infection. This antiviral immune response is activated by recognition of PAMPs via PRRs such as RIG-I/MDA5, resulting in the expression of pro-inflammatory cytokines, chemokines, type I IFN, and ISGs [6, 7]. As a downstream protein from RIG-I, MAVS is a critical part of the antiviral response. In WNV infections, MAVS is essential for induction of innate immunity to ensure effective development and regulation of adaptive immunity against viral infections [92]. Furthermore, the literature demonstrates that type I IFN signaling is critical for early control of TBEV and LGTV replication in the periphery and CNS, thus providing protection against lethal infection [93]. Consequently, depletion of MAVS leads to a disabled antiviral response [120] and a higher susceptibility to viral infections [91]. The impact of aging on MAVS-dependent antiviral activity against TBEV infection is so far unknown. We assume that the importance of the antiviral activity of MAVS against TBEV increases with the increasing age of the organisms. In this study, using LGTV as a model for TBEV infection in the CNS, we report the critical role of MAVS in antiviral activity during aging, leading to protection against fatal LGTV infection. Aging in Mavs$^{-/-}$ mice leads to increased susceptibility to LGTV and early reaching of terminal criteria during the survival experiment. In contrast, WT mice are not susceptible to LGTV independent of age and do not develop clinical symptoms. Therefore, aging appears to have a major impact on MAVS-dependent antiviral activity by enhancing protective effects in aged mice. The extent to which this antiviral activity is affected by aging is discussed in the following sections.

4.2. Relevance of viral replication in the increased susceptibility

In neurotropic viral infections, increased susceptibility usually correlates with high viral replication. WNV-infected young *Mavs*$^{-/-}$ mice showed increased viral replication in the periphery and CNS compared to young WT mice, resulting in an early lethality [92]. Furthermore, Kurhade et al. (2016) showed that young *Mavs*$^{-/-}$ mice succumbed to LGTV infection earlier than young WT mice, which correlates with high viral replication in the CNS of mice [84]. In this study using WT mice and *Mavs*$^{-/-}$ mice of different ages, we report that MAVS is crucial for controlling viral replication in the brain of young mice during LGTV infection. In the absence of MAVS, young mice have increased viral replication in the brain. In contrast, young *Mavs*$^{-/-}$ mice have low viral replication in the lymph nodes and spleens similar to young WT mice. Therefore, MAVS appears to play a minor role in controlling viral replication in the periphery of young mice during LGTV infection. Interestingly, the depletion of MAVS at endpoint analysis leads to increased virus replication in the peripheral organs and brains of adult and old *Mavs*$^{-/-}$ mice. Age-related changes lead to increased susceptibility and mortality from viral infections [121]. This study aimed to clarify whether the increased susceptibility to LGTV infection of aged *Mavs*$^{-/-}$ mice is related to increased virus replication. WT mice of all ages are not susceptible to LGTV infection, which correlates with the overall low virus replication in peripheral organs and brains. While aging leads to highly increased replication in the spleens of *Mavs*$^{-/-}$ mice. Nonetheless, this age-related effect on viral replication is not evident in lymph nodes or brains of *Mavs*$^{-/-}$ mice. Therefore, the data do not fully explain what leads to the increased mortality of aged *Mavs*$^{-/-}$ mice. Since MAVS is critical for the induction of cellular immunity, we analyzed the effects of aging on the MAVS-dependent antiviral response at the cellular level in the following sections.

4.3. Effect of aging on adaptive immune cells in antiviral response

Control of viral replication requires concerted control of cellular immunity. This is also mediated by the infiltration of immune cells. Under normal conditions, there is a continuous transmigration of lymphocytes, dendritic cells and macrophages between the CNS and peripheral blood [74]. Since neurotropic viral infections are associated with inflammation of the CNS, there is increased infiltration of immune cells [42]. In TBEV infection, an increased number of infiltrating T cells was found in the CSF of patients [122]. Furthermore, CNS inflammation also increases the number of B cells in the CNS [123]. These infiltrating immune cells can mediate protective but also neurotoxic properties such as the production of cytokines and chemokines, and non-cytolytic clearance of pathogens from neuronal cells [105]. Cytotoxic T cell mainly mediate cellular immune responses and are able to eliminate infected cells due to their cytotoxic activity. T helper cells are regulators of the immune response through the secretion of cytokines and recruit immune cells to the site of infection [124]. B cells regulate CNS homeostasis and play an important role in the pathogenesis of various CNS diseases. Our data show that the depletion of MAVS during LGTV

infection increases both B cell and activated B cell infiltration into the cerebellum of young mice. This increased infiltration correlates with increased susceptibility to LGTV of cerebellar cells in young *Mavs*$^{-/-}$ mice. However, this increased susceptibility does not result in increased infiltration of T helper cells or cytotoxic T cells into the cerebellum of young *Mavs*$^{-/-}$ mice. The absence of MAVS increases the susceptibility of cerebral cells of young mice. However, in the cerebrum of young *Mavs*$^{-/-}$ mice no increase in B- or T cell infiltration upon LGTV infection is evident.

Aging processes such as immunosenescence lead to the impairment of immune cell compartments [48, 49]. These processes affect both innate and the adaptive immunity. However, innate immunity appears to be better preserved in older organisms, while adverse age-related changes in adaptive immunity occur more frequently. Older organisms have reduced numbers of naïve B- and T cells and lower diversity of their receptors, leading to a less efficient response and more severe viral infections [53, 97]. This phenomenon occurs earlier in cytotoxic T cells than in T helper cells and is a hallmark of immunosenescence in humans [125]. Our data show that aging has a major impact on the number of infiltrating immune cells in the CNS of LGTV-infected *Mavs*$^{-/-}$ mice. With the increasing age of *Mavs*$^{-/-}$ mice, there was a decrease in infiltrating immune cells, independent of virus replication. Here, the MAVS-dependent immune response must be important for susceptibility to LGTV and may lead to a reduced antiviral response in aged *Mavs*$^{-/-}$ mice. However, this work could not prove a major impact of aging on adaptive immunity during LGTV infection in mice. B cell infiltration and activation in the cerebellum of mice is age- and MAVS-dependent, while infiltration of T helper cells and cytotoxic T cell was age- and MAVS-independent. Since WT mice of all ages do not exhibit high virus replication in the CNS during LGTV infection, an increased infiltration of immune cells into the CNS was not to be expected. Our data indicate that aging does not have a major impact on B and T cell infiltration and activation during LGTV infection in mice. Hence, impact of aging on innate immunity is discussed in the following chapter.

4.4. Aging affects innate immune cells in the antiviral response

Microglia are resident macrophages in the CNS. They regulate CNS homeostasis and perform efficient immune surveillance through highly mobile processes [126]. These cells play a phagocytic role, eliminating pathogens and cellular debris that enter the brain. Furthermore, microglia are also able to transform into an activated phenotype under certain conditions to perform inflammatory functions [127]. However, under pathological conditions, activation of microglia can have deleterious effects, such that it can mediate the onset and development of neuroinflammatory responses through a range of transcription factors and multiple cellular signaling pathways [128]. Aging processes can lead to functional limitations and sustained activation of microglia [51]. Our data show that aging reduces the number of microglia in the

cerebellum during LGTV infection in a MAVS- dependent manner. Aging has a major impact on the frequency of activated microglia in the CNS of LGTV-infected mice. The frequency of activated microglia increases with increasing age of mice. This seems to be regulated by MAVS in region-specific manner. This increased activation of microglial cells in aged mice may be important for pathogen clearance and the recruitment of additional immune cells. Nonetheless, sustained microglial activation can result in overexpression of inflammatory cytokines, which can lead to chronic neuroinflammation. Since aged WT mice are not susceptible to LGTV, sustained microglial activation in the cerebrum and cerebellum of aged WT mice could result in an enhanced immune response during LGTV infection. This enhanced immune response may result in a protective effect against LGTV in aged WT mice.

Dendritic cells are antigen-presenting cells that are present in the CNS at steady state [129]. Macrophages are antigen-presenting cells that organize the immune response and control tissue homeostasis. Both dendritic cells and macrophages promote the activation and proliferation of cytotoxic T cells and T helper cells through the secretion of pro-inflammatory cytokines. Under certain conditions, the secretion of pro-inflammatory cytokines can also cause tissue damage in the CNS and promote neurodegenerative diseases [130]. In WNV infection, dendritic cells are required to control virus replication and regulate downstream immune responses [131]. Aging processes lead to a reduced number and type I-IFN secretion of antigen-presenting cells [88]. Our data show that aging in *Mavs*$^{-/-}$ mice reduces dendritic cell infiltration into the CNS during LGTV infection. Furthermore, this correlates with the decreased frequency of activated dendritic cells in the CNS with increasing age of *Mavs*$^{-/-}$ mice. This happens independently of the brain region. Since *Mavs*$^{-/-}$ mice show increased virus replication in the cerebrum and cerebellum compared to WT mice, independent of the age of mice, an increased infiltration of dendritic cells is to be expected. Here, depletion of MAVS only increases the infiltration of dendritic cells and activated dendritic cells into the CNS of young mice. This effect can result in an impaired immune response, leading to more severe LGTV infection in aged *Mavs*$^{-/-}$ mice.

Our data show that aging in *Mavs*$^{-/-}$ mice reduces the infiltration of macrophages into the cerebrum during LGTV infection. Furthermore, this correlates with the reduced frequency of activated macrophages in the cerebrum with the increasing age of *Mavs*$^{-/-}$ mice. Therefore, this happens in a region-dependent manner. The depletion of MAVS only increases the infiltration of macrophages and activated macrophages into the cerebrum of young mice. This effect may result in a region-specific impaired immune response, leading to more severe LGTV infection in aged *Mavs*$^{-/-}$ mice.

4.5. The susceptibility to LGTV is regulated by age and region

Neurotropic virus infections are usually restricted to specific brain regions and do not spread throughout the brain. This can be explained by the fact that different cells or cell subtypes can react differently to viral infections [34, 35]. For example, granule cell neurons from the cerebellum of young mice are less susceptible to some viral infections than cortical neurons from the cerebral cortex of young mice [101]. Furthermore, it is known that cerebellar astrocytes are primed and produce IFNs faster after CNS infection, resulting in improved BBB function and suppression of neuroinflammation [132]. In LGTV infection, viral replication is primarily detected in the olfactory bulb, while less viral replication was detectable in other brain regions [133]. This assumption is supported by our results. Cells of the olfactory bulb from young *Mavs*$^{-/-}$ mice are highly susceptible to LGTV. However, cerebral and cerebellar cells from young *Mavs*$^{-/-}$ mice are also highly susceptible to LGTV. In contrast, cells of the choroid plexus from young *Mavs*$^{-/-}$ mice are not susceptible to LGTV. Here, different cell types in distinct brain regions seem to react differently to LGTV infection. Surprisingly, differential LGTV infection in specific brain regions is age-dependent. Baruch et al. (2014) identified an age- induced type-I IFN signature in the choroid plexus of mice that negatively affects brain function [41]. Our results show that the susceptibility of cells of the choroid plexus to LGTV in *Mavs*$^{-/-}$ mice is increased with age. Age-related effects may regulate the antiviral response in the choroid plexus that lead to an increased susceptibility to LGTV infection. In contrast, cerebellar cells of *Mavs*$^{-/-}$ mice lose their susceptibility to LGTV infection during aging. Here, an age-related protective MAVS-dependent antiviral mechanism in the cerebellum might explain that cerebellar cells from adult and old *Mavs*$^{-/-}$ mice are better protected from LGTV infection. The basic mechanisms behind this have not yet been sufficiently researched.

4.6. Aging determines the local antiviral response within the CNS

Specialized immune mechanisms are known that can control viral infections within the brain in a region-specific manner [134]. Rsad-2 activity in the cerebrum is required to restrict virus spread to other brain regions [38]. Ifi27 display an antiviral phenotype in subsets of cells, suggesting that some ISGs have specific inhibitory functions in restricted tissues [119]. Further studies show that these region-specific antiviral responses can be induced with increasing age [41]. We have already show that LGTV susceptibility is age- and region-specific. Furthermore, this correlates with antiviral activity in specific brain regions. Local cell type-specific IFNβ- expression within the olfactory bulb triggered distal parts of the brain, resulting in the protection from lethal encephalitis [37]. Since cells of the olfactory bulb of mice are highly susceptible to LGTV, leading to rapid detection of infected cells after inoculation [84, 133], locally high induced IFNβ-expression is important to control virus spread [36]. Our data show that aging decreases MAVS-dependent antiviral activity in the olfactory bulb of mice. The absence of MAVS increases antiviral activity in the olfactory bulb of young *Mavs*$^{-/-}$ mice. This antiviral response is highly reduced in the olfactory bulb of old *Mavs*$^{-/-}$ mice. Thus, cells of the olfactory bulb of old *Mavs*$^{-/-}$ mice are highly susceptible to LGTV infection; IFNβ-expression is not induced. Consequently, the type-I and type-II IFN signaling is impaired in old *Mavs*$^{-/-}$ mice. This is reflected in the decreased expression of IFNγ in the olfactory bulb of aged *Mavs*$^{-/-}$ mice. Furthermore, aging highly decreases IRF-7-, OAS-1-, Rsad-2-, and Ifi27-expression in the olfactory bulb of *Mavs*$^{-/-}$ mice. Interestingly, the IRF- 1- expression in the olfactory bulb of mice is not clearly affected by aging or MAVS. This reduced antiviral activity in the olfactory bulb of aged *Mavs*$^{-/-}$ mice may explain their increased susceptibility to LGTV.

Both cerebral cells and cerebellar cells appear to have unique antiviral immune responses to neurotropic viral infections [101]. Our data show that aging reduces the MAVS-dependent antiviral response in the cerebrum of mice. The absence of MAVS increases antiviral activity in the cerebrum of young *Mavs*$^{-/-}$ mice. This antiviral activity is highly reduced in the cerebrum of old *Mavs*$^{-/-}$ mice. Cerebral cells of old *Mavs*$^{-/-}$ mice are highly susceptible to LGTV, but IFNβ- expression is almost not induced. Consequently, the type-I and type-II IFN signaling is impaired in old *Mavs*$^{-/-}$ mice. This is reflected in the reduced expression of IFNγ in the cerebrum of aged *Mavs*$^{-/-}$ mice. Furthermore, aging highly decreases IRF-7-, OAS-1-, Rsad-2-, and Ifi27- expression in the cerebrum of *Mavs*$^{-/-}$ mice.

The depletion of MAVS increases antiviral activity in young *Mavs*$^{-/-}$ mice. This antiviral activity is not always decreased in the cerebellum of old *Mavs*$^{-/-}$ mice. Aging reduces Rsad-2, IRF-7-, IRF- 1- and IFNγ-expression in the cerebellum of *Mavs*$^{-/-}$ mice.

CNS cells of infected WT are not susceptible to LGTV, which correlates with reduced IFNβ- expression in each brain regions. The expression of OAS-1 and IFNβ in the cerebellum of

infected mice appear to be independent of the age of the mice. In contrast, the expression of Ifi27 is increased in the cerebellum of infected aged *Mavs*$^{-/-}$ mice. Aging seems to induce an MAVS- dependent antiviral mechanism in the cerebellum of LGTV infected mice. However, this increased antiviral activity in the cerebellum of aged *Mavs*$^{-/-}$ mice confers only local protection against LGTV, but does not ensure the survival of aged *Mavs*$^{-/-}$ mice. Aging does not affect antiviral activity in the CNS of LGTV-infected WT mice. WT mice have little induced antiviral activity in the distinct brain regions. This correlates with the low viral replication in the CNS of LGTV-infected WT mice.

These results demonstrate that aging determines the MAVS-dependent antiviral activity against LGTV infection in the CNS in a region-specific manner. However, antiviral activity does not correlate with viral replication in individual brain regions of *Mavs*$^{-/-}$ mice. Here, aging leads to decreased viral replication in the olfactory bulb, cerebrum and cerebellum of *Mavs*$^{-/-}$ mice. This decreased viral replication in the olfactory bulb, cerebrum, and cerebellum of aged *Mavs*$^{-/-}$ mice seems not to determine the survival during LGTV infection. Since a slight increase in viral replication is evident when analyzing whole brains from aged *Mavs*$^{-/-}$ mice, other brain regions might be the reason of the increased susceptibility of aged *Mavs*$^{-/-}$ mice during LGTV infection. Further investigations needs to be done to fully explain the increased susceptibility of aged *Mavs*$^{-/-}$ mice.

5. Material and Methods

5.1. Materials

5.1.1. Consumable

Material	Details	Manufacturer
Cell counting chamber slides	Countess	Thermo Fisher Scientific
Ceramic spheres	1/4'', 1/2''	MP Biomedicals
Cover glasses	24 x 50 mm	VWR
Cryo tube	2ml; 1,8 ml	Biozym Sarstedt AG
Culture flasks	T75, T25	Sarstedt AG
Culture plates	6-, 12-l, 24-, 48-, 96 Well	Sarstedt AG
FACS Tubes	5 ml	Sarstedt AG
Filter Tips	1000, 200, 10	Starlab Biozym (safeseal)
Glass potter	5 ml	B. Braun Melsungen AG
Glass racks		B. Braun Melsungen AG
Glass slides	Menzel Gläser Superfrost	VWR
LightCycler Multiwell plate	96, white	Roche Molecular Systems
Micro Fine Insulin syringe	0,3 mm x 8 mm	Becton Dickinson GmbH
Pap Pen		Abcam
Pasteur pipettes	225 mm, glass	Brandt AG
Preparation kit	Scissors, Spatulae, Forceps	Fine Science Tools
Micro Tubes	0,2 ml; 1,5 ml; 2 ml	Sarstedt AG Greiner
Sealing foil	transparent	Roche Molecular Systems
Serological pipette	10 ml + 25 ml	Corning Starlab
Sterican cannula	0.8 mm x 40 mm 0.5 mm x 25 mm	Becton Dickinson GmbH
Syringe	1 ml, 10 ml, 50 ml	B Braun Medical Corp.
Tips	1000 µl, 200 µl, 100 µl, 10 µl	Eppendorf AG Abimed
Tissue stryner	70 µm, 100 µm	Becton Dickinson GmbH
Tube	15 ml, 50 ml	Corning
Vacutainer	Safety-Lok	Becton Dickinson GmbH
Well plate	96, V-Bottom	Carl Roth GmbH + Co. KG

5.1.2. Chemicals

Chemicals	Manufacturer
Chlorofrom	Sigma Aldrich
Cytofix/Cytoperm	Becton Dickinson GmbH
DMEM	Gibco Life Technologies
EDTA	Sigma Aldrich
Ethanol	Th. Geyer GmbH & Co. KG
Fetale calve serum	Capricorn
Glucose	Thermo Fisher Scientific
Glutamax	Gibco Life Technologies
Goat serum	sigma Aldrich
HBSS (10x)	Gibco Life Technologies
HEPES	Gibco Life Technologies
Isoflurane	Baxter
Paraformaldehyde (37%)	Carl Roth GmbH + Co. KG
PBS (10x)	Gibco Life Technologies Biozym
Pen/Strep (10x)	Gibco Life Technologies
Percoll	GE Healthcare
Propanol	AppliChem
RPMI	Gibco Life Technologies
Sodium Pyruvate Solution	sigma Aldrich
Sucrose	Merck KGoA
TEP (10X)	Gibco Life Technologies
Tissue Tek	Sakura
TriFast peqGold	PeqLab
Triton-X 100	Serva Electrophoresis GmbH
TRIZOL	Thermo Fisher Scientific
Trypan Blue Solution (0,4 %)	sigma Aldrich
Tween-20	sigma Aldrich
Tween-80	sigma Aldrich
Vectashield Mounting Medium	Vector Laboratories

5.1.3. Virus strain

LGTV-WT

Langat virus strain TP21 (Laboratory of G. Dobler) was used for different experiments and is named LGTV-WT. The virus was propagated in Vero B4 cells, and Focus-Forming-Units Assay determined virus concentration.

5.1.4. Laboratory Equipment

Device	Type	Manufacturer
Aspirator		A. Hartenstein
Cell Counter	Countess II FL	Thermo Fisher Scientific
Centrifuge	Multifuge X3R Biofuge pico mini spinner Multifuge 3 S-R	Thermo Fisher Scientific Heraeus Sprout Heraeus
Cryostat microtome	Rotation CM3050 S	Leica
Flow cytometer	Attune nxt	Thermo Fisher Scientific
Freezer	- 20 °C - 80 °C	Liebherr Thermo Fisher Scientific
Fridge	Comfort	Liebherr
Homogenisator	FastPrep 24	MP Biomedicals
Hood	F-TA 1200 x 900-900	mc6
Ice Maschine		Scotsman
Incubator	Heracell 150i	Thermo Fisher Scientific
LightCycler 480 Instrument	qRT-PCR	Roche Molecular Systems
Magnetic Stirrers	magnetic stirr + heating	Heidolph
Micropipettes	Research, Research 2, Research plus	Eppendorf AG
Microscope	Primovert	Zeiss
Microscope, stereo	SZX10	Olympus
MilliQ Unit	Integral S	Merck
Nitrogen Tank	Biosafe	Cryotherm
pH Meter	Lab 860	SI Analytics
Pipette controller	Labsolute Integra Pipetboy 2	Th. Geyer GmbH & Co. KG VWR
Shaker	Schüttler MTS 4	IKA

Sterile workbench	Herasafe	Heraeus
Strirrer	MR 3001	Heidolph
Thermomixer	ThermoMixer comfort ThermoMixer F1.5	Eppendorf AG
Vortex	PeqTWIST	peqlab
Water bath		GFL

5.1.5. Computer software

Data collection and processing were done with Microsoft Office Professional Plus 2016 Word, Excel, and PowerPoint. To obtain microscopic pictures Automated Interactive Microscope (AIM) program and ZEN imaging software were used. Image analysis was performed with ImageJ (National Institutes of Health). qRT-PCR results were analyzed and calculated using the LightCycler 480 software (Roche). Preparation of figures and statistical analysis of data was done using GraphPad Prism 8.0 software (GraphPad Software Inc., La Jolla, CA, USA). The log-rank (Mantel-Cox) test was used for statistical significance in survival differences. Group differences were analyzed by two-way ANOVA multiple comparison test. Flow cytometry data were acquired with Attune NxT (Thermo Fisher Scientific) and analyzed using FlowJo 10 (FlowJo Software LLC, BD, USA).

5.2. Methods

5.2.1. Animal experiments

Ethical Statement

The animal experiments were performed according to the German Animal welfare Law (TierSchG BGBl. S. 1105; 25.05.1998). The approved animal codes for the experiments were IMMB-G-01-1507-18.

Mouse strains

Animals were bred and cared for at the animal house at the Otto-von-Guericke University, Magdeburg. C57BL/6OlaHsd (WT) animals were obtained from ENVIGO. WT and transgenic (*Mavs*$^{-/-}$) mice on a C57BL/6OlaHsd background were kept under SPF conditions, and PCR verified the genotype. Mice have maintained individually ventilated IVC Green Line cages (Tecniplast Germany GmbH), separated according to gender. Mice had access to food, water, and libitum, and were kept under standardized conditions. They have a 12 to 12 light-dark cycle with about 250 lux illuminance, 55 % humidity, and 22 °C.

Mouse infection

WT and *Mavs*$^{-/-}$ mice were used. Young (2-3 months), adult (10-12 months), and old (18 - 24 months) mice were used for the experiments. Animals were intraperitoneally injected with 100 µl 1 x 10^4 FFU LGTV-WT. Virus was always diluted in 1 x PBS.

Survival experiment

Mice were intraperitoneally injected with 100 µl 1 x 10^4 FFU of the virus. The health conditions and weight were observed daily and documented. If mice reached the termination criteria, they were directly sacrificed.

For endpoint analysis, brains, spleens, and draining inguinal lymph nodes were collected and analyzed using qRT-PCR.

5.2.2. Quantitative real time PCR (qRT-PCR)

RNA isolation from tissues

Both systemically infected and uninfected mice were killed by CO_2 inhalation. Mice were perfused transcardially with 20 ml 1x PBS. Brains, spleens, and draining inguinal lymph nodes were collected.

Furthermore, to analyze the influence of age on separate brain parts, brains were isolated and separated into olfactory bulb, choroid plexus, cerebrum, and cerebellum. Organs and tissues were stored in Fastprep tubes and directly frozen in liquid nitrogen. One ceramic sphere and Trizol were filled into each tube. Tubes were placed into the Fastprep 24 homogenizer, and organs and tissues were homogenized three times for 20 s at 4,5 m/s. Cell solutions were transferred into a 1,5 ml tube with chloroform. The solution was mixed for 15 s by shaking and incubated for 10 min at RT. Solutions were centrifuged at 13.000 rpm for 15 min at 4 °C. The transparent upper layer was transferred into a 1,5 ml tube with isopropanol. Samples were mixed and incubated for 5 min at RT. The suspensions were centrifuged at 13.000 rpm for 10 min at 4 °C. Two washing steps with 75% ethanol were followed. Samples were resuspended in RNase-free water, and RNA concentration was measured with Nanodrop. RNA was stored at -80 °C.

RNA Isolation from cells

RNA from choroid plexus and Vero cells was extracted using the QIAmp Viral RNA Mini Kit. Pipet 560 µl prepared Buffer AVL containing carrier RNA into a 1,5 ml tube and add 140 µl cell-culture supernatant or organ supernatant of the choroid plexus. Mix by pulse-vortexing for 15 s. Incubate at room temperature for 10 min. Briefly centrifuge the tube and add 560 µl ethanol (100%) to the sample, and mix by pulse-vortexing for 15 s. After mixing, briefly centrifuge the tube. Carefully apply 630 µl of the solution to the QIAamp Mini column (in a 2 ml collection tube) without wetting

the rim. Close the cap, and centrifuge at 8000 rpm for 1 min. Place the QIAamp Mini column into a clean 2 ml collection tube, and discard the tube containing the filtrate. Repeat the last step. Carefully open the QIAamp Mini column, and add 500 µl Buffer AW1. Close the cap, and centrifuge at 8000 rpm for 1 min. Place the QIAamp Mini column in a clean 2 ml collection tube, and discard the tube containing the filtrate. Carefully open the QIAamp Mini column, and add 500 µl Buffer AW2. Close the cap and centrifuge at 14,000 rpm for 3 min. Place the QIAamp Mini column in a new 2 ml collection tube and discard the old collection tube with the filtrate. Centrifuge at full speed for 1 min. Place the QIAamp Mini column in a clean 1,5 ml tube. Discard the old collection tube containing the filtrate. Carefully open the QIAamp Mini column and add 60 µl Buffer AVE equilibrated to room temperature. Close the cap, and incubate at room temperature for 1 min. Centrifuge at 8000 rpm for 1 min. Performing a double elution using 2 x 40 µl Buffer AVE. RNA concentration was measured with Nanodrop. RNA was stored at -80 °C.

cDNA synthesis

The solutions for the master mix are seen in the table µg RNA of each sample, and a 30 µl master mix was used for the reverse transcription into cDNA (**Table 1**). Samples were incubated for 1 h at 37 °C.

Table 1: **Mastermix of cDNA-synthesis**

Solutions	Mastermix 1x	Company
5x First-Strand Buffer	10µl	Invitrogen
dNTP Mix 5mM	5µl	Invitrogen
oligo(dT)$_{12-18}$ Primer	1µl	Bioline
random hexamer Primer	1µl	Bioline
DTT 0.1M	5µl	Invitrogen
RnaseOut	0,3µl	Invitrogen
M-MLV- RT	1µl	Invitrogen
Rnase free water	7µl	Invitrogen
RT-Mix	30µl	
1 µg RNA in 20µl Rnase free water	20µl	Invitrogen

The resulting cDNA mixture was diluted ten times. The samples were measured with LightCycler 480 Instrument II. qRT-PCR was carried out to determine the RNA level of LGTV or ISGs relative

to the housekeeping gene β-actin. Analysis of LGTV/β-actin ratio and ISGs/β-actin ratio were measured with LightCycler Software 480 II. Used primers are seen in the following table (**Table 2**).

Table 2: Primers of qRT-PCR

Primer	Forward	Reverse
ß-actin	5´TGG AAT CCT GTG GCA TCC ATG AAA-3´	5´TAA AAC GCA GCT CAG TAA CAG TCC G-3´
LGTV_NS3	5´AAC GGA GCC ATA GCC AGT GA-3´	5´AAC CCG TCC CGC CAC TC-3´
Ifi27l2a	5´GCT TGT TGG GAA CCC TGT TTG-3´	5´GGA TGG CAT TTG TTG ATG TGG AG-3´
IFN-ß	5´CTT CTC CGT CAT CTC CAT AGG G-3´	5´CAC AGC CCT CTC CAT CAA CT-3´
IFN-γ	5´TGG CTC TGC AGG ATT TTC ATG-3´	5´TCA AGT GGC ATA GAT GTG GAA GAA-3´
OAS1	5´ATG GAG CAC GGA CTC AGG A-3´	5´TCA CAC ACG ACA TTG ACG GC-3´
Rsad-2	5´GTC CTG TTT GGT GCC TGA AT-3´	5´GCC ACG CTT CAG AAA CAT CT-3´

To carry out the qRT-PCR, the KAPA SYBR Fast qPCR Kit Master Mix Universal was used. The PCR reaction mix of 20 µl included a 10 µl master mix, 10 pmol forward and reverse primer, and a 5 µl sample. As a negative control, water was used (**Table 3-Table 5**).

Table 3: Mastermix of β-actin

Solutions	Mastermix 1x	Company
H_2O (Rnase-free)	4,2µl	Invitrogen
ß-actin for 1:10	0,4µl	MWG
ß-actin rev 1:10	0,4µl	MWG
Mastermix	10µl	Sigma
	15µl	
	+ 5µl sample	

Table 4: Mastermix of LGTV

Solutions	Mastermix 1x	Company
H_2O (Rnase-free)	3,6µl	Invitrogen
LGTV_NS3 for 1:10	0,5µl	MWG
LGTV_NS3 rev 1:10	0,5µl	MWG
LGTV_NS3 Probe 1:10	0,4µl	
Mastermix	10µl	Peqlab
	15µl	
	+ 5µl sample	

Table 5: Mastermix of ISGs

Solutions	Mastermix 1x	Company
H_2O (Rnase-free)	4,2µl	Invitrogen
ISG for 1:10	0,4µl	MWG
ISG rev 1:10	0,4µl	MWG
Mastermix	10µl	Sigma
	15µl	
	+ 5µl sample	

The PCR reaction cycle is seen (**Table 6**). It starts with a pre-incubation step at 95°C for 10 minutes. The amplification step contains 45 repetitions at 95°C for 10 seconds, 60°C for 30 seconds, and 72°C for 10 seconds. The melting curve follows at 95°C for 5 seconds, 65°C for 1 minute, and 97°C. In the end, a cooling step follows at 40°C for 30 seconds.

Table 6: PCR reaction cycle

Step Description	Repetition	Step #	Temperature	Time	Ramp Rate
Pre-incubation	1x	1	95 °C	10 min	4,4 °C
Amplification	45x	2	95 °C	10 sec	4,4 °C
			60 °C	30 sec	2,2 °C
			72 °C	10 sec	4,4 °C
Melting curve	1x	3	95 °C	5 sec	4,4 °C
			65 °C	1 min	2,2 °C
			97 °C		0,11 °C
Cooling		4	40 °C	30 sec	2,2 °C

To determine the induction of antiviral proteins, the WT-D0 samples were normalized. The results were shown as fold induction in the graphs.

5.2.3. Flow Cytometry

Dissection Buffer:

1 x HBSS, 45 % Glucose, 1M HEPES

FACS Buffer

1x PBS (Gibco® Life Technologies), 2 mM EDTA, 2 % FCS

Percoll Solutions:

100 % Percoll: Percoll stock + 10 x HBSS

70 % Percoll: 100 % Percoll + 1 x HBSS

30 % Percoll: 100 % Percoll + 1 x HBSS

Both systemically infected and uninfected mice were killed by inhaling an overdose of isoflurane. Mice were perfused transcardially by 60 ml 1x PBS. Brains and spleens were collected. The brain was directly cut into the olfactory bulb, choroid plexus, cerebrum, and cerebellum. Organs or tissues were homogenized with 2 ml dissection buffer in a tissue glass homogenizer. The cell suspension was strained with a 70 µm cell strainer. The suspension was centrifuged for 20 min at 400g and 4°C. The pellet was resuspended in 10 ml 70% percoll solution. 10 ml of 30% percoll solution were slowly layered on the first layer, and 5 ml PBS were slowly layered on the top. The gradient was centrifuged for 35 min at 800 g and 4 °C without a break and an acceleration of one. The myelin layer was removed, and the cell layer was collected between 30% and 70% percoll solution. The cell suspension was washed with PBS and FACS Buffer and resuspended in FACS Buffer. Total cells per brain or spleen were counted with a Neubauer chamber. All samples were saturated with FcR Blocking reagent (MiltenyiBiotec) and stained with antigen-specific fluorescent antibodies (**Table 7**). Cells were fixed with 4 % PFA, and the analysis was done by Attune and FlowJo software. The single-cell staining of the spleen was used for manual compensation in all experiments.

Table 7: Antibody panel for flow cytometry

Target	Fluorochrom	Dilution	Company
CD8	PerCP-Cy5.5	1:200	BioLegend
CD11b	PE	1:400	BioLegend
F4/80	PE-Dazzle	1:300	BioLegend
CD3	PE-Cy7	1:300	BioLegend
CD11c	APC	1:400	BioLegend
MHC-II	Alexa Fluor 700	1:100	BioLegend
L/D	Zombie NIR	1:1000	BioLegend
NK1.1	BV421	1.400	BioLegend
CD4	BV510	1:300	BioLegend
CD19	BV605	1:300	BioLegend
CD45	BV711	1:300	BioLegend
CD86	FITC	1:400	BioLegend

5.2.4. Immunohistochemistry

Sodium citrate Buffer 10 mM, pH 6:

Tri-sodium citrate (dihydrate) in MilliQ H_2O. Add 0.5 % of Tween 20.

Tris Buffered Saline (TBS) 0.1M, pH 7,4:

0.154 mol/L NaCl, 0.1 mol/L Tris in MilliQ H_2O

Blocking Solution:

0.1M TBS, 5 % Goat Serum and 0,2% Triton X-100

Both systemically infected and uninfected mice were killed by CO_2 inhalation. Mice were perfused transcardially with 20 ml 1x PBS. Brains were removed, transferred into 15 ml falcons with 8 ml 1% PFA solution, and kept there for 24 h. After 24 h, the brains were transferred into 15 ml falcons with 30% sucrose solution. Brains were sufficiently saturated when they sunk to the bottom of the tubes. Brains were covered with TissueTek and stored at -20 °C. Brains were cut as 30 µm slices with the cryostat and attached to glass slides. For antigen retrieval, glass recs were filled with sodium citrate buffer and were placed in the water bath. The water bath was set at 100°C, so the solution could slowly reach around 90-95°C (avoid boiling). When the water bath is between 90-95 °C, the slides were placed into the recs and kept there for around 20 min. After 20 min of cooling down, the slides were washed with PBS. For saturation, slides were incubated for 1 h with blocking solution, stained overnight at 4 °C with primary antibody solutions, and afterward stained for 1,5 h with secondary antibody solutions (**Table 8**). Between staining steps, the slides were washed with TBS. Vectashield mounting media and coverslips were used to protect and store the samples. After 24 h of drying, the slides were stored at 4 °C before taking the pictures with a fluorescence microscope.

Table 8: Antibody staining of immunohistochemically

Antigen	Primary Antibody			Secondary Antibody			
	Species	Dilution	Company	Species	Color	Dilution	Company
NS3	chicken	1:1000	Laboratory of Sonja Best	goat anti chicken	AF488 (green)	1:250	Invitrogen
CD45	rat	1:200	Synaptic Systems	goat anti rat	AF546 (gelb)	1:200	Invitrogen
NeuN	guinea pig	1:400	Synaptic Systems	goat anti guinea pig	AF647 (red)	1:500	Jackson-Dianova
IBA1	guinea pig	1:400	Synaptic Systems	goat anti guinea pig	AF647 (red)	1:500	Jackson-Dianova
					DAPI	1:1000	

6. Literature

1. Gesundheitswesen, I.f.Q.u.W.i., *Informed health online*. 2006, Cologne Germany: Institute for Quality and Efficiency in Health Care.
2. Alberts B, J.A., Lewis J, et al. , *Molecular Biology of the Cell. 4th edition.* 2002: New York: Garland Science; 2002. Innate Immunity.
3. Medzhitov, R. and C.A. Janeway, *Innate immunity: The virtues of a nonclonal system of recognition.* Cell, 1997. **91**(3): p. 295-298. DOI: 10.1016/S0092-8674(00)80412-2.
4. Le Bon, A. and D.F. Tough, *Links between innate and adaptive immunity via type I interferon.* Curr Opin Immunol, 2002. **14**(4): p. 432-6. DOI: 10.1016/s0952-7915(02)00354-0.
5. Takeuchi, O. and S. Akira, *MDA5/RIG-I and virus recognition.* Curr Opin Immunol, 2008. **20**(1): p. 17-22. DOI: 10.1016/j.coi.2008.01.002.
6. Kawai, T. and S. Akira, *Innate immune recognition of viral infection.* Nat Immunol, 2006. **7**(2): p. 131-7. DOI: 10.1038/ni1303.
7. Koyama, S., et al., *Innate immune response to viral infection.* Cytokine, 2008. **43**(3): p. 336-41. DOI: 10.1016/j.cyto.2008.07.009.
8. Platanias, L.C., *Mechanisms of type-I- and type-II-interferon-mediated signalling.* Nat Rev Immunol, 2005. **5**(5): p. 375-86. DOI: 10.1038/nri1604.
9. Ivashkiv, L.B. and L.T. Donlin, *Regulation of type I interferon responses.* Nat Rev Immunol, 2014. **14**(1): p. 36-49. DOI: 10.1038/nri3581.
10. Stetson, D.B. and R. Medzhitov, *Antiviral defense: interferons and beyond.* J Exp Med, 2006. **203**(8): p. 1837-41. DOI: 10.1084/jem.20061377.
11. Hoffmann, H.H., W.M. Schneider, and C.M. Rice, *Interferons and viruses: an evolutionary arms race of molecular interactions.* Trends Immunol, 2015. **36**(3): p. 124-38. DOI: 10.1016/j.it.2015.01.004.
12. Lindqvist, R., et al., *Fast type I interferon response protects astrocytes from flavivirus infection and virus-induced cytopathic effects.* J Neuroinflammation, 2016. **13**(1): p. 277. DOI: 10.1186/s12974-016-0748-7.
13. Stetson, D.B. and R. Medzhitov, *Type I interferons in host defense.* Immunity, 2006. **25**(3): p. 373-81. DOI: 10.1016/j.immuni.2006.08.007.
14. Kato, H., et al., *Differential roles of MDA5 and RIG-I helicases in the recognition of RNA viruses.* Nature, 2006. **441**(7089): p. 101-5. DOI: 10.1038/nature04734.
15. Samuel, C.E., *Antiviral actions of interferons.* Clin Microbiol Rev, 2001. **14**(4): p. 778-809, table of contents. DOI: 10.1128/cmr.14.4.778-809.2001.
16. Yoneyama, M. and T. Fujita, *RNA recognition and signal transduction by RIG-I-like receptors.* Immunol Rev, 2009. **227**(1): p. 54-65. DOI: 10.1111/j.1600-065X.2008.00727.x.
17. Carlin, A.F., et al., *An IRF-3-, IRF-5-, and IRF-7-Independent Pathway of Dengue Viral Resistance Utilizes IRF-1 to Stimulate Type I and II Interferon Responses.* Cell Rep, 2017. **21**(6): p. 1600-1612. DOI: 10.1016/j.celrep.2017.10.054.
18. Feng, H., et al., *Interferon regulatory factor 1 (IRF1) and anti-pathogen innate immune responses.* PLoS Pathog, 2021. **17**(1): p. e1009220. DOI: 10.1371/journal.ppat.1009220.
19. Pachter, J.S., H.E. de Vries, and Z. Fabry, *The blood-brain barrier and its role in immune privilege in the central nervous system.* J Neuropathol Exp Neurol, 2003. **62**(6): p. 593-604. DOI: 10.1093/jnen/62.6.593.
20. Sorgeloos, F., et al., *Antiviral type I and type III interferon responses in the central nervous system.* Viruses, 2013. **5**(3): p. 834-57. DOI: 10.3390/v5030834.
21. Schmitt, G., et al., *The great barrier belief: The blood-brain barrier and considerations for juvenile toxicity studies.* Reprod Toxicol, 2017. **72**: p. 129-135. DOI: 10.1016/j.reprotox.2017.06.043.
22. Ek, C.J., et al., *Barriers in the developing brain and Neurotoxicology.* Neurotoxicology, 2012. **33**(3): p. 586-604. DOI: 10.1016/j.neuro.2011.12.009.

23. Monath, T.P., C.B. Cropp, and A.K. Harrison, *Mode of entry of a neurotropic arbovirus into the central nervous system. Reinvestigation of an old controversy.* Lab Invest, 1983. **48**(4): p. 399-410.
24. Nair, S. and M.S. Diamond, *Innate immune interactions within the central nervous system modulate pathogenesis of viral infections.* Curr Opin Immunol, 2015. **36**: p. 47-53. DOI: 10.1016/j.coi.2015.06.011.
25. Ousman, S.S. and P. Kubes, *Immune surveillance in the central nervous system.* Nat Neurosci, 2012. **15**(8): p. 1096-101. DOI: 10.1038/nn.3161.
26. Al-Shujairi, W.H., et al., *Intracranial Injection of Dengue Virus Induces Interferon Stimulated Genes and CD8+ T Cell Infiltration by Sphingosine Kinase 1 Independent Pathways.* PLoS One, 2017. **12**(1): p. e0169814. DOI: 10.1371/journal.pone.0169814.
27. Delhaye, S., et al., *Neurons produce type I interferon during viral encephalitis.* Proc Natl Acad Sci U S A, 2006. **103**(20): p. 7835-40. DOI: 10.1073/pnas.0602460103.
28. Detje, C.N., et al., *Local type I IFN receptor signaling protects against virus spread within the central nervous system.* J Immunol, 2009. **182**(4): p. 2297-304. DOI: 10.4049/jimmunol.0800596.
29. Hanamsagar, R., M.L. Hanke, and T. Kielian, *Toll-like receptor (TLR) and inflammasome actions in the central nervous system.* Trends Immunol, 2012. **33**(7): p. 333-42. DOI: 10.1016/j.it.2012.03.001.
30. Hickey, W.F., *Basic principles of immunological surveillance of the normal central nervous system.* Glia, 2001. **36**(2): p. 118-24. DOI: 10.1002/glia.1101.
31. Carson, M.J., et al., *CNS immune privilege: hiding in plain sight.* Immunol Rev, 2006. **213**: p. 48-65. DOI: 10.1111/j.1600-065X.2006.00441.x.
32. Aloisi, F., F. Ria, and L. Adorini, *Regulation of T-cell responses by CNS antigen-presenting cells: different roles for microglia and astrocytes.* Immunol Today, 2000. **21**(3): p. 141-7. DOI: 10.1016/s0167-5699(99)01512-1.
33. van den Pol, A.N., S. Ding, and M.D. Robek, *Long-distance interferon signaling within the brain blocks virus spread.* J Virol, 2014. **88**(7): p. 3695-704. DOI: 10.1128/jvi.03509-13.
34. Kim, W.G., et al., *Regional difference in susceptibility to lipopolysaccharide-induced neurotoxicity in the rat brain: role of microglia.* J Neurosci, 2000. **20**(16): p. 6309-16. DOI: 10.1523/jneurosci.20-16-06309.2000.
35. Kipp, M., et al., *Brain-region-specific astroglial responses in vitro after LPS exposure.* J Mol Neurosci, 2008. **35**(2): p. 235-43. DOI: 10.1007/s12031-008-9057-7.
36. Durrant, D.M., S. Ghosh, and R.S. Klein, *The Olfactory Bulb: An Immunosensory Effector Organ during Neurotropic Viral Infections.* ACS Chem Neurosci, 2016. **7**(4): p. 464-9. DOI: 10.1021/acschemneuro.6b00043.
37. Detje, C.N., et al., *Upon intranasal vesicular stomatitis virus infection, astrocytes in the olfactory bulb are important interferon Beta producers that protect from lethal encephalitis.* J Virol, 2015. **89**(5): p. 2731-8. DOI: 10.1128/jvi.02044-14.
38. Lindqvist, R., et al., *Cell-type- and region-specific restriction of neurotropic flavivirus infection by viperin.* J Neuroinflammation, 2018. **15**(1): p. 80. DOI: 10.1186/s12974-018-1119-3.
39. Lun, M.P., E.S. Monuki, and M.K. Lehtinen, *Development and functions of the choroid plexus-cerebrospinal fluid system.* Nat Rev Neurosci, 2015. **16**(8): p. 445-57. DOI: 10.1038/nrn3921.
40. Schwerk, C., et al., *The choroid plexus-a multi-role player during infectious diseases of the CNS.* Front Cell Neurosci, 2015. **9**: p. 80. DOI: 10.3389/fncel.2015.00080.
41. Baruch, K., et al., *Aging. Aging-induced type I interferon response at the choroid plexus negatively affects brain function.* Science, 2014. **346**(6205): p. 89-93. DOI: 10.1126/science.1252945.
42. Pinti, M., et al., *Aging of the immune system: Focus on inflammation and vaccination.* Eur J Immunol, 2016. **46**(10): p. 2286-2301. DOI: 10.1002/eji.201546178.
43. Lopez-Otin, C., et al., *The hallmarks of aging.* Cell, 2013. **153**(6): p. 1194-217. DOI: 10.1016/j.cell.2013.05.039.

44. Erickson, K.I., et al., *Exercise training increases size of hippocampus and improves memory.* Proc Natl Acad Sci U S A, 2011. **108**(7): p. 3017-22. DOI: 10.1073/pnas.1015950108.
45. Cherbuin, N., et al., *Being overweight is associated with hippocampal atrophy: the PATH Through Life Study.* International Journal of Obesity, 2015. **39**(10): p. 1509-1514. DOI: 10.1038/ijo.2015.106.
46. Drayer, B.P., *Imaging of the aging brain. Part I. Normal findings.* Radiology, 1988. **166**(3): p. 785-96. DOI: 10.1148/radiology.166.3.3277247.
47. Mattson, M.P. and T.V. Arumugam, *Hallmarks of Brain Aging: Adaptive and Pathological Modification by Metabolic States.* Cell Metab, 2018. **27**(6): p. 1176-1199. DOI: 10.1016/j.cmet.2018.05.011.
48. Stephenson, J., et al., *Inflammation in CNS neurodegenerative diseases.* Immunology, 2018. **154**(2): p. 204-219. DOI: 10.1111/imm.12922.
49. Hurme, M., *Viruses and immunosenescence - more players in the game.* Immun Ageing, 2019. **16**: p. 13. DOI: 10.1186/s12979-019-0152-0.
50. Panda, A., et al., *Human innate immunosenescence: causes and consequences for immunity in old age.* Trends Immunol, 2009. **30**(7): p. 325-33. DOI: 10.1016/j.it.2009.05.004.
51. Kovacs, E.J., et al., *Aging and innate immunity in the mouse: impact of intrinsic and extrinsic factors.* Trends Immunol, 2009. **30**(7): p. 319-24. DOI: 10.1016/j.it.2009.03.012.
52. Chevalier, G., et al., *Neurons are MHC class I-dependent targets for CD8 T cells upon neurotropic viral infection.* PLoS Pathog, 2011. **7**(11): p. e1002393. DOI: 10.1371/journal.ppat.1002393.
53. Goronzy, J.J. and C.M. Weyand, *Mechanisms underlying T cell ageing.* Nat Rev Immunol, 2019. **19**(9): p. 573-583. DOI: 10.1038/s41577-019-0180-1.
54. Ray, D. and R. Yung, *Immune senescence, epigenetics and autoimmunity.* Clin Immunol, 2018. **196**: p. 59-63. DOI: 10.1016/j.clim.2018.04.002.
55. Dorrington, M.G. and D.M. Bowdish, *Immunosenescence and novel vaccination strategies for the elderly.* Front Immunol, 2013. **4**: p. 171. DOI: 10.3389/fimmu.2013.00171.
56. Shrestha, B. and M.S. Diamond, *Role of CD8+ T cells in control of West Nile virus infection.* J Virol, 2004. **78**(15): p. 8312-21. DOI: 10.1128/jvi.78.15.8312-8321.2004.
57. Hayasaka, D., et al., *Mortality following peripheral infection with tick-borne encephalitis virus results from a combination of central nervous system pathology, systemic inflammatory and stress responses.* Virology, 2009. **390**(1): p. 139-50. DOI: 10.1016/j.virol.2009.04.026.
58. Hirano, M., et al., *Tick-borne flaviviruses alter membrane structure and replicate in dendrites of primary mouse neuronal cultures.* J Gen Virol, 2014. **95**(Pt 4): p. 849-861. DOI: 10.1099/vir.0.061432-0.
59. Yshii, L., et al., *Neurons and T cells: Understanding this interaction for inflammatory neurological diseases.* Eur J Immunol, 2015. **45**(10): p. 2712-20. DOI: 10.1002/eji.201545759.
60. Meuth, S.G., et al., *Cytotoxic CD8+ T cell-neuron interactions: perforin-dependent electrical silencing precedes but is not causally linked to neuronal cell death.* J Neurosci, 2009. **29**(49): p. 15397-409. DOI: 10.1523/JNEUROSCI.4339-09.2009.
61. Ehling, P., et al., *CD8(+) T Cell-Mediated Neuronal Dysfunction and Degeneration in Limbic Encephalitis.* Front Neurol, 2015. **6**: p. 163. DOI: 10.3389/fneur.2015.00163.
62. Ishikawa, T., A. Yamanaka, and E. Konishi, *A review of successful flavivirus vaccines and the problems with those flaviviruses for which vaccines are not yet available.* Vaccine, 2014. **32**(12): p. 1326-37. DOI: 10.1016/j.vaccine.2014.01.040.
63. Dobler, G., *Zoonotic tick-borne flaviviruses.* Vet Microbiol, 2010. **140**(3-4): p. 221-8. DOI: 10.1016/j.vetmic.2009.08.024.
64. Mandl, C.W., *Steps of the tick-borne encephalitis virus replication cycle that affect neuropathogenesis.* Virus Res, 2005. **111**(2): p. 161-74. DOI: 10.1016/j.virusres.2005.04.007.

65. Gritsun, T.S., V.A. Lashkevich, and E.A. Gould, *Tick-borne encephalitis.* Antiviral Research, 2003. **57**(1-2): p. 129-146. DOI: 10.1016/s0166-3542(02)00206-1.
66. Lindqvist, R., A. Upadhyay, and A.K. Overby, *Tick-Borne Flaviviruses and the Type I Interferon Response.* Viruses, 2018. **10**(7). DOI: 10.3390/v10070340.
67. Hudopisk, N., et al., *Tick-borne encephalitis associated with consumption of raw goat milk, Slovenia, 2012.* Emerg Infect Dis, 2013. **19**(5): p. 806-8. DOI: 10.3201/eid1905.121442.
68. Dumpis, U., D. Crook, and J. Oksi, *Tick-Borne Encephalitis.* Clinical Infectious Diseases, 1999. **28**(4): p. 882-890. DOI: 10.1086/515195 %J Clinical Infectious Diseases.
69. Mansfield, K.L., et al., *Tick-borne encephalitis virus - a review of an emerging zoonosis.* J Gen Virol, 2009. **90**(Pt 8): p. 1781-1794. DOI: 10.1099/vir.0.011437-0.
70. Grard, G., et al., *Genetic characterization of tick-borne flaviviruses: new insights into evolution, pathogenetic determinants and taxonomy.* Virology, 2007. **361**(1): p. 80-92. DOI: 10.1016/j.virol.2006.09.015.
71. Pletnev, A.G., V.F. Yamshchikov, and V.M. Blinov, *Nucleotide sequence of the genome and complete amino acid sequence of the polyprotein of tick-borne encephalitis virus.* Virology, 1990. **174**(1): p. 250-63. DOI: 10.1016/0042-6822(90)90073-z.
72. Mackenzie, J.S., D.J. Gubler, and L.R. Petersen, *Emerging flaviviruses: the spread and resurgence of Japanese encephalitis, West Nile and dengue viruses.* Nat Med, 2004. **10**(12 Suppl): p. S98-109. DOI: 10.1038/nm1144.
73. Mandl, C.W., et al., *Sequence of the genes encoding the structural proteins of the low-virulence tick-borne flaviviruses Langat TP21 and Yelantsev.* Virology, 1991. **185**(2): p. 891-5. DOI: 10.1016/0042-6822(91)90567-u.
74. Blom, K., et al., *Cell-Mediated Immune Responses and Immunopathogenesis of Human Tick-Borne Encephalitis Virus-Infection.* Frontiers in Immunology, 2018. **9**. DOI: ARTN 217410.3389/fimmu.2018.02174.
75. Haglund, M. and G. Günther, *Tick-borne encephalitis--pathogenesis, clinical course and long-term follow-up.* Vaccine, 2003. **21 Suppl 1**: p. S11-8. DOI: 10.1016/s0264-410x(02)00811-3.
76. Shaw, A.C., D.R. Goldstein, and R.R. Montgomery, *Age-dependent dysregulation of innate immunity.* Nat Rev Immunol, 2013. **13**(12): p. 875-87. DOI: 10.1038/nri3547.
77. Lauri I. A. Pulkkinen, S.J.B., Maria Anastasina, *Tick-Borne Encephalitis Virus: A Structural View.* Viruses, 2018. **10**. DOI: 10.3390/v10070350.
78. Leonova, G.N., et al., *Comprehensive assessment of the genetics and virulence of tick-borne encephalitis virus strains isolated from patients with inapparent and clinical forms of the infection in the Russian Far East.* Virology, 2013. **443**(1): p. 89-98. DOI: 10.1016/j.virol.2013.04.029.
79. Loew-Baselli, A., et al., *Seropersistence of tick-borne encephalitis antibodies, safety and booster response to FSME-IMMUN (R) 0.5 ml in adults aged 18-67 years.* Human Vaccines, 2009. **5**(8): p. 551-556. DOI: DOI 10.4161/hv.5.8.8571.
80. Robert-Koch-Institut, *Epidemiologisches Bulletin*, Robert-Koch-Institut, Editor. 2021.
81. Kunze, U., et al., *The Golden Agers and Tick-borne encephalitis. Conference report and position paper of the International Scientific Working Group on Tick-borne encephalitis.* Wien Med Wochenschr, 2005. **155**(11-12): p. 289-94. DOI: 10.1007/s10354-005-0178-0.
82. CDC, *Yellow Book*. 2020: Oxford University Press Inc.
83. Baker, D.G., et al., *Toll-like receptor 7 suppresses virus replication in neurons but does not affect viral pathogenesis in a mouse model of Langat virus infection.* J Gen Virol, 2013. **94**(Pt 2): p. 336-347. DOI: 10.1099/vir.0.043984-0.
84. Kurhade, C., et al., *Type I Interferon response in olfactory bulb, the site of tick-borne flavivirus accumulation, is primarily regulated by IPS-1.* J Neuroinflammation, 2016. **13**: p. 22. DOI: 10.1186/s12974-016-0487-9.
85. Montgomery, R.R., *Age-related alterations in immune responses to West Nile virus infection.* Clin Exp Immunol, 2017. **187**(1): p. 26-34. DOI: 10.1111/cei.12863.
86. Kong, K.F., et al., *Dysregulation of TLR3 impairs the innate immune response to West Nile virus in the elderly.* J Virol, 2008. **82**(15): p. 7613-23. DOI: 10.1128/jvi.00618-08.

87. Gomez, C.R., et al., *Innate immunity and aging.* Experimental Gerontology, 2008. **43**(8): p. 718-728. DOI: 10.1016/j.exger.2008.05.016.
88. Goldberg, E.L., A.C. Shaw, and R.R. Montgomery, *How Inflammation Blunts Innate Immunity in Aging.* Interdiscip Top Gerontol Geriatr, 2020. **43**: p. 1-17. DOI: 10.1159/000504480.
89. de Veer, M.J., et al., *Functional classification of interferon-stimulated genes identified using microarrays.* J Leukoc Biol, 2001. **69**(6): p. 912-20.
90. Der, S.D., et al., *Identification of genes differentially regulated by interferon alpha, beta, or gamma using oligonucleotide arrays.* Proc Natl Acad Sci U S A, 1998. **95**(26): p. 15623-8. DOI: 10.1073/pnas.95.26.15623.
91. Kumar, H., et al., *Essential role of IPS-1 in innate immune responses against RNA viruses.* J Exp Med, 2006. **203**(7): p. 1795-803. DOI: 10.1084/jem.20060792.
92. Suthar, M.S., et al., *IPS-1 is essential for the control of West Nile virus infection and immunity.* PLoS Pathog, 2010. **6**(2): p. e1000757. DOI: 10.1371/journal.ppat.1000757.
93. Weber, E., et al., *Type I interferon protects mice from fatal neurotropic infection with Langat virus by systemic and local antiviral responses.* J Virol, 2014. **88**(21): p. 12202-12. DOI: 10.1128/JVI.01215-14.
94. Sun, Q., et al., *The specific and essential role of MAVS in antiviral innate immune responses.* Immunity, 2006. **24**(5): p. 633-42. DOI: 10.1016/j.immuni.2006.04.004.
95. Geissmann, F., et al., *Development of monocytes, macrophages, and dendritic cells.* Science, 2010. **327**(5966): p. 656-61. DOI: 10.1126/science.1178331.
96. Fuentes, E., et al., *Immune System Dysfunction in the Elderly.* An Acad Bras Cienc, 2017. **89**(1): p. 285-299. DOI: 10.1590/0001-3765201720160487.
97. Weiskopf, D., B. Weinberger, and B. Grubeck-Loebenstein, *The aging of the immune system.* Transpl Int, 2009. **22**(11): p. 1041-50. DOI: 10.1111/j.1432-2277.2009.00927.x.
98. Kierdorf, K., et al., *Microglia emerge from erythromyeloid precursors via Pu.1- and Irf8-dependent pathways.* Nature Neuroscience, 2013. **16**(3): p. 273-280. DOI: 10.1038/nn.3318.
99. Kreutzberg, G.W., *Microglia: a sensor for pathological events in the CNS.* Trends Neurosci, 1996. **19**(8): p. 312-8. DOI: 10.1016/0166-2236(96)10049-7.
100. Stoll, G. and S. Jander, *The role of microglia and macrophages in the pathophysiology of the CNS.* Prog Neurobiol, 1999. **58**(3): p. 233-47. DOI: 10.1016/s0301-0082(98)00083-5.
101. Cho, H., et al., *Differential innate immune response programs in neuronal subtypes determine susceptibility to infection in the brain by positive-stranded RNA viruses.* Nature Medicine, 2013. **19**(4): p. 458-+. DOI: 10.1038/nm.3108.
102. Stout-Delgado, H.W., et al., *Aging impairs IFN regulatory factor 7 up-regulation in plasmacytoid dendritic cells during TLR9 activation.* J Immunol, 2008. **181**(10): p. 6747-56. DOI: 10.4049/jimmunol.181.10.6747.
103. Sridharan, A., et al., *Age-associated impaired plasmacytoid dendritic cell functions lead to decreased CD4 and CD8 T cell immunity.* Age (Dordr), 2011. **33**(3): p. 363-76. DOI: 10.1007/s11357-010-9191-3.
104. Yao, Y. and R.R. Montgomery, *Role of Immune Aging in Susceptibility to West Nile Virus.* Methods Mol Biol, 2016. **1435**: p. 235-47. DOI: 10.1007/978-1-4939-3670-0_18.
105. Zegenhagen, L., et al., *Brain heterogeneity leads to differential innate immune responses and modulates pathogenesis of viral infections.* Cytokine Growth Factor Rev, 2016. **30**: p. 95-101. DOI: 10.1016/j.cytogfr.2016.03.006.
106. Patil, A.M., et al., *Type I IFN signaling limits hemorrhage-like disease after infection with Japanese encephalitis virus through modulating a prerequisite infection of CD11b(+)Ly-6C(+) monocytes.* J Neuroinflammation, 2021. **18**(1): p. 136. DOI: 10.1186/s12974-021-02180-5.
107. Samuel, M.A. and M.S. Diamond, *Alpha/beta interferon protects against lethal West Nile virus infection by restricting cellular tropism and enhancing neuronal survival.* J Virol, 2005. **79**(21): p. 13350-61. DOI: 10.1128/jvi.79.21.13350-13361.2005.

108. Levy, D.E., I. Marié, and A. Prakash, *Ringing the interferon alarm: differential regulation of gene expression at the interface between innate and adaptive immunity.* Curr Opin Immunol, 2003. **15**(1): p. 52-8. DOI: 10.1016/s0952-7915(02)00011-0.
109. Brien, J.D., et al., *Interferon regulatory factor-1 (IRF-1) shapes both innate and CD8(+) T cell immune responses against West Nile virus infection.* PLoS Pathog, 2011. **7**(9): p. e1002230. DOI: 10.1371/journal.ppat.1002230.
110. Qian, F., et al., *Impaired interferon signaling in dendritic cells from older donors infected in vitro with West Nile virus.* J Infect Dis, 2011. **203**(10): p. 1415-24. DOI: 10.1093/infdis/jir048.
111. Szretter, K.J., et al., *The interferon-inducible gene viperin restricts West Nile virus pathogenesis.* J Virol, 2011. **85**(22): p. 11557-66. DOI: 10.1128/jvi.05519-11.
112. Zhang, W., et al., *OASs in Defense of Mycobacterial Infection: Angels or Demons?* Curr Issues Mol Biol, 2021. **40**: p. 221-230. DOI: 10.21775/cimb.040.221.
113. Steinbusch, M.M.F., et al., *The antiviral protein viperin regulates chondrogenic differentiation via CXCL10 protein secretion.* J Biol Chem, 2019. **294**(13): p. 5121-5136. DOI: 10.1074/jbc.RA119.007356.
114. Lindqvist, R. and A.K. Överby, *The Role of Viperin in Antiflavivirus Responses.* DNA Cell Biol, 2018. **37**(9): p. 725-730. DOI: 10.1089/dna.2018.4328.
115. Helbig, K.J., et al., *Viperin is induced following dengue virus type-2 (DENV-2) infection and has anti-viral actions requiring the C-terminal end of viperin.* PLoS Negl Trop Dis, 2013. **7**(4): p. e2178. DOI: 10.1371/journal.pntd.0002178.
116. Al Shujairi, W.H., et al., *Viperin is anti-viral in vitro but is dispensable for restricting dengue virus replication or induction of innate and inflammatory responses in vivo.* J Gen Virol, 2021. **102**(10). DOI: 10.1099/jgv.0.001669.
117. Huang, H., et al., *IFI27 is a potential therapeutic target for HIV infection.* Ann Med, 2022. **54**(1): p. 314-325. DOI: 10.1080/07853890.2021.1995624.
118. Ullah, H., et al., *Antiviral Activity of Interferon Alpha-Inducible Protein 27 Against Hepatitis B Virus Gene Expression and Replication.* Front Microbiol, 2021. **12**: p. 656353. DOI: 10.3389/fmicb.2021.656353.
119. Lucas, T.M., J.M. Richner, and M.S. Diamond, *The Interferon-Stimulated Gene Ifi27l2a Restricts West Nile Virus Infection and Pathogenesis in a Cell-Type- and Region-Specific Manner.* J Virol, 2015. **90**(5): p. 2600-15. DOI: 10.1128/JVI.02463-15.
120. Fredericksen, B.L., et al., *Establishment and maintenance of the innate antiviral response to West Nile Virus involves both RIG-I and MDA5 signaling through IPS-1.* J Virol, 2008. **82**(2): p. 609-16. DOI: 10.1128/jvi.01305-07.
121. Xie, G., et al., *Dysregulation of Toll-Like Receptor 7 Compromises Innate and Adaptive T Cell Responses and Host Resistance to an Attenuated West Nile Virus Infection in Old Mice.* J Virol, 2016. **90**(3): p. 1333-44. DOI: 10.1128/jvi.02488-15.
122. Tomazic, J. and A. Ihan, *Flow cytometric analysis of lymphocytes in cerebrospinal fluid in patients with tick-borne encephalitis.* Acta Neurol Scand, 1997. **95**(1): p. 29-33. DOI: 10.1111/j.1600-0404.1997.tb00064.x.
123. Machado-Santos, J., et al., *The compartmentalized inflammatory response in the multiple sclerosis brain is composed of tissue-resident CD8+ T lymphocytes and B cells.* Brain, 2018. **141**(7): p. 2066-2082. DOI: 10.1093/brain/awy151.
124. Morgan, J., et al., *Classical CD4 T cells as the cornerstone of antimycobacterial immunity.* Immunol Rev, 2021. **301**(1): p. 10-29. DOI: 10.1111/imr.12963.
125. Franceschi, C., et al., *Biomarkers of immunosenescence within an evolutionary perspective: the challenge of heterogeneity and the role of antigenic load.* Exp Gerontol, 1999. **34**(8): p. 911-21. DOI: 10.1016/s0531-5565(99)00068-6.
126. Nimmerjahn, A., F. Kirchhoff, and F. Helmchen, *Resting microglial cells are highly dynamic surveillants of brain parenchyma in vivo.* Science, 2005. **308**(5726): p. 1314-8. DOI: 10.1126/science.1110647.
127. Amor, S., et al., *White matter microglia heterogeneity in the CNS.* Acta Neuropathol, 2022. **143**(2): p. 125-141. DOI: 10.1007/s00401-021-02389-x.

128. Cai, B., et al., *A synthetic diosgenin primary amine derivative attenuates LPS-stimulated inflammation via inhibition of NF-κB and JNK MAPK signaling in microglial BV2 cells.* Int Immunopharmacol, 2018. **61**: p. 204-214. DOI: 10.1016/j.intimp.2018.05.021.
129. Santos, E.S., et al., *Tolerogenic Dendritic Cells Reduce Cardiac Inflammation and Fibrosis in Chronic Chagas Disease.* Front Immunol, 2020. **11**: p. 488. DOI: 10.3389/fimmu.2020.00488.
130. Colton, C.A., *Immune heterogeneity in neuroinflammation: dendritic cells in the brain.* J Neuroimmune Pharmacol, 2013. **8**(1): p. 145-62. DOI: 10.1007/s11481-012-9414-8.
131. Roe, K., et al., *Dendritic cell-associated MAVS is required to control West Nile virus replication and ensuing humoral immune responses.* PLoS One, 2019. **14**(6): p. e0218928. DOI: 10.1371/journal.pone.0218928.
132. Daniels, B.P., et al., *Regional astrocyte IFN signaling restricts pathogenesis during neurotropic viral infection.* J Clin Invest, 2017. **127**(3): p. 843-856. DOI: 10.1172/JCI88720.
133. Schreier, S., K. Cebulski, and A. Kröger, *Contact-dependent transmission of Langat and tick-borne encephalitis virus in type I interferon receptor-1 deficient mice.* J Virol, 2021. **95**(8). DOI: 10.1128/jvi.02039-20.
134. Wacher, C., et al., *Coordinated regulation and widespread cellular expression of interferon-stimulated genes (ISG) ISG-49, ISG-54, and ISG-56 in the central nervous system after infection with distinct viruses.* J Virol, 2007. **81**(2): p. 860-71. DOI: 10.1128/jvi.01167-06.

7. Appendix

7.1. Abbreviations

APC	Antigen Presenting Cell
BBB	Blood-Brain-Barrier
BCs	B Lymphocytes
C	Capsid
CNS	Central Nervous System
CP	Choroid Plexus
CSF	Cerebrospinal Fluid
CTL	Cytotoxic T Cell
DCs	Dendritic Cells
DENV	Dengue Virus
dpi	Day Post Infection
E	Envelope
ER	Endoplasmatic Reticulum
FFU	Focus Forming Unit
GFP	Green Fluorescent Protein
HBV	Hepatitis B Virus
IFN	Interferon
IFNAR	IFN A Receptor
IL	Interleukin
IRF	Interferon Regulatory Factor
ISG	Interferon Stimulating Gene
Jak	Janus kinase
JEV	Japanese Encephalitis Virus
KO	Knockout
LGTV	Langat Virus
LIV	Louping-Ill Virus
M	Membrane
MAVS	Mitochondrial Antiviral Signaling Protein
MDA5	Melanoma Differentiation-Associated Protein 5
MEF	Mouse Embryonic Fibroblast
MHC-I	Class I Major Histocompatibility Complex
MOI	Multiplicity Of Infection
NK cells	Natural Killer Cells
NS	Non-Structural

OB	Olfactory Bulb
OHFV	Omsk Hemorrhagic Fever Virus
ORF	Open Reading Frame
PAMPS	Pathogen Associated Molecular Patterns
POWV	Powassan Virus
PRR	Pathogen Recognition Receptor
qRT-PCR	Quantitative real time polymerase chain reaction
RIG-I	Retinoic Acid-Inducible Gene-I
RLR	RIG-I-like Receptors
STAT	Signal Transducer and Activator of Transcription
TBEV	Tick-Borne Encephalitis Virus
TCR	T Cell Receptor
Th cell	T Helper Cell
TLR	Toll-like Receptors
TNF	Tumor Necrosis Factor
Tyk	Tyrosine kinase
Type I IFN	Type I Interferon System
WNV	West Nile Virus
WT	Wildtype (C57BL/6OlaHsd)
YFV	Yellow Fever Virus
ZIKV	Zika Virus

7.2. Figures

7.3. Tables